P.J.M. de Laat

International Institute for Hydraulic and Environmental Engineering, Delft, the Netherlands

Model for unsaturated flow above a shallow water-table, applied to a regional sub-surface flow problem

Centre for Agricultural Publishing and Documentation

Wageningen - 1980

ISBN 90 220 0725 1

The author graduated on 22 February 1980 as Doctor in de Landbouwwetenschappen at the Agricultural University, Wageningen, the Netherlands, on a thesis with the same title and contents.

Abstract

Laat, P.J.M. de (1980) Model for unsaturated flow above a shallow water-table, applied to a regional sub-surface flow problem. Agric. Res. Rep. (Versl. landbouwk. Onderz.) 895, ISBN 90 220 0725 1, (vii) + 126 p., 42 figs, 6 tables, 182 refs, 2 appendices, Eng. and Dutch summaries.
Also: Doctoral thesis, Wageningen.

A mathematical model is developed to simulate transient unsaturated flow above a shallow water-table. The unsaturated zone, here extending from just below the phreatic level to soil surface, is schematized into a root zone and a subsoil. In the root zone the gradient of the hydraulic potential is assumed equal to zero. Vertical flow in the subsoil is described by a combination of steady-state situations corresponding to the upper and lower boundary flux, respectively. Transient flow is solved by a sequence of steady-state situations, subject to boundary flux conditions at the soil surface and from below the water table. The solution uses time increments of the order of days and is efficient in terms of computer costs.

To verify the model for an actual field situation, it is linked at the upper boundary to a model for evapotranspiration and at the lower boundary to a model for two-dimensional horizontal saturated flow. The resulting quasi three-dimensional model is applied to a field-size flow problem. Results agree closely with observed water-table elevations. The composite model is further used to predict consequenses of groundwater extraction.

Free descriptors: capillary rise, percolation, saturated-unsaturated flow, evapotranspiration, groundwater extraction, prediction.

Contents

1 Introduction

The reclamation and protection of land from the sea and inland waters in the Netherlands during the past centuries resulted in the development of large polder areas. The excellent opportunities for water management in these areas provided optimum conditions for crop growth, at least from a quantitative point of view. Qualitative problems arose due to the deterioration in quality of the supplemented surface water and, particularly in the lowest polders, to the intrusion of saline groundwater.

It is only since the beginning of this century that serious attention has been given to the water management problems in the eastern and southern part of the country. Although the land is above mean sea level, flooding was frequent in some places and large areas suffered from too high water-tables. It is well-known that wet conditions in the beginning of the growing season may seriously affect agricultural crop production. It delays the sowing and planting of crops, but also the seedling emergence and growth because of low temperatures and high concentrations of carbon dioxide in the root zone of the soil. To ensure favourable conditions for crop growth at the beginning of the growing season, the drainage in many of the higher areas with mainly aeolian soils has been drastically improved.

Although the average annual rainfall excess in the Netherlands is between 200 and 300 mm, the potential evapotranspiration exceeds precipitation during the growing season (April to September) by more than 100 mm. If this amount is available for the crop in the root zone, water supply is optimum for crop production. However, most of the (sandy) soils in the eastern and southern part of the country are not even able to retain the amount that is needed in a year for which 'average weather conditions' apply. With a shallow water-table a considerable part of this deficit may be supplemented by the transport of soil moisture from the groundwater reservoir to the root zone. The upward movement of soil moisture in the region above the water table is termed capillary rise. This process depends on the depth of the water table. It becomes insignificant for the water supply of the crop if the prevailing water-table depth is more than 3-5 m below soil surface.

The rapid expansion of population and industry during the past decades resulted in a considerable increase in the demand for domestic and industrial water. As surface water in general is of poor quality, and as there is hardly any fresh groundwater in the west, the amounts extracted from the eastern and southern parts of the country are rapidly increasing. In those areas where the implemented drainage system is (more than) adequate, an additional extraction of groundwater results in an undesirable drawdown of the water table. The effect of a drawdown on the availibility of water for the crop in areas with relatively high water-tables is twofold. It reduces the amount of soil moisture initially available in the root zone and it hampers capillary rise. As a result of

the development described above, some of the areas which previously had an abundance of water now show a shortage.

This study concerns groundwater flow in shallow water-table aquifers and in particular flow in the unsaturated region between the soil surface and the phreatic level. Although the water movement in a partly saturated soil may be described by one single equation, the flow regions above and below the phreatic surface were traditionally treated as two separate systems. One of the reasons for the separate approach is that flow in the unsaturated zone is predominantly vertical, and in the saturated part in a horizontal direction. Moreover, the numerical solution of the governing equation requires much more effort in the unsaturated zone than in the saturated region. The available solutions of three-dimensional, saturated-unsaturated problems using a single equation are, therefore, restricted to small-size flow systems.

A less-rigorous approach treats flow in the saturated and unsaturated region separately and uses a special procedure to link both sub-systems. The partial differential equation governing non-steady unsaturated flow is highly non-linear. For stability and convergence the solution requires that time and space are discretized to small steps. The restriction with respect to the length of the time increment is imposed upon the entire system. Therefore, for the less-rigorous approach to be attractive in terms of computer costs, it is necessary that the numerical solution of the equation governing unsaturated flow is replaced by a more efficient simulation model. The approximate solutions, available at present, are unsuitable for a complete transient analysis, as they consider flow in an upward or downward direction only. Moreover, most of the solutions assume that the water table is at infinite depth.

For a shallow water-table in a sandy aquifer, the characteristic time of the unsaturated flow system is of the order of days. With a time increment of approximately this length, the flow system can be described by a succession of steady-state situations. This approach is used in this study to develop a model for unsaturated flow.

In order to verify this model for an actual field situation, it is linked at the upper boundary to a model for evapotranspiration, and at the lower boundary to a model for two-dimensional horizontal saturated flow. The combined model is applied to an area of 36 km^2 around the pumping site ''t Klooster' in the east of the country. The amount of surface water runoff from this area is relatively small. It was selected for this study to reduce the effect of the surface water system on the verification of the combined saturated-unsaturated flow model.

Finally, the model is used to predict consequences of groundwater extraction on the water-table elevation and real evapotranspiration.

2 Transport of water in soil

2.1 SOIL WATER POTENTIAL

In an isothermal system the driving force for transport of soil water is the gradient of potential energy. The 'International Soil Science Society' (Aslyng, 1963; Bolt, 1975) uses concepts based on energy and thermodynamics to define the condition of water in soil (see e.g. Taylor, 1968; Hillel, 1971). The total potential energy is described as the amount of work liberated by removing a unit mass of soil water from a certain location in the soil in the form of pure free water at the same temperature and to transfer this quantity isothermally to a reference level where it is defined as having a potential of zero. The components of the total potential Ψ_t are the pressure potential Ψ_p, the osmotic or solute potential Ψ_o and the gravitational potential Ψ_g. Thus

$$\Psi_t = \Psi_p + \Psi_o + \Psi_g \tag{1}$$

The pressure potential results from a pressure that differs from the existing atmospheric pressure. Pressure ($N \cdot m^{-2}$) is equivalent to energy per unit volume ($J \cdot m^{-3}$). Since the density ρ is mass per volume it follows that the pressure potential (expressed in energy per unit mass)

$$\Psi_p = \frac{p}{\rho} \tag{2}$$

where p is the pressure with respect to atmospheric pressure. In the unsaturated soil the pressure potential is negative due to the attractive forces of the soil matrix. Buckingham (1907) introduced the term 'capillary potential' to indicate that the potential results from capillary effects. Nowadays the term 'matric potential' is preferred as the pressure p is, especially in clayey soils, also affected by adsorption, by attraction between water molecules and ions in the electrical double layer of clay particles and by small deviations in the soil air pressure from the existing atmospheric pressure. In particular with respect to the last mentioned effect see Stroosnijder (1976). At the free water surface atmospheric pressure exists (by definition), so that p equals zero. Below this level, in the saturated region, the attraction of the soil matrix is negligible. Pressure merely results from the hydrostatic pressure, so that values for Ψ_p are positive. The pressure potential in the saturated zone has been termed 'submergence potential' (Rose, 1966). Although the pressure above and below the free water level results from quite different forces, p is considered in this study as a single continuous quantity, extending from the saturated to the unsaturated region.

The osmotic or solute potential reduces the total potential energy in the presence

of a membrane whose permeability to water molecules differs from that to the molecules of the dissolved salts. When dealing with water movement in soil it is assumed that the solute can move freely with the soil water. Hence

$$\Psi_o \equiv 0 \tag{3}$$

This condition implies that the soil water potential is defined with respect to free water of similar chemical composition as the soil moisture located at reference level.

The gravitational potential is the energy due to the earth gravitational field. If g is the gravity constant, the required energy to lift a mass of water m over a height z above reference level equals mgz. So the gravitational potential per unit mass

$$\Psi_g = gz \tag{4}$$

as g can be considered a constant over the distances involved.

The driving force for transport of water in a porous medium is then given by

$$\nabla\Psi_t = \nabla\Psi_p + \nabla\Psi_g = \nabla(\frac{p}{\rho}) + g\nabla z \tag{5}$$

If at a height z above reference level pressure p exists, the total potential energy per unit mass at this particular location in the soil may be written as

$$\Psi_t = \int_0^p \frac{1}{\rho}\, d\alpha + g \int_0^z d\beta \tag{6}$$

The potential Ψ_t represents a scalar quantity if its gradient describes a vector field without a rotational component. It can be shown (De Wiest, 1966) that Ψ_t as given by Eqn 6 generates an irrotational vector field, provided that the density ρ is a function of p only. Actually, the density of the soil water also varies with solute concentration and temperature. In this study the soil water is assumed to be homogeneous and imcompressible, so that for isothermal systems the total water potential (energy per unit mass) is given by

$$\Psi_t = \frac{p}{\rho} + gz \qquad (J \cdot kg^{-1}) \tag{7}$$

as here ρ can be considered a constant. Multiplying Eqn 7 by the constant ρ yields the pressure equivalent of the water potential (energy per unit volume)

$$P = \rho gz + p \qquad (J \cdot m^{-3} \text{ or } Pa) \tag{8}$$

Dividing Eqn 7 by the constant g results in a quantity known as hydraulic head or hydraulic potential (energy per unit weight)

$$\phi = z + \frac{p}{\rho g} \qquad (m) \tag{9}$$

2.2 GENERAL EQUATION OF FLOW

In the absence of other forces, such as thermal and electrical gradients, a difference in the total potential energy between two locations in the soil is the driving force to move water from the location where the potential is high to the location where a lower value exists. The resulting volume flux density q related to the potential gradient is known as Darcy's law, written in vectorial form as

$$\vec{q} = -k(\nabla p + \rho g \nabla z) \tag{10}$$

where the hydraulic conductivity k ($m^2 \cdot s^{-1} \cdot Pa^{-1}$) depends on the characteristics of the soil matrix, the dynamic viscosity of the fluid and the degree of saturation. If the value of k is the same in each flow direction, the porous medium is said to be hydraulically isotropic. Though the flux density vector q has the dimension of velocity ($m \cdot s^{-1}$), the term velocity is more properly used for the actual velocity of the water in the pore space of the soil matrix. In groundwater hydrology q is preferably termed 'specific discharge'.

In the unsaturated soil the pressure of water is usually measured with a tensiometer and below the free water surface with a piezometer. Both methods measure the pressure at a certain location in the soil relative to atmospheric pressure as a height of a water column, called pressure head ψ. If the density ρ in the apparatus equals the density of the soil water, $p = \rho g \psi$. It is therefore convenient to use the gradient of the hydraulic head to write Eqn 10 as

$$\vec{q} = -K[(\frac{1}{\rho g})\nabla p + \nabla z] = -K\nabla\phi \tag{11}$$

where the hydraulic conductivity K (= $\rho g k$) is expressed in the practical unit ($m \cdot s^{-1}$).

The continuity equation for flow in non-deformable media, stating the Law of Conservation of Mass, may be written as

$$\frac{\partial \rho \theta}{\partial t} = -\nabla \cdot \rho q \tag{12}$$

where t is time and θ the volume fraction of water per unit volume soil matrix. Taking ρ again as a constant and combining Eqns 11 and 12 results in a general equation of flow, written in vector notation as

$$\frac{\partial \theta}{\partial t} = \nabla \cdot (K \nabla \phi) \tag{13}$$

For flow in anisotropic media a more general equation is obtained by expanding Eqn 13 as follows

$$\frac{\partial \theta}{\partial t} = \frac{\partial}{\partial x}\left(K_x \frac{\partial \phi}{\partial x}\right) + \frac{\partial}{\partial y}\left(K_y \frac{\partial \phi}{\partial y}\right) + \frac{\partial}{\partial z}\left(K_z \frac{\partial \phi}{\partial z}\right) \tag{14}$$

where the x,y,z directions are chosen in the three principal directions of the hydraulic

conductivity K_x, K_y and K_z. When solving multi-dimensional flow problems, anisotropy should be taken into account because generally the natural porous medium has a stratified structure. Since transformation of isotropic flow problems into a problem for anisotropic media is relatively simple, the equations in Section 2.3 are conveniently derived for isotropic soils. For a thorough discussion on anisotropy in porous media the reader is referred to Childs (1969).

2.3 PARTICULAR FORMS OF THE GENERAL EQUATION

When modelling complicated systems simplifying assumptions have to be made. Some of these simplifications are necessary for a mathematical description of the system. An example is the assumption that Darcy's law, which is in accordance with the equation of Hagen-Poiseuille for laminar flow in a circular tube, also holds for flow in porous media. The validity of Darcy's law especially in unsaturated soil is still a matter of discussion (Swartzendruber, 1963 and 1968; Thames & Evans, 1968; Vachaud, 1969). Other assumptions are necessary to obtain an analytic or adequate numerical solution of the problem: for example, considering flow in one or two directions only, or neglecting the variation in hydraulic conductivity. These simplifying assumptions result in a number of differential equations each of which holds for a certain class of flow problems which are characterized by the assumptions made when deriving the formula. Many equations have been given the name of the author who first suggested its use. Equations frequently cited when discussing saturated and unsaturated flow will be dealt with in this section.

It should be realized that the general equation as formulated in Eqn 13 is general in so far as it describes the flow in a three-dimensional, non-homogeneous, saturated or unsaturated porous medium, but is less general in so far as it is restricted to isothermal flow of an incompressible homogeneous fluid in a rigid soil without other driving forces than those defined by the hydraulic head. Problems on mixed saturated-unsaturated flow in this study and most of the problems discussed in literature on this subject satisfy or nearly satisfy these restrictions. Therefore Eqn 13 will be used as the basic equation for further consideration.

The development of flow equations for transport of water in porous media came from two different disciplines. Saturated flow problems have been studied by groundwater hydrologists in relation to civil engineering and unsaturated flow has always been the domain of the soil scientist in relation to agriculture. This separate development may be illustrated by the fact that Buckingham when introducing the capillary potential in 1907 dit not even mention Darcy's law from 1856 and it took 20 years before Israelson (1927) noted the connection. The delayed progress made in the development of unsaturated flow theory compared with that of saturated flow has been mainly due to the difference in the nature of the potentials. In saturated media the potentials involving position and pressure are easily obtained where as it was not until 1928 with the introduction of the tensiometer (Richards, 1928) that unsaturated flow potentials could be measured. Moreover, empirical relations between pressure and moisture content and between pressure and hydraulic conductivity are required for the solution of unsaturated flow equations. These relations are difficult and tedious to obtain and are both subject to hysteresis.

Therefore analogy of flow through porous media to heat conduction was first recognized for saturated flow.

2.3.1 Saturated flow

For saturated flow the earlier defined proportionality factor k in the equation of Darcy as formulated in Eqn 10 is a function of the properties of the soil matrix and the fluid. Many investigators have tried to describe this parameter in terms of the characteristics of the medium as well as those of the liquid. In this connection use has been made of the experimentally derived equation of Poiseuille. According to this equation the rate of (laminar) flow through a tube of uniform cross-section is proportional to the hydraulic gradient, which is essentially Darcy's law for a column filled with porous material. From considerations on the proportionality constant of both equations, it follows that (Rose, 1966)

$$k = \frac{Ar^2}{\eta} \tag{15}$$

where A is a dimensionless constant, r the 'effective' radius of the pores and η the dynamic viscosity of the liquid. The constant A results from the fact that the flow through a porous medium is very irregular compared with laminar flow through a tube. It contains dimensionless characteristics on the geometry of the soil matrix. A reliable expression to relate the constant A to the porosity, shape of the grains, grain-size distribution and other geometrical properties of the porous medium has not been found. Muskat (1937) suggested to lump A and r^2 into one parameter that is a function of the structure of the medium alone and entirely independent of the nature of the fluid. This parameter has later been termed 'inherent', 'intrinsic' or 'specific' permeability. This concept of inherent permeability is rather not used by soil scientists, because soils are in general by no means inert in the physicochemical sense (Childs, 1969). This is well-known from farming practice where the structure of clayey soils is improved by the application of certain fertilizers. However, in the more inert sandy porous media in the absence of air, the concept of inherent permeability proved to be useful and it is generally applied by groundwater hydrologists. Denoting the intrinsic permeability by κ, the proportionality constant k is given by

$$k = \frac{\kappa}{\eta} \tag{16}$$

The hydraulic conductivity K, which appears in Darcy's law expressed in terms of hydraulic head may then be written as

$$K = \rho g k = \frac{\rho g \kappa}{\eta} \tag{17}$$

Since ρ has been assumed a constant and the fluid homogeneous, the hydraulic conductivity K may still be considered as a characteristic of the (saturated) porous medium alone.

Laplace's equation, earlier derived for the steady conduction of electricity and

heat was introduced for steady flow in homogeneous saturated media before the end of the last century by Slichter (1899). With $\partial\theta/\partial t = 0$ and K is a constant this equation follows directly from Eqn 13

$$\nabla^2\phi = \frac{\partial^2\phi}{\partial x^2} + \frac{\partial^2\phi}{\partial y^2} + \frac{\partial^2\phi}{\partial z^2} = 0 \tag{18}$$

In a horizontal, completely confined aquifer of uniform thickness the specific discharge in vertical direction can be disregarded and Eqn 18 reduces to

$$\frac{\partial^2\phi}{\partial x^2} + \frac{\partial^2\phi}{\partial y^2} = 0 \tag{19}$$

For semi-confined or leaky aquifers the vertical flux is still small enough to write the continuity equation as

$$\frac{\partial Dq_x}{\partial x} + \frac{\partial Dq_y}{\partial y} = -q_i \tag{20}$$

where D is the thickness of the aquifer and q_i is the leakage through the upper confining layer. Substituting $q_x = -K\partial\phi/\partial x$ and $q_y = -K\partial\phi/\partial y$ into Eqn 20 and assuming the hydraulic conductivity $\overline{K}$ to be a constant in vertical direction yields

$$\frac{\partial}{\partial x}\left(T\frac{\partial\phi}{\partial x}\right) + \frac{\partial}{\partial y}\left(T\frac{\partial\phi}{\partial y}\right) = q_i \tag{21}$$

where $T = \overline{K}D$ is termed the transmissivity, a function of x and y in non-homogeneous media. The flux q_i may be written in terms of the characteristics of the confining layer and the hydraulic head of the adjoining aquifer. Using Darcy's law

$$q_i = -K'\frac{\phi' - \phi}{D'} = -\frac{\phi' - \phi}{c} \tag{22}$$

where ϕ' is the hydraulic head in the adjoining aquifer, K' the hydraulic conductivity and D' the thickness of the confining layer. K' and D' are usually expressed as the resistance $c = D'/K'$. If ϕ' varies with time, q_i is also a function of time and Eqn 21 describes transient flow in a non-homogeneous, non-deformable, semi-confined aquifer.

An important class of problems describing essentially horizontal flow are based on the Dupuit-Forchheimer assumptions. Dupuit (1863) derived an equation for radial flow in an unconfined aquifer assuming that for small inclinations of the free water surface the streamlines may be taken as horizontal. Furthermore he assumed that along each vertical line the hydraulic head is equal to the height of the free water surface above the horizontal impermeable base (thus $\partial q_x/\partial z = \partial q_y/\partial z = 0$). Applying the equation of continuity to flow in any column with a free surface height h above the impermeable base, Forchheimer (1886) derived a general equation for flow in unconfined aquifers with water tables of low slope. The equation of continuity requires that

$$\frac{\partial}{\partial x}(hq_x) + \frac{\partial}{\partial y}(hq_y) = -\mu \frac{\partial h}{\partial t} \tag{23}$$

where μ is the 'drainable porosity' or 'specific yield', defined as the volume of water extracted from the groundwater per unit area and per unit descent of h. The Dupuit assumptions allow the equations of Darcy to be written as $q_x = -\bar{K}\partial h/\partial x$ and $q_y = -\bar{K}\partial h/\partial y$, which combined with Eqn 23 yield the equation of Boussinesq (1904)

$$\frac{\partial}{\partial x}\left(\bar{K}h \frac{\partial h}{\partial x}\right) + \frac{\partial}{\partial y}\left(\bar{K}h \frac{\partial h}{\partial y}\right) = \mu \frac{\partial h}{\partial t} \tag{24}$$

Although Muskat (1937) in a comprehensive discussion strongly took issue with the Dupuit-Forchheimer theory and preferred to await the development of a more satisfactory solution, the theory has become very popular because it is easy to apply. The errors resulting from the Dupuit-Forchheimer assumptions generally depend on the curvature of the free surface and tend to be larger for the approximated shape of the water table than for the calculated flow rates. For one particular flow problem Charny (see Polubarinova-Kochina, 1962) has shown that the Dupuit-Forchheimer assumptions lead to the exact solution for the rate of flow.

The right side of Eqn 24 represents the change in time of the total volume of water stored in a column of unit cross-sectional area due to a variation in the height of the water table. It has the dimension of a flux. The dimensionless parameter μ is a function of x, y and t. When the changes in h are small as compared with the thickness of the aquifer, $\bar{K}h$ may be considered as a function of x and y alone. Substituting the transmissivity $T = \bar{K}h$ into Eqn 24 yields a non-linear diffusion equation developed by Jacob (1950)

$$\frac{\partial}{\partial x}\left(T \frac{\partial h}{\partial x}\right) + \frac{\partial}{\partial y}\left(T \frac{\partial h}{\partial y}\right) = \mu \frac{\partial h}{\partial t} + \Sigma q_i \tag{25}$$

where the additional term $\Sigma q_i = q_1 + q_2 + q_3 + \ldots$ represents sources and sinks such as leakage through a confining layer, rainfall, pumpage, etc. The transmissivity T is a function of x and y, while q_i may vary with x, y and t. Positive values of q_i represent a sink, negative values a source function. For steady flow conditions the term $\mu\partial h/\partial t$ disappears and Eqn 25 reduces to a form similar to the equation for semi-confined flow (Eqn 21). These types of equation are known as Poisson equations.

2.3.2 Unsaturated flow

Considering flow in unsaturated porous media, the hydraulic conductivity becomes a function of the water content, expressible as $k = k(\theta)$, and the general equation of flow may be reproduced in the form

$$\frac{\partial \theta}{\partial t} = \nabla \cdot k(\theta)\{\nabla p + \rho g \nabla z\} \tag{26}$$

Equation 26 can be solved only if a unique relation exists between k and θ as well as between θ and p. Haines (1930) was among the first to report experimental evidence, using sand and uniform glass spheres, that $\theta(p)$ is not a single-valued function. In rigid soils unique relations between θ and p exist if the change in θ is monotonic, i.e. the moisture content is either continuously increasing or decreasing. Between these two extreme relations, known as the 'wetting' and 'drying' moisture characteristic, a family of so-called 'scanning'-curves determine the relation between θ and p dependent on the past history. Hysteresis effects in the relation between k and θ appear to be less sizable (Nielsen & Biggar, 1961; Elrick & Bowman, 1964; Top & Miller, 1966; Poulovassilis, 1969), but if k is expressed as k(p) hysteresis in the moisture characteristic is imposed on the relation between k and p.

To convert Eqn 26 into an equation with one dependent variable, the left side is written as

$$\frac{\partial \theta}{\partial t} = \frac{d\theta}{dp} \frac{\partial p}{\partial t} = C(p) \frac{\partial p}{\partial t} \tag{27}$$

where C(p) is defined as the specific moisture capacity. Writing Eqn 26 as a function of p, Richards (1931) derived the following equation for unsaturated flow in non-homogeneous, isotropic, porous media

$$C(p) \frac{\partial p}{\partial t} = \frac{\partial}{\partial x} (k(p) \frac{\partial p}{\partial x}) + \frac{\partial}{\partial y} (k(p) \frac{\partial p}{\partial y}) + \frac{\partial}{\partial z} (k(p) \frac{\partial p}{\partial z}) + \rho g \frac{\partial k(p)}{\partial z} \tag{28}$$

which is usually referred to as Richards' equation (Swartzendruber, 1969). The use of Eqn 28 is restricted to the class of problems in which the matric pressure changes monotonically, as it fails to take into account hysteresis effects in the relations k(p) and $\theta(p)$. A modified hysteretic version of Richards' equation has been proposed by Miller & Miller (1956), but its use is limited as hysteretic relationships are difficult to obtain in practice.

Buckingham (1907) has expressed Darcy's law in terms of θ with the introduction of

$$D(\theta) = k(\theta) \frac{dp}{d\theta} \qquad (m^2 \cdot s^{-1}) \tag{29}$$

which later Childs & Collis-George (1950) noted as being mathematically identical to a diffusion coefficient. Application of the soil-water diffusivity D requires that $dp/d\theta$ exists, which is not the case for saturated media where p varies and θ remains a constant. Richards (1931) suggested that writing Eqn 28 in terms of the other dependent variable θ is just a matter of mathematical expediency if p is a single-valued function of θ. However, ∇p can only be expressed in terms of $\nabla \theta$ when θ is continuous and thus the medium homogeneous. With reference to these restrictions, Eqn 28 written in terms of θ yields the transport-diffusion equation

$$\frac{\partial \theta}{\partial t} = \frac{\partial}{\partial x} (D(\theta) \frac{\partial \theta}{\partial x}) + \frac{\partial}{\partial y} (D(\theta) \frac{\partial \theta}{\partial y}) + \frac{\partial}{\partial z} (D(\theta) \frac{\partial \theta}{\partial z}) + \rho g \frac{\partial k(\theta)}{\partial z} \tag{30}$$

which was presented in this form by Philip (1957a). Equation 30 is a non-linear Fokker-Planck equation. The class of flow problems to which it in general refers is absorption and infiltration into homogeneous unsaturated soil. For one-dimensional horizontal flow and other instances where gravity may be neglected Eqn 30 reduces to the non-linear diffusion equation

$$\frac{\partial \theta}{\partial t} = \frac{\partial}{\partial x}\left(D(\theta)\,\frac{\partial \theta}{\partial x}\right) \qquad (31)$$

for which analytical and quasi-analytical solutions have been obtained (Philip, 1969).

A form of transport of water in porous media that has not been discussed is the water-vapour movement. Vapour movement is a process of diffusion rather than mass flow and may conveniently be included in the diffusivity term in the Fokker-Planck equation (Philip, 1957a). However, vapour movement becomes only a significant fraction of the total unsaturated transport when the soil is very dry and the rate of liquid flow close to zero (Rose, 1963a, 1963b). Hence vapour movement may be neglected (Miller & Klute, 1967). This conclusion is only warranted in view of the assumption made earlier that isothermal transport of a homogeneous liquid is considered. For conditions that are no longer isothermal, vapour diffusion becomes the dominant system in the total moisture transport in very dry soil (Philip, 1957b). Rosema (1974), following an approach of Philip & de Vries (1957), showed that for wet conditions Eqn 28 cannot be used to describe the diurnal change in the total moisture flux in the top layer of a bare soil. For an analysis of the simultaneous transport of water and heat from the point of view of irreversible thermodynamics the reader is referred to e.g. Cary & Taylor (1962) and Cary (1963, 1966).

2.4 METHODS FOR SOLUTION OF FLOW PROBLEMS

To solve problems of groundwater flow a system (real or abstract) is derived to simulate the operation of the prototype system with the limits of accuracy required by the problem under study (Dooge, 1973 and 1977). Such a simulation system is termed a model. The process of simulation is then the operation of the model to predict the response of the prototype system. In this sense, differential equations governing groundwater flow are models, and simulation of a groundwater flow system involves the solution of a differential equation. Mathematical models use analytical or numerical techniques to obtain this solution.

A mathematical model represents an abstract system. Real simulation systems include physical and analogue models. These direct simulation methods are first reviewed briefly. Mathematical models, which are of primary interest for this study, are discussed in more detail afterwards.

2.4.1 Direct simulation methods

Physical models comprise one-dimensional flow in soil columns and two or three

dimensional flow in sand tanks. The porous medium is usually homogeneous, isotropic and consists of artificial or natural granular material. For saturated flow the model is often a scaled-down version of the aquifer, which involves the use of scale factors. Since the same laws governing flow apply to both the model and the prototype system, physical models are in particular useful for comparison with theory. Application of sand tank models to regional flow problems have not been reported, probably due to the restrictions imposed by the scale factors (Prickett, 1975).

Analogue solutions of groundwater flow problems are based on the principle that systems belonging to an entirely different physical category are described by essentially the same equations as those governing flow in porous media. Similarity of Darcy's law to the equation for laminar flow of a viscous fluid through a circular tube has already been mentioned. A model for transient, unsaturated, vertical flow based on this analogy was built by Wind (1972). The model consists of a number of vessels each representing one soil layer. When appropriate scale factors are used, the shape of the vessel, its liquid content and level represent the moisture characteristic, moisture content and matric pressure, respectively. The non-hysteretic flow process is simulated by the flow of a viscous fluid through a number of tubes connecting the vessels. The model has been successfully used for flow in heavy soils with a high water-table and under wet conditions.

A viscous fluid analogue for saturated groundwater flow is the parallel plate model. This model is usually called Hele-Shaw model, because Hele-Shaw (1898) first noticed the analogy between the equation for two-dimensional laminar flow of a viscous fluid through a narrow interspace between two parallel plates and the equation of Laplace. It can be shown that Poiseuille's law applied to this flow system is the analogue to Darcy's law for groundwater flow (Lamb, 1932, p. 582). The model is used in vertical position to simulate two-dimensional steady or transient unconfined flow for a variety of boundary conditions (e.g. Awan & O'Donnell, 1972). Non-homogeneity of the porous medium is imitated by variations of the width of the interspace. In horizontal position the model has long been used to study steady confined and unconfined flow problems. Santing (1958) extended its use to simulate the diffusion equation with the introduction of a number of vessels on top of the model to imitate storage capacity. The model is suitable to simulate numerous groundwater flow problems including steady, transient, confined and unconfined flow in homogeneous or non-homogeneous media in the presence of sources and sinks, rainfall and evaporation. A disadvantage of the model lies in the fact that the transmissivities are constant in time and difficult to change once the model is constructed and the width of the interspace has been fixed. Viscous flow models are restricted to simulate two-dimensional flow problems. The models are difficult to construct and the complicated operation requires a temperature controlled environment.

The analogy of Darcy's law and Ohm's law governing the steady flow of an electrical current through a conductive medium has led to numerous electrical analogue models for groundwater flow. The model may be a continuous or discrete representation of the porous medium. Continuous systems are used to study steady groundwater flow problems. The conductive material may be an electrolyte in an insulated tank or solid material from which the conductive Teledeltos paper is most commonly used. The shape of the

conductive medium is a scaled-down version of the aquifer. Teledeltos paper is used to solve two-dimensional homogeneous flow problems. For the simulation of two-dimensional flow problems with liquid models non-homogeneity of the aquifer may be imitated by varying the bottom level of the tank. De Josselin de Jong (1962) combined two liquid tanks by a resistor network to study steady flow in two aquifers separated by a confining layer.

With a discrete electrical analogue model the properties of the porous medium are simulated by a network consisting of electrical elements. The network is a scaled-down version of the hydrologic prototype. At the nodes appropriate electrical voltages and current sources can be introduced to represent corresponding boundary conditions and sources or sinks. The electrical elements simulating transmission and storage are resistance and capacitance. Resistance network analogues are used to solve steady flow problems. Herbert (1968) showed that problems of two and three dimensional transient flow may be solved by a stepwise solution, considering the time-variant flow process as a succession of steady-states. This method is rather time consuming and introduces extra errors due to discretizing the time parameter. Transient flow problems are more conveniently handled with resistance-capacitance networks. Resistance-capacitance analogues are the most versatile analogue models for analysing sub-surface flow systems, but there is a limit to the complexity of the flow system they can handle (Bouwer, 1967). This refers in particular to the inclusion of transient unsaturated flow (Wind & Mazee, 1979).

Comparing results from analogue models with numerical solutions obtained with a digital computer, Prickett & Lonnquist (1969) concluded that digital methods are less time consuming for model construction and operation, and superior for non-linear problems. For the simulation of large groundwater flow systems requiring many time increments and a large core storage, analogue models are less costly to operate than digital models but the data handling is more difficult. This problem can be solved by combining resistance network and digital computer into a hybrid computer model. This allows the groundwater flow problem to be programmed as for a pure digital computer solution, but the non-linear partial differential equation is solved by a resistance network. Since the solution with the resistance network is almost instantaneously obtained it serves as a subroutine in the digital computer program which reduces the computational time drastically (Vemuri & Dracup, 1967).

Apart from viscous fluid and electrical analogue models there are several other simulation techniques based on analogy (Karplus, 1958) from which the stretched membrane analogue model is worth mentioning. The model consists of a thin rubber sheet stretched with uniform tension. The shape of the membrane due to a point load which represents a source or sink is governed by Poisson's equation. The tension of the sheet and the vertical deflections are analogous to aquifer transmissivity and hydraulic head variations, respectively. The model is simple and inexpensive when used to simulate steady flow problems of multiple wells in homogeneous aquifers. De Josselin de Jong (1961) pointed out that accurate solutions can be obtained with an optical technique for the observation of the simulated flow pattern.

2.4.2 *Mathematical models*

Mathematical models describe the prototype system by a set of algebraic formulas. The nature of the formula depends on the approach used to solve the groundwater flow problem. This approach may range from a pure black box analysis, via conceptual models to the mathematical physics approach. Strictly speaking, it is difficult to distinguish between the different approaches, since almost every mathematical model contains to a certain extent conceptual elements. The mathematical physics approach results in differential equations, and the particular forms of the general equation derived in Section 2.3 are generally accepted to belong to this category.

Mathematical models use analytical or numerical methods to solve the governing equation of flow. The solution requires that the geometry of the one, two or three dimensional region in which flow is considered is specified as well as the conditions that apply at the boundary of the flow domain. If at the boundary the value of the dependent variable is given, the boundary condition is known as the Dirichlet condition. Flux, or Neumann conditions refer to situations for which the flux (or zero flux) normal to the boundary is specified. If for different parts of the boundary different types of boundary conditions apply, the system is known as a mixed boundary value problem. The use of derivative boundary conditions for the solution of a steady-state flow problem requires that the net flow out of the flow domain equals zero. Moreover, to arrive at a unique solution for a typical Neumann problem an additional parameter is needed. Well-defined boundary conditions are sufficient to obtain a particular solution of a steady-state flow problem. But for the solution of a transient flow problem, the initial condition as well as changes in boundary values with time have to be specified.

Analytical methods

Much effort has been made to derive analytical solutions of flow problems. In general analytical solutions can only be obtained for homogeneous media and when sufficient simplifying assumptions are made. For saturated flow these have led to a great number of groundwater formulas. Well-known formulas are the Theis and Hantush equations for transient radial flow to a well. These equations are important for an approximation of the performance of wells and aquifer in the absence of sufficient data. For this purpose the properties of the aquifer and its boundary conditions are idealized. Imaginary wells are used to reproduce the same disturbing effects as the idealized geological boundary. A solution may then be obtained by using the principle of superposition for the effects of real and imaginary wells in an infinite aquifer (e.g. Walton & Neill, 1960).

A semi-analytical solution is obtained with the boundary element method (Brebbia, 1978). The boundary of the two-dimensional flow domain is divided into a series of elements. Van der Veer (1978) used a continuous distribution of sinks, sources and vortices over each element to generate a flow pattern in the domain. The solution found by enforcing the flow pattern to satisfy the boundary conditions, is obtained by numerical techniques and is exact in the region enclosed by an approximate boundary.

For the derivation of the Theis and Hantush formulas the Boltzmann substitution has

been used to transform the partial differential equation into an ordinary differential equation. This reduction in the number of independent variables is known as similarity substitution and is only useful if the variables removed from the equation are also removed from the governing conditions by the same substitution. The Boltzmann similarity substitution may also be used to solve the Fokker-Planck equation for unsaturated flow. This results in a semi-analytical solution for which an efficient numerical method was introduced by Philip (1955).

Pure analytical solutions which are found completely by mathematical analysis cannot be obtained for transient unsaturated flow unless some non-realistic assumptions are made. For instance, assuming D and k to be constants, the one-dimensional Fokker-Planck equation reduces to the linear diffusion equation

$$\frac{\partial \theta}{\partial t} = D \frac{\partial^2 \theta}{\partial x^2} \qquad (32)$$

for which solutions for a great number of boundary conditions are readily available (Crank, 1956; Carslaw & Jaeger, 1959).

For solving practical problems, analytical and semi-analytical methods are often unsuitable. However, from solutions obtained with such methods one can gain a better understanding of the fundamental structure of the flow problem than with an incidental numerical solution.

Numerical methods

The solution of differential equations governing flow may be approached numerically using a finite element or finite difference method. With finite element methods, the flow problem is either reformulated using variational calculus (e.g. the Rayleigh-Ritz method) or balanced using weighted residual principles (e.g. the method of Galerkin). For two-dimensional flow a solution is obtained by first sub-dividing the flow region into elementary sub-areas, the elements. The size of the elements may vary, the shape is usually triangular or quadrangular. The independent variable in the interior of the element is expressed in terms of its value at the corner points. Application of finite element methods results in a set of simultaneous equations. Various techniques to solve sets of simultaneous equations are discussed later in this section.

The finite element method is a quite recent development in the field of sub-surface hydrology (Zienkiewicz, 1967). Its relative merits compared with the 'classical' finite difference technique have to be further established, as the number of comparisons between both methods is still limited. A distinct advantage of the finite element method is the ability to generate easily any irregular grid to describe the flow domain. For a regular grid of triangular elements, the method yields for the two-dimensional equation of Laplace the same set of simultaneous equations as generated by a finite difference technique (Remson et al., 1971).

For a finite difference approach a grid has to be defined with dimensions depending

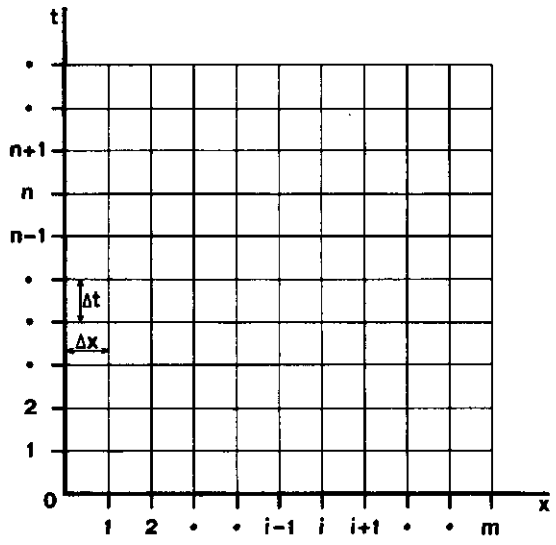

Fig. 1. The finite difference grid for Eqn 32 with distance x and time t.

on the number of independent variables that appear in the partial differential equation. If the one-dimensional diffusion equation (32) is taken as an example, the grid will have two co-ordinates: distance x and time t, as shown in Fig. 1. Every point in this finite difference grid corresponds to a specific point in space at a specific instant in time. It is convenient to choose a regular grid with constant Δt and Δx but this is by no means a requirement (e.g. Tyson & Weber, 1964). If the co-ordinates in the x,t plane are indicated by i and n, the solution at any given grid point or node (i,n) is θ_i^n. For n = 0 initial values for θ have to be given and if the flow domain is divided into m equal intervals, boundary conditions for i = 0 and i = m have to be specified for each time level n.

The finite difference approach replaces the derivatives of the partial differential equation by their finite difference analogue. This approach may lead to an explicit or implicit finite difference scheme. An explicit scheme is obtained if the time derivative is replaced by a forward difference approximation between the n and n+1 time level and the space derivatives are replaced by their finite difference analogues at the n time level. Applied to Eqn 32 this yields

$$\frac{\theta_i^{n+1} - \theta_i^n}{\Delta t} = D \frac{\frac{\theta_{i+1}^n - \theta_i^n}{\Delta x} - \frac{\theta_i^n - \theta_{i-1}^n}{\Delta x}}{\Delta x} \qquad (33a)$$

which can be written as

$$\theta_i^{n+1} = \theta_i^n + D \frac{\Delta t}{(\Delta x)^2} (\theta_{i-1}^n - 2\theta_i^n + \theta_{i+1}^n) \qquad (33b)$$

In Eqn 33b the unknown value of the dependent variable at time level n+1 is explicitly expressed in terms of known values at the time level n. To solve Eqn 33b Dirichlet con-

ditions have to be specified. Flux conditions involve an extra equation. For instance, if at the boundary x_m the flux q_m^n is specified an imaginary node is introduced as follows

$$D \frac{\theta_{m+1}^n - \theta_{m-1}^n}{2(\Delta x)} = q_m^n \tag{34a}$$

to be written as

$$\theta_{m+1}^n = \frac{2(\Delta x)}{D} q_m^n + \theta_{m-1}^n \tag{34b}$$

With the introduction of imaginary nodes when flux conditions are specified at the boundary, θ can be solved at the end of the first time increment through a repeated application of Eqn 33b. Once these values are computed, Eqn 33b is used again to move the solution forward by another time increment. Although the explicit finite difference scheme appears to be a simple straightforward technique, it has found little application in the field of sub-surface hydrology (Remson et al., 1971). The reason is that the method is unstable and leads to a meaningless solution due to the amplification of round-off errors, unless the inequality

$$\frac{D\,\Delta t}{(\Delta x)^2} < \frac{1}{2} \tag{35}$$

is satisfied (Richtmyer & Morton, 1967). Moreover, Eqn 35 is a requirement for the finite difference approximation to converge to the true solution when in the limit Δx and Δt approach to zero. Because stability and convergence criteria imposed on an explicit finite difference scheme often lead to unacceptable restrictions on the choice of Δx and Δt, an implicit scheme is usually preferred. Such a scheme is obtained if the time derivative is replaced by a backward difference approximation between the n-1 and n time level. If this scheme is applied to Eqn 32, the resulting equation

$$\frac{\theta_i^n - \theta_i^{n-1}}{\Delta t} = D \frac{\theta_{i-1}^n - 2\theta_i^n + \theta_{i+1}^n}{(\Delta x)^2} \tag{36}$$

contains three unknowns. If for the first time level Eqn 36 is written for each node, this results in (m-1) equations with (m-1) unknowns. Through a simultaneous solution of this set of equations values for θ at the first time level are obtained. The procedure is repeated to move the solution forward in time. The truncation of the Taylor series which is used to convert the partial differential equation into a finite difference form results in a truncation error. This error can be reduced with the Crank-Nicolson scheme, which uses the central time difference by approximating the space derivatives half way time level n-1 and n. The Crank-Nicolson approximation of the linear diffusion equation (32) is

$$\frac{\theta_i^n - \theta_i^{n-1}}{\Delta t} = D \frac{\frac{1}{2}(\theta_{i-1}^n - 2\theta_i^n + \theta_{i+1}^n) + \frac{1}{2}(\theta_{i-1}^{n-1} - 2\theta_i^{n-1} + \theta_{i+1}^{n-1})}{(\Delta x)^2} \tag{37}$$

The central (37) and backward (36) difference approximations lead to similar implicit schemes, which are unconditionally stable. The second order accuracy of the Crank-Nicolson scheme usually results in a faster convergence. The coefficient matrix which is obtained from Eqns 36 and 37 has a tridiagonal form. It is efficiently solved by a Gaussian elimination technique known as the tridiagonal algorithm.

If two space parameters (x,y) are involved the implicit finite difference approximation yields equations with five unknowns. Peaceman & Rachford (1955) proposed a method which enables the application of the tridiagonal algorithm for the two-dimensional problem. The method is known as the alternating direction implicit (ADI) method. It requires two advanced time levels for a complete application. Time level n is approached with an equation equivalent to Eqn 36 where the finite difference analogue of $\partial^2\theta/\partial y^2$ is evaluated at time level n-1. Next lines parallel to the x co-ordinate are solved, one at a time in the direction of increasing y. For the second step the treatment of the space parameters is the reverse, i.e. the finite difference approximation for $\partial^2\theta/\partial x^2$ is evaluated explicitly in terms of the known values at time level n and $\partial^2\theta/\partial y^2$ is expressed implicitly for time level n+1. The ADI technique is unconditionally stable and the resulting coefficient matrix for each line has the advantageous tridiagonal form. According to Rushton (1974), singularities in the flow domain may impose restrictions on the use of the method. Many successful applications in the field of saturated (e.g. Pinder & Bredehoeft, 1968) as well as unsaturated (e.g. Rubin, 1968) groundwater flow have been reported. The ADI technique can be extended to solve three-dimensional problems (Douglas & Gunn, 1964).

The finite difference and finite element methods have in common that they both give rise to a set of linear (or linearized) equations. For the solution of a system of simultaneous equations direct and iterative methods may be used. A direct method is the above-mentioned tridiagonal or Thomas algorithm, which can be applied to coefficient matrices that show a tridiagonal form. This algorithm effectively reduces the implicit scheme to two explicit schemes. It is obtained through a decomposition of the coefficient matrix into a lower triangular matrix and an upper triangular matrix. First the lower triangular matrix is solved by forward substitution and then the upper triangular matrix is solved by backward substitution. Since this method greatly reduces the number of computational steps when compared with other Gaussian elimination methods it is economical with respect to computer costs (Isaacson & Keller, 1966). Applications of the tridiagonal algorithm in the field of sub-surface hydrology are numerous, e.g. Hanks & Bowers (1962), Liakopoulos (1965), Rubin (1969), Jensen & Hanks (1967), Freeze (1969).

Most of the sub-surface flow equations are non-linear. Only if the coefficients of the derivatives in the differential equation are a function of the dependent variable does the implicit finite difference scheme generate a set of non-linear difference equations. This applies in particular to equations describing unsaturated flow in which functions appear such as $k(\theta)$, $D(\theta)$ and $C(p)$. Since direct methods solve the coefficient matrix only once to advance the solution from time level n to n+1, the values of the dependent variable at the advanced time level cannot be used to obtain the average values of the coefficients. The most obvious and simple approach is the use of coefficients evaluated for the known value of the dependent variable at time level n. Since

the values of the coefficients often change rapidly with a small variation in the value of the dependent variable, this results in a loss of accuracy unless small time steps are employed. The linearization technique may be improved if extrapolated values of the dependent variable from previous time levels are used to estimate the values of the coefficients. This technique used by Rubin & Steinhardt (1963) is less suitable for systems where the value of the dependent variable is not monotonically increasing or decreasing. Douglas & Jones (1963) proposed a predictor-corrector technique which is particularly suited to mildly non-linear, one-dimensional, parabolic differential equations. The method is stable when used in combination with the tridiagonal algorithm. It involves two applications of the Crank-Nicolson scheme. The first step, known as the predictor, solves the system of equations for time level $n+\frac{1}{2}$. This facilitates the evaluation of the coefficients at this time level. For the second step, known as the corrector, the Crank-Nicolson scheme is applied to advance the solution from time level n to n+1, using the predicted values of the coefficients at time level $n+\frac{1}{2}$. With hysteresis the non-linearity may render the solution unstable and less accurate. Predictor-corrector techniques have been used by e.g. Molz & Remson (1970), Hornberger et al., (1970), Hornberger & Remson (1970). A disadvantage of the method is that it requires twice as much computer time. Even more time-consuming is a method used by Klute et al. (1965) where the system of equations is repeatedly solved to improve the values of the coefficients in the non-linear equations.

With complicated problems or when the non-linearities are more pronounced, iterative methods are preferred to the direct Gaussian elimination technique. Moreover, iterative methods are the only means to solve coefficient matrices which result from differencing elliptic equations. If the linear two-dimensional Laplace equation (19) is taken as an example, the most simple Jacobi iterative scheme which results from differencing this elliptic equation is written (with $\Delta x = \Delta y$) as

$$\phi_{i,j}^{r+1} = (\phi_{i-1,j}^{r} + \phi_{i+1,j}^{r} + \phi_{i,j-1}^{r} + \phi_{i,j+1}^{r})/4 \tag{38}$$

where r is the iteration index and i,j indicates the location or the node in the x,y plane. For the solution of an elliptic problem an initial guess for $\phi_{i,j}^{0}$ is required to start the iteration. If the scheme is executed in a specific order, earlier improved values of ϕ can be used to speed up the rate of convergence. This technique is known as Gauss-Seidel iteration and can be written for Eqn 19 as

$$\phi_{i,j}^{r+1} = (\phi_{i-1,j}^{r+1} + \phi_{i,j-1}^{r+1} + \phi_{i+1,j}^{r} + \phi_{i,j+1}^{r})/4 \tag{39}$$

The rate of convergence is greatly improved with a scheme known as the successive over-relaxation (SOR) method. It uses an acceleration parameter ω and can be written for Eqn 19 as

$$\phi_{i,j}^{r+1} = (1 - \omega)\phi_{i,j}^{r} + \frac{\omega}{4}(\phi_{i-1,j}^{r+1} + \phi_{i,j-1}^{r+1} + \phi_{i+1,j}^{r} + \phi_{i,j+1}^{r}) \tag{40}$$

where generally $1 \leq \omega \leq 2$. For certain problems an optimum value for ω may be obtained from theoretical considerations, for other problems empirical formulas or trial and

error procedures have to be used. Many applications of point-iterative methods (Gauss-Seidel and SOR) to transient and steady flow problems have been reported in literature. They include saturated (e.g. Remson et al., 1965; Freeze & Witherspoon, 1966; Taylor & Luthin, 1969) as well as unsaturated (e.g. Watson, 1967; Ibrahim & Brutsaert, 1968; Wisler et al., 1968) flow conditions.

Instead of improving the value of the dependent variable for each node independently, a block or line successive over-relaxation (LSOR) method may be used. If LSOR is applied to the two-dimensional problem (19), the iterative scheme for each horizontal line of the x,y difference grid can be written as

$$\phi_{i,j}^{r+1} = (1 - \omega)\phi_{i,j}^{r} + \frac{\omega}{4} (\phi_{i-1,j}^{r+1} + \phi_{i+1,j}^{r+1} + \phi_{i,j-1}^{r+1} + \phi_{i,j+1}^{r}) \qquad (41)$$

The system of equations generated with Eqn 41 is efficiently solved with the tridiagonal algorithm, since $\phi_{i,j-1}^{r+1}$ is known from previously obtained values for the nodes on line j-1.

A more implicit solution is obtained with the alternating direction implicit procedure (ADIPIT), the iterative variant of the ADI method. Each iteration cycle consists of solving simultaneous sets of equations for rows and then for columns. The rate of convergence greatly depends on the choice of the acceleration parameter which varies in a cyclic manner (Wachspress, 1966). Applications of LSOR and ADIPIT methods have been reported by e.g. Bredehoeft & Pinder (1970), Prickett (1975), Vauclin et al. (1975).

With the above-mentioned techniques, stable and convergent solutions can be obtained for relatively simple, non-linear flow problems. For complicated problems Stone (1968) proposed a more powerful technique known as the strongly implicit procedure (SIP). However difficulties arise when the finite difference approach is used to solve multi-dimensional, saturated-unsaturated flow problems for heterogeneous media or where the geometric boundary of the flow domain is irregular (Vachaud et al., 1975). These difficulties do not occur with the application of the finite element technique. This method is flexible for use in an irregular flow domain and allows at the boundary a change from Dirichlet to Neumann conditions during a single time increment.

A recent numerical approach, commonly referred to as numerical simulation is used to solve transient one-dimensional unsaturated flow problems. For this purpose the soil column is divided into a number of layers. To each separate layer and for a small time increment, Darcy's law and the principle of continuity are applied. This results in the calculation of a flux which is used to compute a new value for the moisture content of each layer. Since all flow rates are calculated independently of each other the procedure is essentially an explicit method to which the earlier mentioned restrictions apply. Kastanek (1971, 1973) proposed a numerical simulation technique in which the number of layers varies automatically in accordance with the changing moisture profile. De Wit & van Keulen (1972) and van Keulen (1975) used a special computer language developed by IBM, the Continuous System Modelling Program (CSMP), which greatly reduces the programming effort.

Numerical methods have proved to be an important tool in the solution of complicated flow problems. Nevertheless, mathematical analysis of flow processes is of importance to gain a better understanding of the structure of the solution and for comparison with results obtained through a numerical approach. Analytical or semi-analytical methods are particularly useful when a first estimate of quantitative aspects of a flow system is required.

Analogue methods are used to solve a wide variety of flow problems. The construction of a resistance-capacitance network does not necessarily require more time than the setup of a numerical computer program. Analogue models are less costly to operate, but computer methods are more efficient in handling input and output of data. The size of the core memory of the computer and the running costs are limiting factors in the application of numerical methods to large problems (Freeze & Witherspoon, 1968). However these limits are rapidly extending due to advances in the field of computer technology. As computer programs are easily changed and adapted to other problems, they are in many cases considered superior to direct simulation methods.

3 Saturated-unsaturated flow

3.1 THE TRADITIONAL APPROACH

As a result of the traditional approach to treat flow in porous media of which part is saturated and part unsaturated separately, an interface between both flow systems must be defined. For this purpose the level in the soil where the pressure is atmospheric, known as free water level, water table or phreatic surface is most commonly used. It has the advantage that it is easily measured in the field and constitutes a flow line when there is steady flow without accretion from the overlying unsaturated region. The actual saturated zone extends to a little above the free water level due to capillary rise. The region of complete saturation above the water table was originally termed capillary fringe ('capillaire zone') by Versluys (1916). The height of the capillary fringe depends on the air entry value, i.e. the negative pressure at which the soil begins to desaturate. Gradually a less well-defined definition has come into use to include the height above the water table at which desaturation becomes considerable or even to include the entire region of unsaturated flow. Some textbooks on groundwater flow (e.g. Verruijt, 1970; Bear, 1972) misuse the term 'capillary rise' for the height of the capillary fringe. Capillary rise refers to a phenomenon (Breaster et al., 1971) and the height of capillary rise is a quantity used with respect to well-prescribed conditions of unsaturated flow (Wesseling, 1957).

When solving saturated groundwater flow problems, the phreatic level is usually taken as the upper boundary of the flow domain, disregarding water movement in the overlying unsaturated zone. Since the conductivity in the region just above the water table is approximately equal to the saturated hydraulic conductivity, some authors (e.g. Youngs, 1969) include the capillary fringe in the flow domain. However the height of the capillary fringe is generally small compared with the saturated thickness of the aquifer and for practical purposes the phreatic level is taken as the upper boundary of the saturated region.

Another concept inherent to the separate approach to saturated-unsaturated flow is specific yield. It is often defined as the volume of water released from a soil column of unit area, extending from the water table to the soil surface if the water table is lowered a unit distance. For the analysis that follows it is necessary to define more precisely the fluxes in the vicinity of a moving water-table.

Consider a change in the position of the phreatic level $\Delta h = h_2 - h_1$ during a single time increment Δt, and assume that flow in the unsaturated soil column is in vertical direction only (Fig. 2). The average flux during the time increment across the soil surface at a height h_s above datum level, is denoted by q_s (positive upwards). In an attempt to define similarly the flux across the water table, difficulties arise as its position

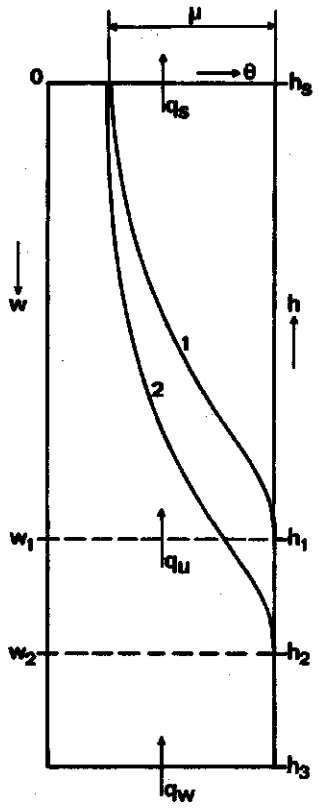

Fig. 2. The different levels at which the vertical fluxes are defined. The numbers (1) and (2) indicate possible soil moisture distributions corresponding to the water-table elevations h_1 and h_2, respectively.

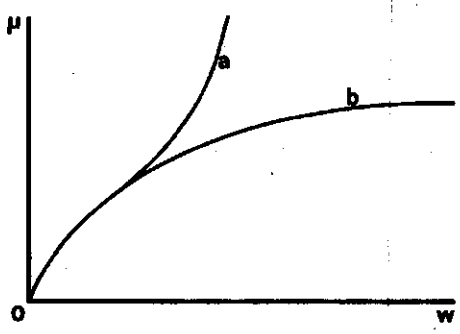

Fig. 3. Typical relations between the specific yield μ and the depth of the water table w for the situation that water is released from an initially saturated column at a steady rate across the soil surface (Curve a) or at a steady rate across the water table (Curve b).

is not stationary. If storage changes occur between the levels h_1 and h_2, the flux across the initial level h_1 is definitely not equal to the flux across the final level h_2. To avoid ambiguities due to a moving water-table, a third level h_3 is defined just below h_2, so that $h_2 - h_3$ is very small. The flux q_w across the lower level h_3 is taken as 'the flux across the water table'. Disregarding horizontal flow components in the small region just below the water table, the flux across level h_2 is equal to q_w.

According to the definition given above, the specific yield μ may be formulated as

$$\mu = (q_w - q_s)\ \Delta t/\Delta h \qquad (42)$$

Fig. 3 shows typical relations between the specific yield μ and w, the depth of the water table below soil surface. Curve a represents the situation when water is released from an initially saturated column at a steady rate across the surface ($q_w = 0$), and Curve b for a steady rate across the water table ($q_s = 0$). In the field of saturated groundwater flow, the definition of specific yield is generally meant to refer to the latter situation where in isotropic, homogeneous soils μ approaches an approximate constant value when the water table is sufficiently deep. When solving unconfined flow problems the specific yield is usually considered as a constant property, characteristic of the aquifer. Its value is taken equal to the average air content at the soil surface (Fig. 2, where for the situations (1) and (2) equilibrium conditions are assumed). The fallacy of

this approach for rapid fluctuations or shallow water-tables has been pointed out by Childs (1960) and is extensively discussed by dos Santos & Youngs (1969).

For the solution of unconfined flow problems that take into account flow from or to the unsaturated zone, μ is usually defined as

$$\mu = (q_w - q_u)\ \Delta t/\Delta h \tag{43}$$

where q_u (Fig. 2) represents the flux into the unsaturated zone (positive) or recharge at the phreatic surface from the overlying unsaturated region (negative). The definition of μ with Eqn 43 is equivalent to that with Eqn 42 if the level h_1 is taken at the soil surface. In practice, the level for h_1 is chosen such that q_u approaches a constant value equal to the long term average flux across the soil surface. This yields an approximate constant value of μ, which facilitates the solution of equations for saturated unconfined flow.

Writing Eqn 43 in differential form for two space dimensions gives

$$\mu \frac{\partial h}{\partial t} + q_u = q_w(x,y,t,h) \tag{44}$$

where μ and q_u may be functions of x, y and t. If for convenience, q_u is considered as the only source or sink function, the right side of Eqn 25 may be replaced by Eqn 44 to yield

$$\frac{\partial}{\partial x}\left(T(x,y)\ \frac{\partial h}{\partial x}\right) + \frac{\partial}{\partial y}\left(T(x,y)\ \frac{\partial h}{\partial y}\right) = q_w(x,y,t,h) \tag{45}$$

Equation 45 describes steady flow in a non-homogeneous unconfined aquifer. Transient flow may be approached by a succession of steady-state situations (Muskat, 1937). If the time dependent function q_w is given for each time step, the use of Eqn 45 does not require the concept of specific yield.

It should be realized that the exact formulation of the saturated unconfined flow problem is far more complicated. When considering three-dimensional flow in an isotropic unconfined aquifer, the geometry of the phreatic surface is a priori unknown. After Verruijt (1970, p. 171), the continuity equation for a small element along the free surface may be written as

$$\mu \frac{\partial h}{\partial t} = q_z - q_u - q_x \frac{\partial h}{\partial x} - q_y \frac{\partial h}{\partial y} \tag{46}$$

where $q_{x,y,z}$ represents the specific discharge in the appropriate co-ordinate direction, q_u the upward flux into the unsaturated zone and h is the z co-ordinate of the free surface. Since the hydraulic head $\phi(x,y,z,t) = z + p/\rho g$ and $p = 0$ at the free surface it follows for $z = h$ that

$$\phi(x,y,h,t) = h \tag{47}$$

or

$$h = \phi(x,y,h(x,y,t),t) = \phi(x,y,z,t)\Big|_{z=h} \tag{48}$$

Partial differentiation of h yields

$$\frac{\partial h}{\partial x} = \frac{\partial \phi}{\partial x} + \frac{\partial \phi}{\partial z}\frac{\partial h}{\partial x} \quad \text{or} \quad \frac{\partial \phi}{\partial x} = \frac{\partial h}{\partial x}\left(1 - \frac{\partial \phi}{\partial z}\right) \tag{49a}$$

$$\frac{\partial h}{\partial y} = \frac{\partial \phi}{\partial y} + \frac{\partial \phi}{\partial z}\frac{\partial h}{\partial y} \quad \text{or} \quad \frac{\partial \phi}{\partial y} = \frac{\partial h}{\partial y}\left(1 - \frac{\partial \phi}{\partial z}\right) \tag{49b}$$

$$\frac{\partial h}{\partial t} = \frac{\partial \phi}{\partial t} + \frac{\partial \phi}{\partial z}\frac{\partial h}{\partial t} \quad \text{or} \quad \frac{\partial \phi}{\partial t} = \frac{\partial h}{\partial t}\left(1 - \frac{\partial \phi}{\partial z}\right) \tag{49c}$$

Substituting Darcy's law (11) for the specific discharges into Eqn 46 gives for the elevation $h = h(x,y,t)$ of the moving free surface

$$\mu \frac{\partial h}{\partial t} = K \frac{\partial \phi}{\partial x}\frac{\partial h}{\partial x} + K \frac{\partial \phi}{\partial y}\frac{\partial h}{\partial y} - K \frac{\partial \phi}{\partial z} - q_u \tag{50}$$

Multiplying Eqn 50 by $\left(1 - \frac{\partial \phi}{\partial z}\right)$ and substituting Eqn 49 yields the boundary condition at the free surface

$$\mu \frac{\partial \phi}{\partial t} = K\left(\frac{\partial \phi}{\partial x}\right)^2 + K\left(\frac{\partial \phi}{\partial y}\right)^2 + K\left(\frac{\partial \phi}{\partial z}\right)^2 - K\left(\frac{\partial \phi}{\partial z}\right) - q_u\left(1 - \frac{\partial \phi}{\partial z}\right) \tag{51}$$

Equation 51 and the equation for saturated flow, rewritten as

$$\nabla \cdot (K \nabla \phi) = 0 \tag{52}$$

have to be solved simultaneously, subject to appropriate boundary conditions at the fixed frontiers to determine $\phi(x,y,z,t)$ everywhere in the flow domain. Since solutions are only possible in a very limited number of cases, the Dupuit-Forchheimer assumptions are generally applied to exclude the vertical flow component. The advantages are that the number of independent variables is reduced by one and the solution of the resulting equation (the equation of Boussinesq (24)) directly yields the position of the free surface. However the equation is still non-linear and two-dimensional analytical solutions have not been obtained. A numerical approach was presented by Lin (1972) resulting in a complex finite difference scheme which is efficiently solved using the ADI technique.

There are several methods to linearize either the equation of Boussinesq or the free surface boundary condition (51). A linearization technique often applied to problems where the change in h is small compared with the total thickness of the aquifer, replaces $\overline{Kh}$ by the average transmissivity T, resulting in the diffusion equation (25) which is linear in h. The objections to the use of the diffusion equation to saturated-unsaturated flow problems result from the following simplifications:

1. the assumptions made to facilitate a numerical solution (Dupuit-Forchheimer approximation and linearization),

2. the flow is restricted to the saturated domain,
3. the change in volume of water per unit area per unit change in head is instantaneous and constant,
4. the flux q_u is independent of the saturated flow system.

The objections are less severe or disappear for flow in horizontal, thick aquifers in which the water table is sufficiently deep (say more than 5 m below soil surface) and where fluctuations in the position of the free water level are small and slow. However, with transient flow to a gravity well (pumping test) and flow in shallow water-table aquifers, the above assumptions are seriously violated. Since Theis (1935) derived an exponentional integral for non-steady flow to a well in a homogeneous, isotropic aquifer which is pumped at a steady rate, Theis' formula has extensively been used to determine the formation constants (μ and T). It has long been recognized that, as a result of the rapid drawdown in the vicinity of the well just after pumping has started, deviations from Theis' non-equilibrium curve occur. According to Walton (1960) the specific discharge at the very early stages of pumping in an unconfined aquifer is small due to a delay in yield (slow drainage) and merely results from a compression of the aquifer and expansion of the water. During the next stage the delayed yield reaches the water table and the aquifer behaves as a semi-confined aquifer tending to equilibrium conditions. At late time μ approaches a constant value and the time drawdown curve merges with Theis' non-equilibrium curve.

In this connection Boulton (1955, 1963) introduced the concept of 'delayed yield'. He assumed that part of the specific yield, μ_A is instantaneous and that a part μ_B, resulting from a unit drawdown at time τ reaches the water table according to the empirical formula $\alpha\mu_B \exp\{-\alpha(t - \tau)\}$, where $t > \tau$ and $1/\alpha$ is the delay index, an empirical constant often expressed in minutes or hours. When water is extracted from a well in an unconfined aquifer, the flux q_w resulting from the drawdown of the water table is given by

$$q_w = \mu_A \frac{\partial h}{\partial t} + \alpha\mu_B \int_0^t \frac{\partial h}{\partial \tau} e^{-\alpha(t-\tau)} d\tau \qquad (53)$$

and the delay in yield causes $q_w = q_w(t)$. Although Boulton's convolution integral is a valuable tool for pumping test evaluation it has received its share of criticism. Boulton (1963) conceded that the method is only capable of expressing μ as a function of time and does not predict the variation with distance to the well. Since the effects of vertical hydraulic gradients and slow drainage are both lumped into the empirical coefficient α, which is 'devoid of any apparent physical meaning' (Neuman, 1972), the discussion on which phenomenon is predominant in the delayed water-table response has not yet ceased. Moreover it has been shown that the characteristic term for slow drainage may also be derived without the assumption of delayed yield (Streltsova, 1972; Neuman, 1972; Cooley & Case, 1973).

Saturated groundwater flow involving shallow water-tables has been extensively studied with respect to drainage of agricultural lands. Most of the studies were restricted to the falling water-table case with or without recharge from rainfall (e.g. Edelman, 1947; Kirkham & Gaskell, 1951; Kraijenhoff van de Leur, 1958; Isherwood, 1959; Maasland, 1959). Laboratory experiments carried out by Luthin & Worstell (1956) and

Vachaud et al. (1973) clearly showed the variable nature of μ. Where with pumping tests this variability merely results from the rapid drawdown of the free water level, the specific yield in the shallow water-table case rather depends on the depth of the water table below surface. For this reason Brutsaert et al. (1961) proposed an approximate solution which treats μ as a function of the elevation of the free water level.

The traditional approach to unsaturated flow considers transport of soil moisture in the vertical direction only. Most of the papers deal with infiltration into a homogeneous, semi-infinite medium. The unsaturated zone extends from the soil surface to a depth at which the moisture content may be considered as time-invariant, while the phreatic surface is assumed at infinite depth.

Papers on unsaturated flow that include a water table, which are particularly of interest for this study, are much less numerous. Exact analytical solutions have not been presented. A few approximate solutions were obtained for the drainage of an initially saturated soil column. Gardner (1962) assumed the moisture content to be a linear function of the hydraulic head and Youngs (1960) and Youngs & Aggelides (1976) assumed a constant specific yield. Childs & Poulovassilis (1962) have presented a solution to the shape of a falling water-table moving with a constant velocity. Capillary rise from a water table has been solved for steady-state situations (Wind, 1955; Wesseling, 1957; Gardner, 1958) or by linearization (Philip, 1966). The first numerical solution to one-dimensional vertical flow was presented by Klute (1952). Since then many numerical models for flow in the unsaturated zone have been published, but very few use the water table as the lower boundary and until 1968 none of these models included interaction with the underlying saturated zone.

3.2 THE RIGOROUS APPROACH

Although Richards' equation applies to transient flow in a rigid system above as well as below the water table, the differences in the nature of the flow are reasons to treat saturated and unsaturated flow separately. In the unsaturated zone the hydraulic gradient in the horizontal direction is usually a negligible fraction of the gradient in the vertical direction since the boundary conditions at the soil surface (rainfall, evaporation) are relatively uniform over large areas. Consequently flow is predominantly vertical, often governed by large gradients in the matric pressure in combination with a low hydraulic conductivity. Below the water table the soil is saturated and matric pressure gradients do not exist, while the hydraulic conductivity is always at its maximum. In many saturated flow systems the hydraulic gradient in the vertical direction may be neglected and flow is predominantly horizontal, governed by gravity. Hence, the advantage of a separate treatment is that, for unsaturated flow, it is often sufficient to solve the one-dimensional form of Richards' equation, where for saturated flow the relatively simple two-dimensional form of the (linearized) Boussinesq equation can be used. A disadvantage is that effects of unsaturated flow on unconfined groundwater flow, as studied by Kraijenhoff van de Leur (1962) in a scaled granular model cannot be considered. Moreover from a fluid dynamic point of view the water table is an artificial

boundary and the necessity of a unified approach to saturated-unsaturated flow was stressed long ago (e.g. Childs, 1960; Stallman, 1961). There have been a number of multi-dimensional steady-state solutions to saturated-unsaturated flow problems, which are obtained by analogue models (e.g. Bouwer & Little, 1959) and numerical methods (e.g. Reisenauer, 1963; Luthin & Taylor, 1966; Amerman, 1976). For a transient analysis Richards' equation can be used or a combination of equations for saturated and unsaturated flow which in some way or another have to be linked. For the simulation of non-steady flow, viscous analogue models cannot be used because of the non-linear relationships C(p) and k(p). A solution of Richards' equation for saturated-unsaturated flow systems with an electrical analogue would be extremely difficult and, if ever possible, very expensive. In the absence of analytical solutions numerical methods are the only means to solve transient saturated-unsaturated flow problems. This approach was first applied by Rubin (1968), who solved transient drainage of a partly saturated slab of soil into a ditch, a classical problem, known as the ditch drainage case or falling water-table case. Rubin used the two-dimensional form of Richards' equation (28) and expressed the flow problem in the vertical plane in terms of the hydraulic head as

$$C(p)\,\frac{\partial \phi}{\partial t} = \frac{\partial}{\partial x}\left(k(p)\,\frac{\partial \phi}{\partial x}\right) + \frac{\partial}{\partial z}\left(k(p)\,\frac{\partial \phi}{\partial z}\right) \qquad (54a)$$

The flow system is schematically shown in Fig. 4. The height of the slab is D and the length 2L, but because of symmetry only half the slab is considered. The origin of the co-ordinates x and z are assumed in the lower left corner. The slab rests on an impermeable base. Initially the water table is at a height z_i and equilibrium conditions are assumed everywhere in the flow region. It follows for the initial condition at $t = 0$ that

$$\phi = z_i \qquad 0 \leq x \leq L \qquad 0 \leq z \leq D \qquad (54b)$$

For $t > 0$ the water level in the ditches is lowered to a height z_w and remains constant. In the absence of infiltration and evaporation the soil surface as well as the bottom of the slab act as an impermeable boundary. From symmetry consideration this is also true for the vertical boundary at $x = L$. Since a seepage face is allowed to develop three

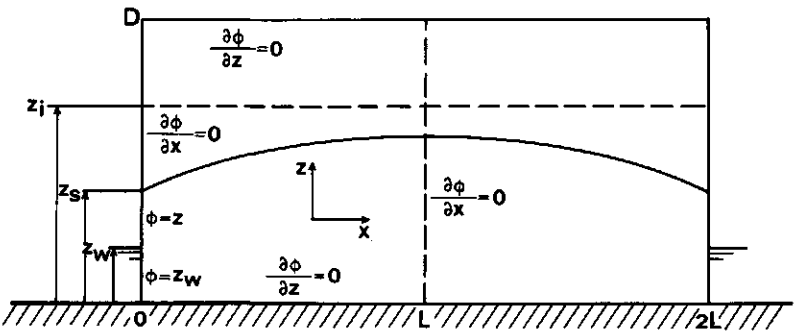

Fig. 4. Schematic presentation and boundary conditions of the falling water-table case.

types of boundary conditions exist at $x = 0$. Between the top of the seepage face and the soil surface the matric pressure is negative and outflow is impossible, hence this part acts as an impermeable boundary. At the seepage face the matric pressure is atmospheric, so the hydraulic head ϕ equals the height z above the impervious base. Below the water level in the ditch the hydraulic head equals z_w. It follows that the boundary conditions for $t > 0$ may be formulated as

$$\frac{\partial \phi}{\partial z} = 0 \qquad 0 \leq x \leq L \qquad z = 0 \quad \text{and} \quad z = D \qquad (54c)$$

$$\frac{\partial \phi}{\partial x} = 0 \qquad 0 \leq z \leq D \qquad x = L \qquad (54d)$$

$$\frac{\partial \phi}{\partial x} = 0 \qquad z_s \leq z \leq D \qquad x = 0 \qquad (54e)$$

$$\phi = z \qquad z_w \leq z \leq z_s \qquad x = 0 \qquad (54f)$$

$$\phi = z_w \qquad 0 \leq z \leq z_w \qquad x = 0 \qquad (54g)$$

Difficulties in solving the flow problem (54) do not only arise from its non-linearity. The governing equation is parabolic in the unsaturated zone and of an elliptical type in the saturated region, where $C(p) = 0$. The position of the free surface separating both regions is time dependent. Moreover, the height of the seepage face is a priori unknown and constitutes part of the solution. A forward finite difference scheme that determines the position of the water table explicitly seems to be obvious. Taylor & Luthin (1969) used an explicit scheme for the unsaturated part of the soil when solving an axisymmetrical flow problem towards a well that completely penetrates the aquifer and discharges at a constant rate. The boundary conditions are similar to those used by Rubin (1968) except for the outer radius where a constant head is assumed. An additional problem is the water level in the well which is continuously adjusted to yield the prescribed discharge. Application of the explicit finite difference scheme for nodes for which $p \leq 0$ yields values for θ and ϕ and is followed by a solution of ϕ for nodes for which $p > 0$ using SOR. The exact position of the free surface follows from a linear interpolation between nodes at which p changes sign. The position of the seepage face at the well is obtained from extrapolation of the free surface. The calculations are repeated for an adjusted water level in the well if the computed outflow differs too much from the prescribed discharge.

Explicit numerical methods were not used by other investigators to solve saturated-unsaturated flow problems, because they require for stability reasons a small mesh size especially in the unsaturated zone in the vicinity of the well. It was found that the length of the time step should be small enough to restrict the change in hydraulic head during the step to values less than 1 mm. Rubin (1968) and later Vachaud et al. (1975) solved the ditch drainage case with an iterative alternating direction implicit procedure (ADIPIT) in which the values of k are evaluated at the old time level while C is time centered. The method is restricted to flow in homogeneous systems and not suitable for infiltration problems in the presence of a sharp wetting front. The unknown position

of the seepage face requires an adjustment if after a complete set of iterations the computed ϕ values indicate an upward or sideward flow away from the seepage zone. Vachaud/Vauclin et al. (1975) compared their numerical simulation favourably with laboratory experiments. The results indicated that the decline of the water table, the total volume of outflow and the duration of the transfer are seriously affected by flow in the unsaturated zone.

Verma & Brutsaert (1970) tried a number of implicit methods (including ADIPIT) to solve the ditch drainage case. They found that the unknown position of the free surface and the unknown length of the seepage face rather than the non-linearity of the flow equation were most critical in causing slow convergence, especially for more realistic problems in which the unsaturated zone was not entirely in or near the capillary fringe. The implicit scheme they finally adopted is preceded by an explicit step to predict θ in the unsaturated region. The finite difference corrector, implicit in ϕ, results in a set of simultaneous linear equations which are solved by Gaussian elimination. Next the position of the free surface and the θ values are compared with values obtained from the explicit step. If they are found different, a smaller value of Δt is used or the length of the seepage face is adjusted. It is obvious that the use of a direct method to solve the coefficient matrix reduces the computation time as compared with iterative methods. The authors did not indicate the effect of the explicit step on the maximum length of Δt to be used.

A less rigorous approach to the ditch drainage case was reported by Hornberger et al. (1969). The implicit finite difference scheme of Remson et al. (1967) was used, which was solved with a Gauss-Seidel iteration. Non-realistic boundary conditions were imposed on a small flow system (0.3 m × 0.5 m); a constant hydraulic head at the vertical lateral boundaries, ignoring the development of a seepage face. Small time increments and lengthy computations were required because no attempt was made to predict the position of the free surface. From comparison with models that do not take into account the unsaturated zone, the authors concluded that unsaturated flow does not have a significant effect on the position of the water table.

Guitjens & Luthin (1971) studied the effect of hysteresis in the soil moisture characteristic on the drawdown and recovery of a water table in an unconfined aquifer. The boundary conditions of their axisymmetrical problem are similar to those used by Rubin (1968) except for the outer radius where a constant hydraulic head is employed. The steady-state drawdown becomes the initial situation for the recovery cycle. Hysteresis is included with the method of independent domains as explained in more detail by Poulovassilis (1962). The flow equation is approximated with a backward finite difference scheme which is solved with the Gauss-Seidel iterative procedure. Computations at the well wall only include points above the water level in the well. Positive values found for p at the well wall are put to zero which yields the seepage face. The authors concluded that the effects of hysteresis on water-table recoveries are negligible.

The solved problems discussed so far all deal with two-dimensional plane or axisymmetrical saturated-unsaturated flow in shallow water-table aquifers. Their common interest concerns the effect of the unsaturated zone on unconfined groundwater flow and

the general conclusion is that this effect is more pronounced for rapid drawdown or in the presence of steep gradients of the free water level.

To investigate the delayed response of the water table in an aquifer that is pumped at a constant rate, Cooley (1971) developed a finite difference model for axisymmetrical flow to a well that includes the unsaturated zone and takes into account the compressibility of water and soil in the saturated region. For this purpose the general equation (13) is rewritten without neglecting possible changes in ρ and the porosity n as

$$\nabla \cdot (\rho K \nabla \phi) = \frac{\partial}{\partial t} (\rho n s_w) \tag{55}$$

where s_w is the degree of water saturation. Expanding the term on the right of Eqn 55 yields

$$\frac{\partial}{\partial t} (\rho n s_w) = \rho n \frac{\partial s_w}{\partial t} + \rho s_w \frac{\partial n}{\partial t} + n s_w \frac{\partial \rho}{\partial t} \tag{56}$$

or

$$\frac{\partial}{\partial t} (\rho n s_w) = \rho n \frac{\partial s_w}{\partial t} + s_w \rho^2 g n (c_f + c_w) \frac{\partial \phi}{\partial t} \tag{57}$$

where the formation compressibility c_f is defined as

$$c_f = \frac{1}{n} \frac{dn}{dp} \tag{58}$$

and for the compressibility of the water c_w holds

$$c_w = \frac{1}{\rho} \frac{d\rho}{dp} \tag{59}$$

The specific storage s_s is given by

$$s_s = \rho g n (c_f + c_w) \tag{60}$$

and is defined as the volume of water released from a unit volume of porous medium as a result of compression of the medium and expansion of the water when the hydraulic head is lowered one unit. Substituting Eqn 60 into Eqn 57 yields

$$\frac{\partial}{\partial t} (\rho n s_w) = \rho n \frac{\partial s}{\partial t} + \rho s_w s_s \frac{\partial \phi}{\partial t} \tag{61}$$

With the specific moisture capacity $C(p) = d\theta/dp = (n/\rho g)(ds_w/d\phi)$, Eqn 55 may be written as

$$\nabla \cdot (\rho K \nabla \phi) = \rho [\rho g C(p) + s_w s_s] \frac{\partial \phi}{\partial t} \tag{62}$$

The development of Eqn 62 involves the assumption that the formation compressibility may be expressed in terms of fluid pressure rather than effective stress. It is furthermore assumed that the compressibility is constant with time and that with desaturation c_f may be neglected since its effect is small compared with that of changes in s_w. Cooley (1971)

used a radial, simplified version of Eqn 62 by neglecting spacial variation of ρ and found that for an isotropic, non-homogeneous medium LSOR was, out of three different solution techniques, most efficient. The boundary conditions are similar to those used by Taylor & Luthin (1969). The seepage face and the head in the well corresponding to a constant discharge were found by iteration. Underrelaxation often appeared necessary to maintain stability. It was found that for unconfined flow or when the aquifer is overlain by an aquitard, for which analytical solutions exist at late time and early time, the numerical solution converges towards the analytical one with decreasing time step and mesh sizes.

Neuman (1973) used the same equation as Cooley (1971) but for anisotropic media, so that K in Eqn 62 represents a tensor. The equation is solved by the Galerkin method in conjunction with a finite element discretization scheme. The solution of the coefficient matrix is obtained with an iterative Gaussian elimination technique. After each iteration the boundary conditions that involve the seepage face are adjusted if necessary. As the type of boundary condition is allowed to change during the solution for a single time increment the method is superior to a finite difference technique. With examples that include the two-dimensional transient seepage through an earth dam and a layered hill slope cut by a ditch, Neuman showed an inverted shape of the water table which could not be obtained with the classical free surface approach. The same model including evaporation from the soil and transpiration from the crop is used for flow in the vertical plane (Neuman et al., 1975).

A rather complete treatment of three-dimensional transient flow in saturated-unsaturated non-homogeneous porous media was presented by Freeze (1971). The flow equation, similar to Eqn 62 is written in terms of the pressure head ψ ($\psi = p/\rho g$) and takes into account anisotropy and hysteresis in the relations K(p) and θ(p). The finite difference equations are solved with a vertically oriented LSOR. The scheme is time centered in ψ and values for K, ψ, n and θ are extrapolated for the first iteration from previous time steps. It was found that the change in pressure head during a single time increment should not exceed 10 cm, so that the time step during early stages of pumping is restricted to less than 0.01 s. If convergence cannot be achieved, the step is recalculated for a smaller value of Δt. The three-dimensional example comprises groundwater withdrawal from a single well in an aquifer (53 m × 40 m × 6 m), which gives an idea of the size of problems that can be tackled.

Rovey (1975) applied a three-dimensional finite difference model to a 64 km reach of the Arkansas River of South-eastern Colorado. The model is based on a linearized form of Richards' equation, where C(p) and K(p) are evaluated for values of p at the beginning of the time step and are held constant during each time increment. The three-dimensional version of the model only applies to a section of 6 × 6 km^2 and interacts with two-dimensional model segments at its upstream and downstream ends. The allowable change in head for which a stable solution of the implicit finite difference equations could be obtained is 30 cm, resulting in a time step of 30 d. The very coarse mesh that is used in vertical direction could not be refined since this would require too much computer time and storage.

3.3 COMPUTATIONAL DIFFICULTIES

A review of available numerical solutions to transient multi-dimensional, saturated-unsaturated flow problems is given in Table 1. Except for the paper by Pikul et al. (1974), all of the papers listed use a single equation to model saturated-unsaturated flow. It can be seen that the size of the flow problems solved is small. The reason is the non-linearity of the flow equation which does not allow an efficient numerical technique to be used. It is well-known that in the presence of a sharp wetting front, the change in matric pressure can be as much as a few thousands of mbar over a depth of less than 10 cm. But also for capillary rise it is not unusual to find pF values (pF = lg[-p]) greater than 4 during a dry summer within 100 cm above the water table. Therefore the mesh size in the vertical direction must be a few centimetres only, in order not to lose a significant part of the k(p) and θ(p) relations, since almost the full range of these highly non-linear relations applies to a vertical distance of less than one metre. Now, if we consider a shallow water-table aquifer with a depth of 20 m and a water table within 5 m below surface, the number of nodes required in the vertical direction could be estimated as follows. If the mesh size for the first metre below soil surface is taken as 5 cm, for the next metre as 10 cm, for the remaining part of the unsaturated zone as 20 cm and in the saturated zone as 1 m, about 60 nodes would be required. Freeze (1971) claimed that the large computer he was using could accommodate 30,000 nodal points, which restricts the flow region in the horizontal plane to less than 23 × 23 nodes, or a few square kilometres if the horizontal mesh size is allowed to be as large as 100 m. Because of the restriction in the mesh size most of the papers listed in Table 1 consider two-dimensional flow systems of a few square metres only.

More serious is the time step restriction imposed upon the finite difference solution to obtain convergence. The length of the time step is closely related to the maximum change in matric pressure in any of the nodes. In some of the papers listed in Table 1 the maximum change in pressure for which convergence can be obtained is indicated and appears to be of the order of a few mbar or less. Other investigators report that the number of iterations required to obtain a solution is considerably increased for rapidly changing events. Most of the problems are solved with a variable time step, which at the start of the experiment is often less than one second. To avoid excessive amounts of computer time the conditions of the flow problems are relatively wet; the absolute value of the matric pressure never exceeds a few hundreds of mbar.

Several authors (Verma & Brutsaert, 1970; Guitjens & Luthin, 1971; Freeze, 1971) suggested that from similitude considerations the simulation results of a scaled-down version of the prototype may be extrapolated to the real system. Breaster et al. (1971) showed that similitude affects the soil moisture characteristics. A small-scale numerical model, based on relations for k(p) and θ(p) that apply to the real system, tends to exaggerate the effect of the unsaturated zone on the flow in the system. Moreover the scale factor for the space co-ordinates is also used to reduce p. It follows that the same numerical difficulties are faced whether a small-scale or real-size numerical model is used since the range in matric pressure that corresponds to a significant change in θ is reduced proportionally.

Table 1. Review of available numerical solutions to multi-dimensional, transient, saturated-unsaturated flow problems.

Dimension	Type of problem	Size of flow problem	Numerical approximation	Solution method
Rubin (1968)				
2-D vertical plane	Ditch drainage case	0.3 m × 0.3 m	Linearized implicit finite difference scheme	ADIPIT
Taylor & Luthin (1969)				
2-D axisymmetrical	Flow to well in shallow water-table aquifer	2.0 m × 1.2 m	Explicit finite difference scheme in unsaturated zone	Gauss-Seidel in saturated zone
Hornberger et al. (1969)				
2-D vertical plane	Ditch drainage case	0.3 m × 0.5 m	Linearized implicit finite difference scheme	Gauss-Seidel
Verma & Brutsaert (1970)				
2-D vertical plane	Ditch drainage case	3.0 m × 3.0 m	Explicit predictor followed by implicit corrector	ADI
Guitjens & Luthin (1971)				
2-D axisymmetrical	Flow to well (effect of hysteresis)	3.7 m × 2.5 m	Implicit finite difference scheme	Gauss-Seidel
Cooley (1971)				
2-D axisymmetrical	Flow to well (delayed water-table response)	20 m × 396 m	Implicit finite difference scheme	LSOR
Freeze (1971)				
3-D	General	53 m × 40 m and 6 m deep	Implicit finite difference scheme	Vertically oriented LSOR
Neuman (1973/1975)				
2-D vertical plane	Several	Several	Implicit Galerkin-type finite element scheme	Iterative application of Gauss elimination
Pikul et al. (1974)				
quasi 2-D vertical plane	Several	Several	Predictor-corrector technique applied to Richards as well as Boussinesq equation	Tridiagonal Algorithm. Linkage procedure may require iteration
Vachaud/Vauclin et al. (1975)				
2-D vertical plane	Ditch drainage case	3.0 m × 2.0 m	Linearized implicit finite difference scheme	ADIPIT
Rovey (1975)				
3-D	Stream-aquifer system	6000 m × 6000 m and variable depth	Linearized implicit finite difference scheme	Gauss elimination

3.4 ALTERNATIVE SOLUTIONS

In an attempt to find an alternative for the single-equation model to solve field-size flow problems in shallow water-table aquifers, it should be realized that the solutions presented so far are rather academic. The problems are solved to show the significance of the unsaturated zone to groundwater flow and have been chosen such that unsaturated lateral flow is of importance. However, in the field, water gradients are low, the Dupuit-Forchheimer assumptions are approximately valid in the saturated zone and lateral unsaturated flow is insignificant compared with lateral saturated flow. These conditions allow the three-dimensional flow system to be described in terms of vertical flow in the unsaturated part and horizontal flow in the saturated region. A solution in the vertical plane to this quasi three-dimensional flow system based on coupled one-dimensional Richards and Boussinesq equations was presented by Pikul et al. (1974). Their model first solved the equation of Boussinesq, written as

$$K \frac{\partial}{\partial x} \left(h \frac{\partial h}{\partial x}\right) = \mu(x,t) \frac{\partial h}{\partial t} + q_u(x,t) \qquad (63)$$

by using the predictor-corrector technique of Douglas and Jones, where values for the specific yield μ and the discharge (positive) or recharge (negative) from the unsaturated zone q_u of the previous time step are used. Next, in each of the nodes of the horizontal mesh, the same technique is applied to solve Richards' equation. The unsaturated zone is assumed to extend from the lower end of the root zone where the flux is prescribed to the water table where zero pressure exists. The principle of continuity, applied to each unsaturated column yields q_u which is used in Eqn 63 for the next time step. The specific yield is derived from

$$\mu(x,t) = n - \theta_m(x,t) \qquad (64)$$

where θ_m is (rather arbitrarily) defined as 'the minimum soil moisture content below the depth from which moisture may be removed directly by evapotranspiration'. The change in the height of the water table appears to be critical for the determination of the length of the time step. A large change in the water-table position makes an adjustment of the lower boundary of the unsaturated model desirable after each time step and may require an iterative solution to both equations to satisfy the internal boundary condition. The model performs rather poorly when lateral unsaturated flow is of importance. Only when the water-table movement is relatively small and the length of the unsaturated columns can be taken as a constant, is the model more efficient than a single-equation model.

One could draw the conclusion that the present state in the development of computer technology prohibits the numerical solution to field-size saturated-unsaturated flow systems. On the other hand one could also state that the numerical techniques available to-day are inadequate to solve unsaturated flow efficiently, because the problem of the small mesh size that is required in the unsaturated zone has not been solved. For the solution of a field-size problem, the horizontal mesh sizes are a hundred or thousand fold the mesh size in the unsaturated zone in vertical direction. This gives rise to the

discrepancy that on the one hand the hydraulic head is calculated with an accuracy of a few centimetres where on the other hand data are used that represent an 'average' over a large non-homogeneous area. According to Freeze (1971), complex models are open to the charge that their sophistication outruns the available data. However, it is rather a deficiency of the numerical method that requires the sub-surface flow to be calculated to such a high degree of detail and precision in order to obtain a solution, that the results are far out of proportion to what is usually wanted in practice. The discrepancy between the numerical solution and the actual situation in the field is even more severe close to the soil surface. In particular the validity of Richards' equation for flow in the root zone may be questioned in the presence of water uptake by the roots, non-capillary pore space, osmotic and temperature gradients, non-continuous wetting phase, water vapour diffusion, tillage, etc. Moreover, a number of hydrological processes that occur above the soil surface and greatly affect the sub-surface flow are often poorly described, such as evapotranspiration, interception and overland flow. It should also be realized that the small time increments that have to be used require an abundance of data which are usually not available.

If the numerical approximation to Richards' equation for the simulation of unsaturated flow is abandoned what alternative is available? In fact there is a wide variety of possibilities ranging from pure black box analyses to complicated conceptual models based on the original equations of Darcy and continuity. The choice depends very much on the type of problem to be solved, the input that is available and the output that is wanted.

3.5 SCOPE OF PRESENT STUDY

The objective of this study is the development of a mathematical model to solve field-size saturated-unsaturated flow problems in relation to evapotranspiration from shallow water-table aquifers. It is assumed that fluctuations in the position of the water table are small compared with the total saturated thickness of the unconfined aquifer. The upper boundary for two-dimensional horizontal saturated flow is taken as a fixed level, just beneath the lowest water-table elevation occurring in the considered period. Above this level, which serves as an interface between the saturated and unsaturated system, flow is assumed in vertical direction. This results in a quasi three-dimensional model (see Chapter 5), the structure of which is similar to the one proposed by Pikul et al. (1974). As a result of this schematization storage changes in the unconfined aquifer only occur in the unsaturated zone. At the soil surface the system is linked to a model for evapotranspiration.

Unsaturated flow is simulated in each node of the two-dimensional horizontal grid, which is defined to describe the saturated system. At the upper and lower boundary of the model for unsaturated flow Neumann conditions apply. A linking procedure is required to solve both fluxes in relation to the sub-system for evapotranspiration and saturated flow.

Evapotranspiration is calculated with the formula of Penman (1948), which has been adapted to cropped surfaces. As the storage of heat in the soil is neglected, estimates

of evapotranspiration are most accurate if the method is applied to periods of a few days. Actual evapotranspiration depends on moisture conditions in the unsaturated zone.

Apart from a proper linking procedure to solve the Neumann conditions, the model for unsaturated flow should have the following properties.

1. It should compute the change in the position of the free water level for changing boundary conditions.
2. It should satisfactorily approximate the soil moisture conditions close to the soil surface for the calculation of actual evapotranspiration.
3. The model must allow the use of time steps with a length of the order of days.
4. The solution technique must be efficient in terms of computer time and storage requirement.

It should be noted that except in the vicinity of the upper and lower boundary of the model, it is not necessary for unsaturated flow to be described in detail.

Though a large number of approximate solutions to unsaturated flow problems exist, none of these has the above mentioned properties. In order to arrive at a model that solves field-size saturated-unsaturated flow systems in shallow water-table aquifers, a solution technique for unsaturated flow that meets the above requirements is proposed and outlined in the next chapter.

4 Development of a model for unsaturated flow

4.1 STEADY-STATE RELATIONS

In the same paper in which Richards (1931) derived the general equation for unsaturated flow (28), he proposed a solution to a steady-state situation that includes a water table. For steady vertical flow the differential form of the continuity equation reduces to

$$\frac{dq}{dz} = 0 \tag{65}$$

where q is the vertical flux and z the vertical co-ordinate direction, both taken positive upward. Integration of Eqn 65 yields

$$q = \bar{q} = \text{constant} \tag{66}$$

which appears to be a trivial result. It follows for the fluxes across the upper and lower boundary that for steady flow

$$q_s = q_w = \bar{q} \tag{67}$$

which implies a stationary position of the water table as may be seen from Eqn 42. The flux $\bar{q}$ is given by Darcy's law

$$\bar{q} = -K \frac{d\phi}{dz} \tag{68}$$

and the hydraulic head is defined as

$$\phi = p/\rho g + z \tag{69}$$

In view of the analysis to follow, it is convenient to adopt, from this stage onwards, more practical units for some of the quantities appearing in Eqns 68 and 69. The pressure p will be expressed in mbar. It has the advantage that its numerical value is approximately equal to the pressure head ψ (cm), often used in literature. If the distance in each of the co-ordinate directions is expressed in cm, the hydraulic potential ϕ is also in the unit cm. As it is intended to express time in days, q and K are most conveniently in the unit $cm \cdot d^{-1}$.

Substituting Eqn 69 in Eqn 68 yields

$$\bar{q} = -K(p) \left(\frac{1}{\rho g} \frac{dp}{dz} + 1\right) \tag{70}$$

Separating the variables in Eqn 70 and solving for z gives

$$z = -\frac{1}{\rho g} \int_0^p \frac{K(p)}{\bar{q} + K(p)} \, dp \qquad (71)$$

where the reference level is chosen at the stationary phreatic surface at which level $z = 0$ and $p = 0$.

Richards (1931) used a linear relation between K and p to solve Eqn 71 analytically for upward flow. Many other empirical K(p) relations have been proposed more recently, some of which allow an analytical solution to Eqn 71. A review is given by Raats & Gardner (1971). The relation between p and z for a particular steady flux $\bar{q}$ is termed pressure profile $z(p,\bar{q})$. By numerical integration of Eqn 71 pressure profiles can be calculated for any given relation between K and p.

Transport of water in the unsaturated zone in an upward direction is called capillary rise. During the first half of this century many experiments were carried out to determine the maximum height of capillary rise for many different types of soil. The definition of the 'maximum height of capillary rise' was often vague and could refer to transient, steady or equilibrium conditions. Well-known is a method where tubes filled with air-dry soil are supplied at the base with water of constant pressure. The maximum height of capillary rise is reached when the advance of the wetting front is negligible. At this stage, according to Moore (1939), the sum of the maximum height of capillary rise and the pressure corresponding to the 'moisture content of the wetting front' is equal to zero. The experiment carried out by Shaw & Smith (1927) is an example of the determination of the maximum height of capillary rise for steady flow conditions. Tubes ranging in length from 1.2 to 3.0 m, uniformly packed with Yolo sandy loam and Yolo loam are initially wetted and permanently supplied with water at the base. Capillary rise is measured for a period of ten months. From the experiment the authors concluded that the maximum height of capillary rise equals three metres, as for this depth of the water table, evaporation from the surface during the considered period is negligible. In the Netherlands an early comprehensive description of water in the unsaturated zone was presented by Versluys (1916). The unsaturated zone is divided from the water table upwards into a capillary zone (fully saturated), a funicular zone (unsaturated, continuous liquid phase) and a pendular zone (unsaturated, discontinuous liquid phase). Versluys distinguished between heights of capillary rise and funicular rise. The rather artificial tripartition of the unsaturated flow region became quite popular and has led many investigators to determine heights of rise according to these concepts.

A proper definition of the height of capillary rise as defined in Eqn 71 is the height above the water table at which a given steady upward flux can be maintained for a given matric pressure at this height. A systematic application of Eqn 71 to compute heights of capillary rise for different values of the flux $\bar{q}$ was first carried out by Wind (1955). The analytical solution to Eqn 71 was obtained with an empirical K(p) relation which may be formulated as

$$K = a(-p)^{-n} \tag{72}$$

where a and n are constants (n = 1.5). Wesseling (1957) used Eqn 72 with n = 2 to compute from Eqn 71 maximum heights of capillary rise for a range of values of $\bar{q}$. The maximum height for a particular steady flux is found by integrating Eqn 71 from p = 0 to a value of p which corresponds with the so-called wilting point or by integrating to a value of p approaching minus infinity as suggested by Gardner (1958). For practical purposes the matric pressure for wilting can be taken equal to -16000 mbar or pF 4.2, where pF ≡ lg(-p). Given the relation between moisture content and matric pressure $\theta(p)$, usually termed the soil moisture characteristic or pF-curve, pressure profiles are easily transformed into moisture profiles $z(\theta,\bar{q})$.

Rijtema (1969) calculated moisture profiles for a great number of soils using data available from literature. From these data the K(p) relation and soil moisture characteristic of medium fine sand are presented in Figs 5a and 5b, respectively. Integration of Eqn 71 for this K(p) relation yields the pressure profiles presented in Fig. 5c. Van der Molen (1972) showed that with simple integration techniques acceptable results may be obtained. For $\bar{q} < 0$ (steady percolation) the profiles have a distinct vertical shape, merging with the equilibrium profile at the lower end. For the development of a model for unsaturated flow it is convenient to schematize these profiles into a vertical part and into a part that coincides with the equilibrium profile as shown in Fig. 5c. Moisture profiles computed from the pressure profiles with the aid of the soil moisture characteristic in Fig. 5b are presented in Fig. 5d. The soil physical data of medium fine sand given in the Figs 5a and 5b and the derived steady-state profiles (Figs 5c and 5d) will be used throughout this chapter to illustrate calculation techniques. The symbols that will be used are explained in Fig. 6. The lower boundary of the unsaturated zone is chosen as a fixed level just below the lowest water-table depth occurring in the period to be considered. This level serves as an interface between the saturated and unsaturated sub-system. The vertical co-ordinate ζ equals zero at the lower boundary and is taken as positive in an upward direction. The upper layer of the unsaturated zone in which most of the roots are present is termed root zone or effective root zone and the remaining part of the unsaturated zone is called subsoil. For convenience the entire unsaturated zone is taken as homogeneous although without appreciable difficulties most calculation procedures may be used for situations where different soil physical data apply to different layers. The depth of the root zone is constant and equals D_r while the interface between the root zone and the subsoil is at a height ζ_{rs}. Flow is assumed to be in the vertical direction only and is taken to be positive upwards. The flux across the interface between the root zone and the subsoil at $\zeta = \zeta_{rs}$ is denoted by q_{rs} and the flux across the upper and lower boundary by q_s and q_w, respectively. Figure 6 shows an equilibrium distribution of soil moisture for a depth w of the phreatic level below surface. The soil moisture distribution corresponds to the moisture profile for $\bar{q} = 0$ as shown in Fig. 5d where θ is given as a function of the height z above the water table. The same co-ordinate system is indicated in Fig. 6, while it should be noted that the level for z = 0 (the phreatic level) changes with time, depending on the value for z_{rs},

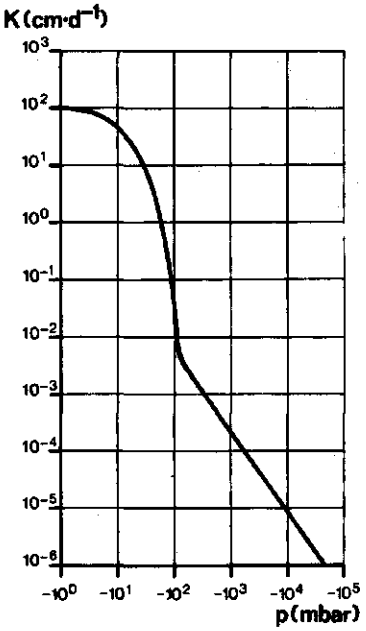

Fig. 5a. Relation between hydraulic conductivity K and matric pressure p for a medium fine sandy soil.

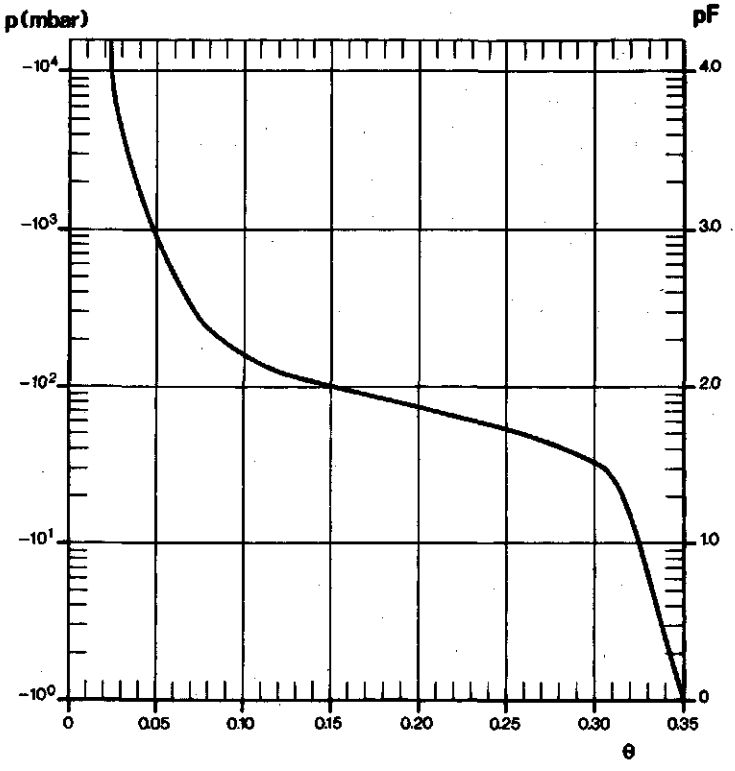

Fig. 5b. Soil moisture characteristic or pF-curve for a medium fine sandy soil giving the relation between matric pressure p and moisture content θ.

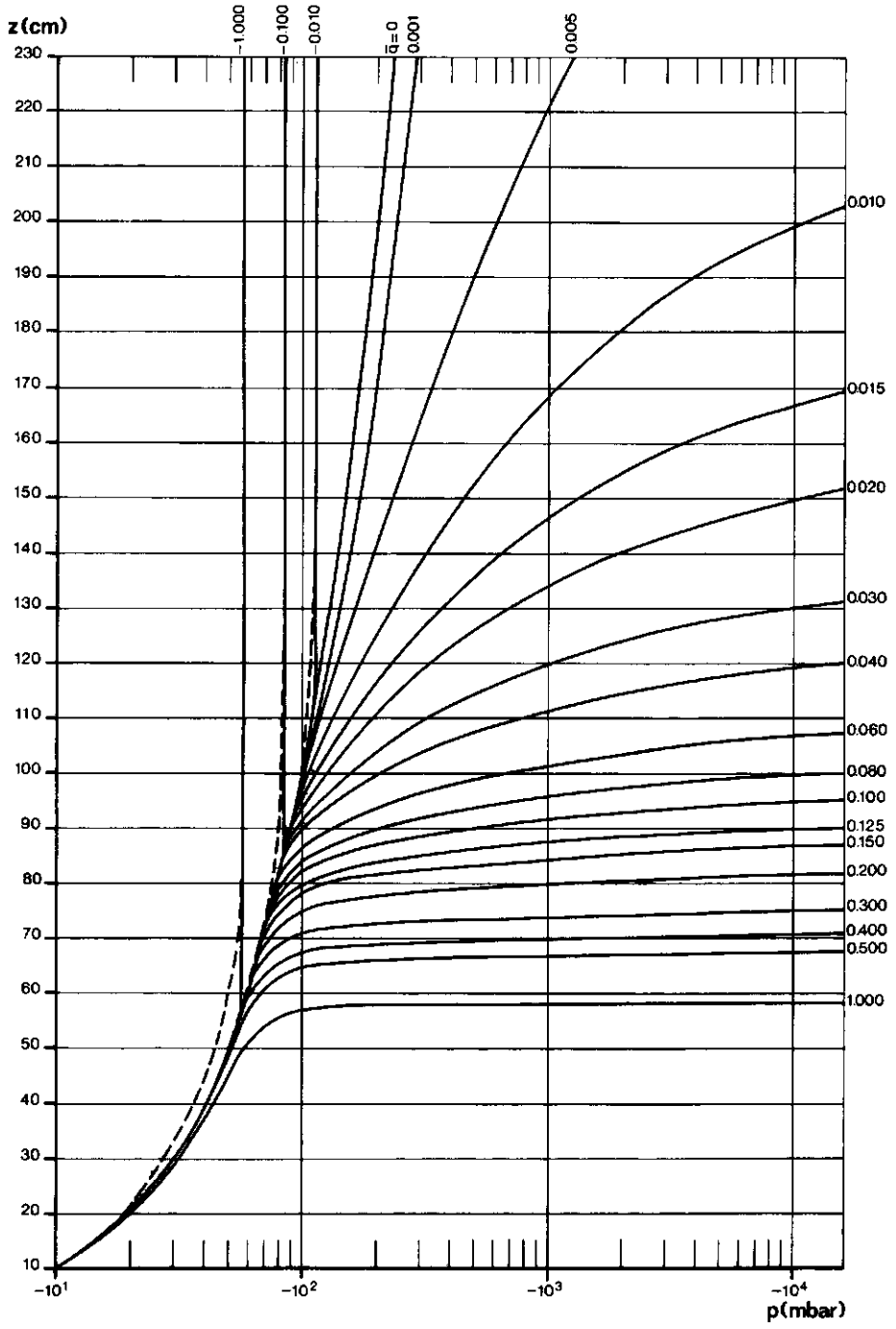

Fig. 5c. Pressure profiles, giving the relation between the height above the water table z and matric pressure p for different values of the steady flux $\bar{q}$ ($cm \cdot d^{-1}$). For $\bar{q} < 0$ the actual profile (---) differs slightly from the schematized profile.

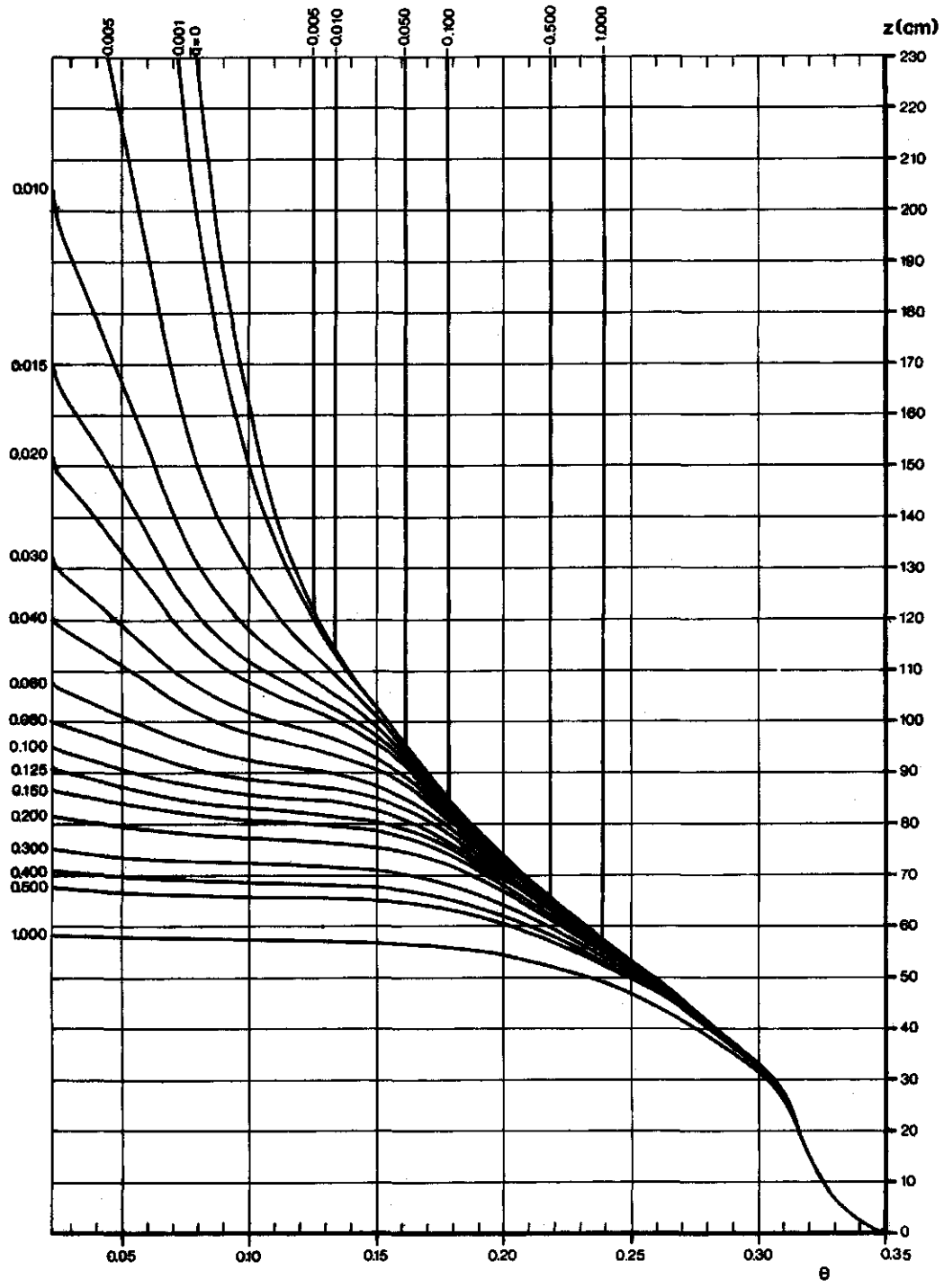

Fig. 5d. Moisture profiles, giving the relation between the height above the water table z and moisture content θ for different values of the steady flux $\overline{q}$ (cm·d^{-1}).

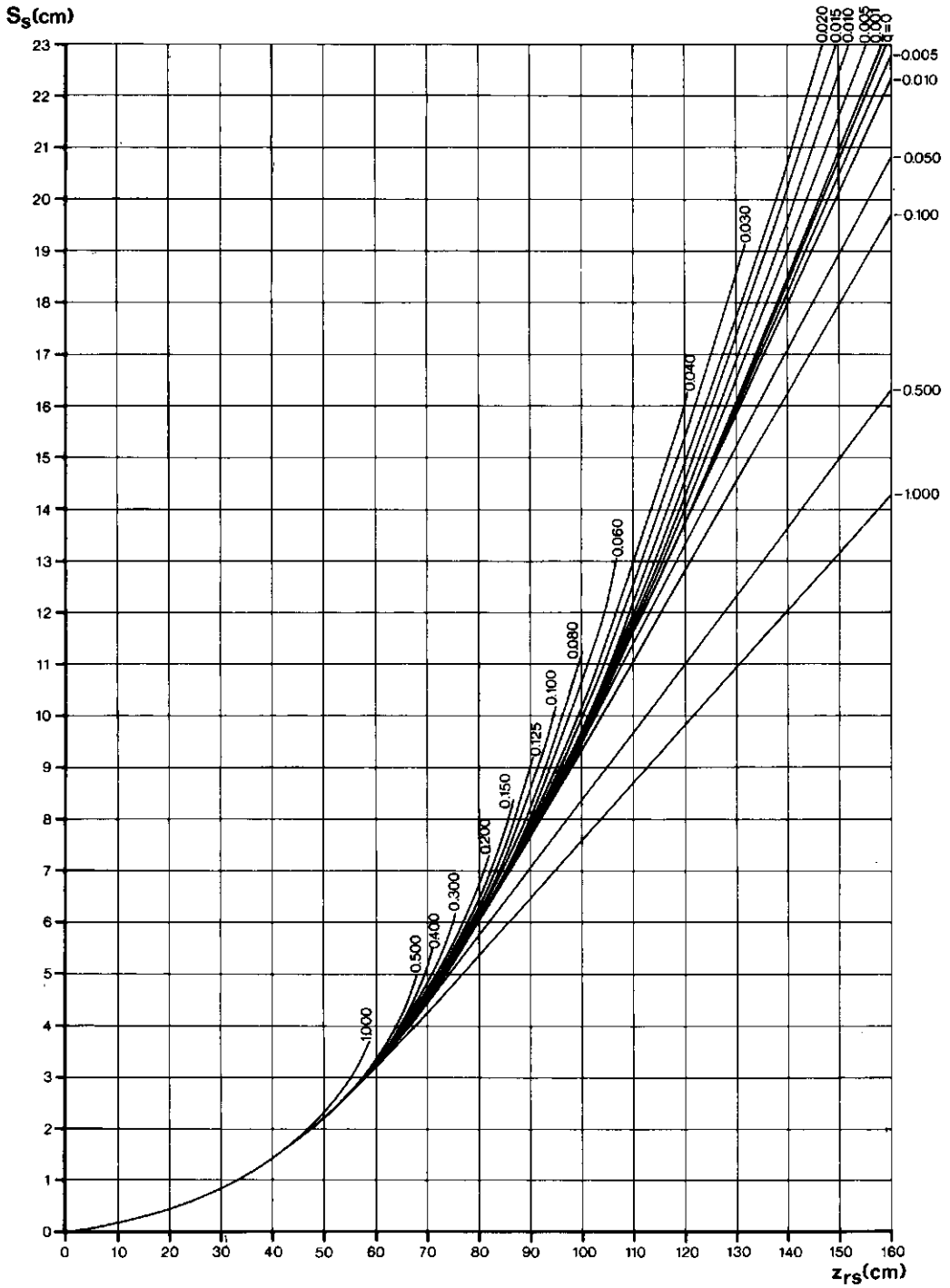

Fig. 5e. Relation between the saturation deficit of the subsoil S_s and the depth of the water table below the interface root zone - subsoil z_{rs} for different values of the steady flux $\bar{q}$ (cm·d^{-1}).

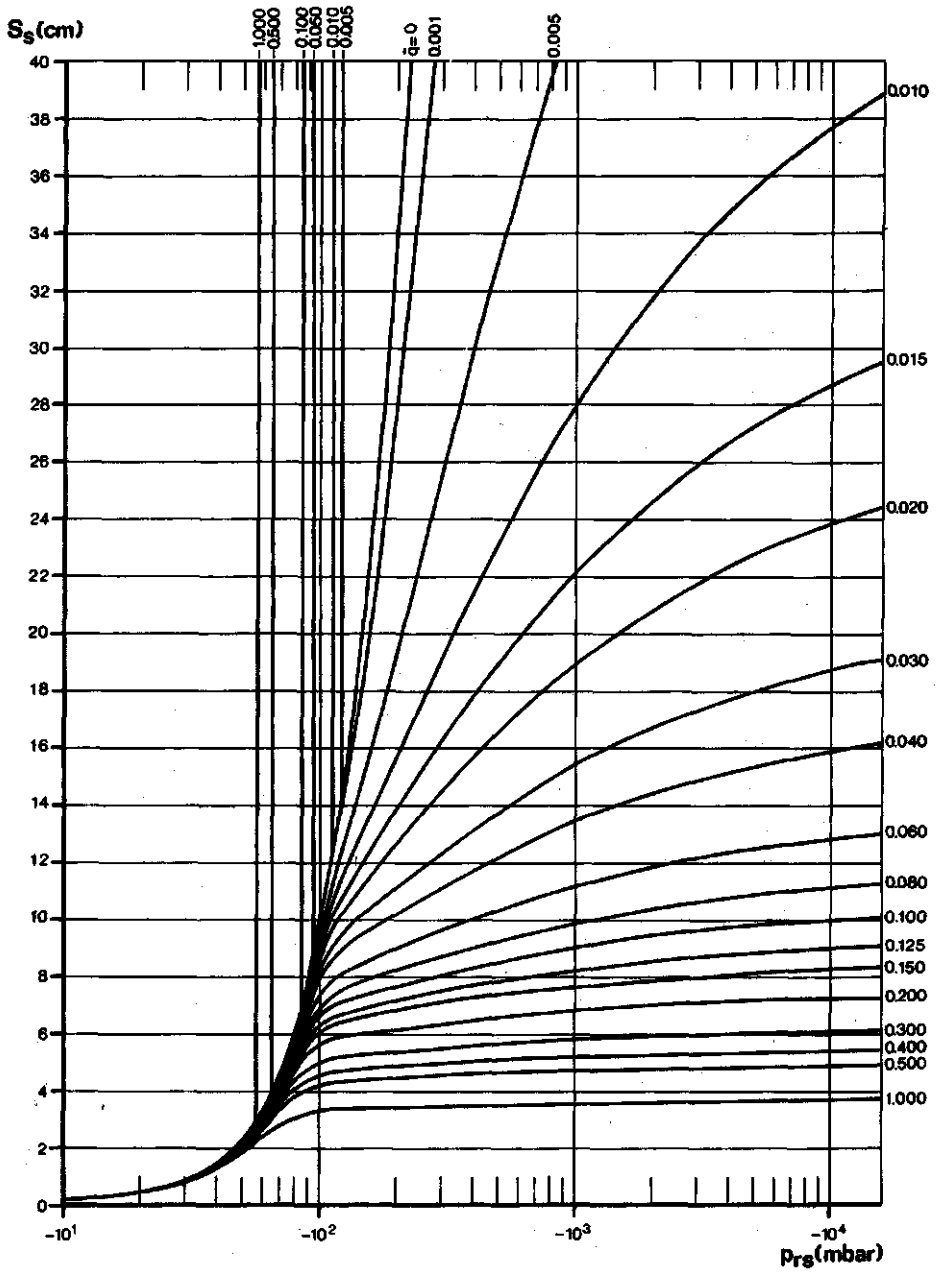

Fig. 5f. Saturation deficit curves for the subsoil giving the relation between the saturation deficit S_s and the pressure at the interface root zone - subsoil p_{rs} for different values of the steady flux $\bar{q}$ ($cm \cdot d^{-1}$).

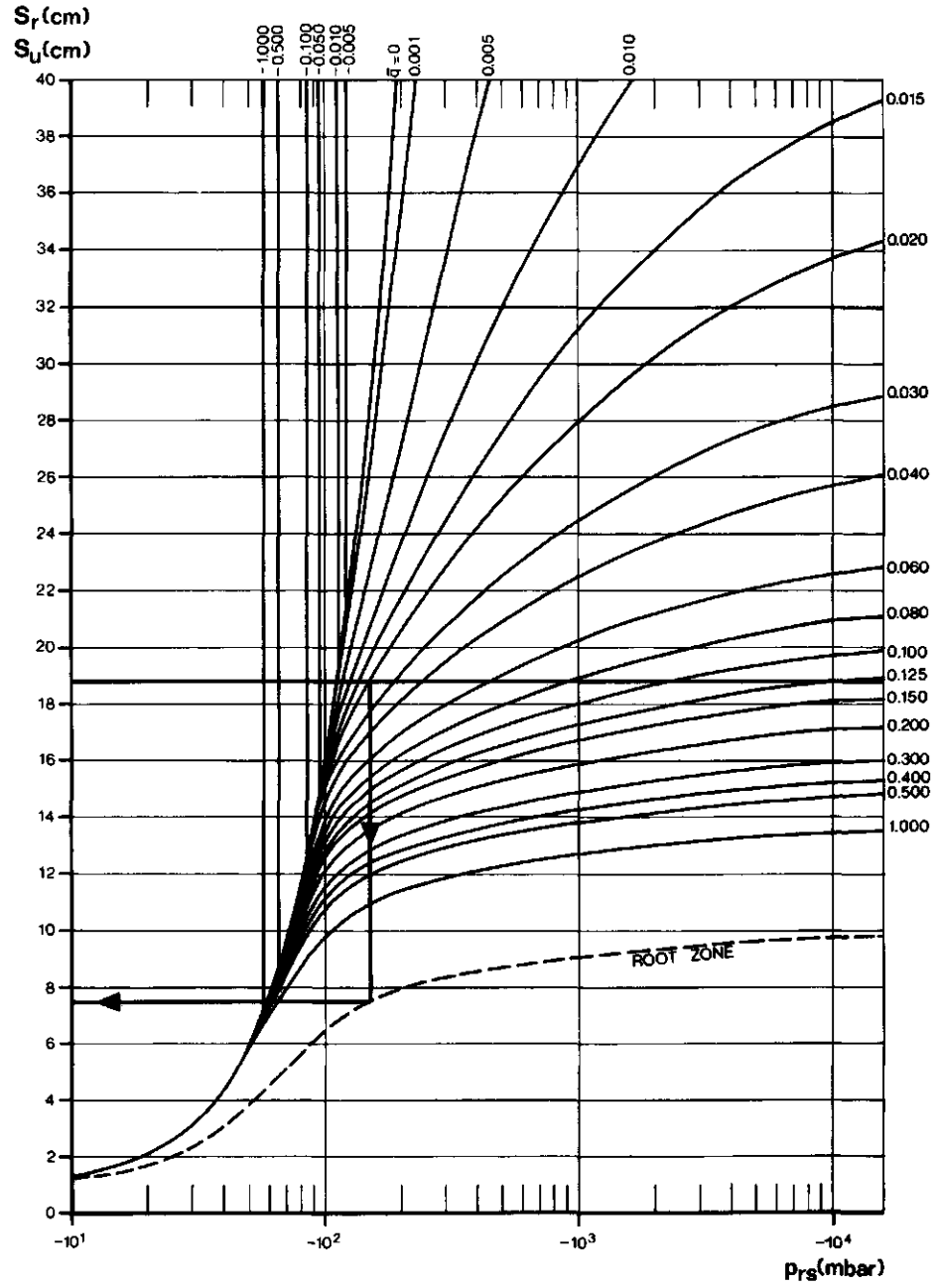

Fig. 5g. Saturation deficit curves for the entire unsaturated zone giving the relation between the saturation deficit S_u and the pressure at the interface root zone - subsoil p_{rs} for different values of the steady flux $\bar{q}$ ($cm \cdot d^{-1}$). Saturation deficit curve (---) for the root zone giving the relation between the saturation deficit S_r and the pressure at the interface root zone - subsoil p_{rs}.

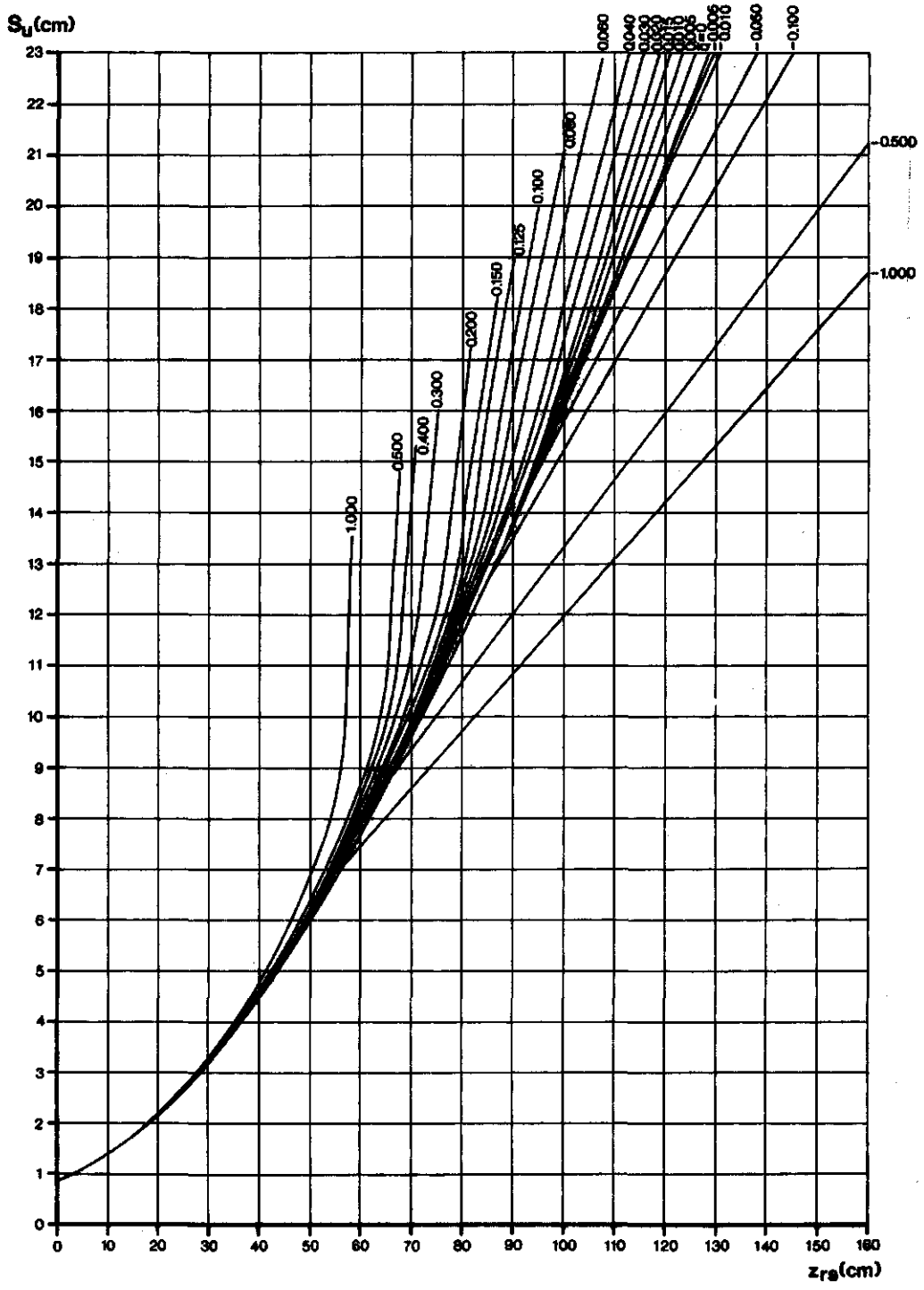

Fig. 5h. Relation between the saturation deficit of the entire unsaturated zone S_u and the depth of the water table below the interface root zone - subsoil z_{rs} for different values of the steady flux $\bar{q}$ (cm·d^{-1}).

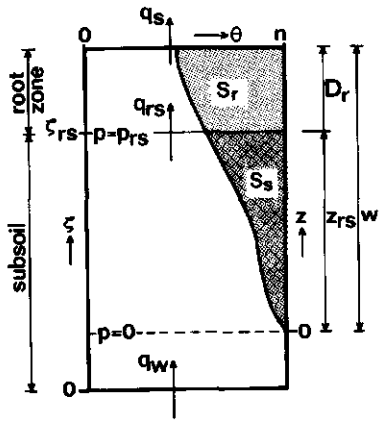

Fig. 6. Schematic presentation of the unsaturated flow system.

the distance between the lower side of the root zone and the water table. At the phreatic level p = 0 and at the height $\zeta = \zeta_{rs}$ the matric pressure is denoted by p_{rs}. De Laat (1976) showed that for a moving water-table 'saturation deficits' may be used to facilitate calculation techniques. The saturation deficit of the unsaturated zone S_u is the amount of water needed to completely saturate the soil and equals the volume of air present between the lower boundary and the soil surface. The saturation deficit of the subsoil S_s may be written as

$$S_s = \int_0^{\zeta_{rs}} [n - \theta(\zeta)]d\zeta \tag{73a}$$

or, since $n - \theta(\zeta) = 0$ for $0 \leq \zeta \leq \zeta_{rs} - z_{rs}$

$$S_s = \int_{\zeta_{rs}-z_{rs}}^{\zeta_{rs}} [n - \theta(\zeta)]d\zeta \tag{73b}$$

Substituting for $\zeta = z + (\zeta_{rs} - z_{rs})$ it follows that $z = 0$ for $\zeta = \zeta_{rs} - z_{rs}$ and $z = z_{rs}$ for $\zeta = \zeta_{rs}$, whence

$$S_s = \int_0^{z_{rs}} [n - \theta(z)]dz \tag{73c}$$

which is an expression for S_s in a moving co-ordinate system. The saturation deficit of the root zone S_r may be written as

$$S_r = \int_{\zeta_{rs}}^{\zeta_{rs}+D_r} [n - \theta(\zeta)]d\zeta \tag{74a}$$

or, applying the same substitution for ζ as above

$$S_r = \int_{z_{rs}}^{z_{rs}+D_r} [n - \theta(z)]dz \qquad (74b)$$

And it follows for the saturation deficit of the entire unsaturated zone, $S_u = S_r + S_s$.

4.2 PSEUDO STEADY-STATE APPROACH

Wesseling (1957) used moisture profiles to calculate the maximum amount of soil water that is available for crop growth. The procedure may be described as follows. At the beginning of the growing season equilibrium conditions are assumed. The soil moisture distribution equals the moisture profile for $\bar{q} = 0$ and is indicated by the broken line in Fig. 7 for an initial depth of the water table w = 100 cm. Based on data obtained by Verhoeven (1953) for a light clay soil during the extremely dry summer of 1947, Wesseling assumed that the moisture content at the surface at the end of the growing season corresponds to pF 4.2 and increases linearly with depth in the root zone. For small rooting depths, as in the example in Fig. 7 where D_r = 30 cm, the moisture distribution is assumed uniform and the matric pressure at a depth D_r likewise equals pF 4.2. The maximum amount of soil moisture that is available from the subsoil by capillary rise to the root zone is found by assuming steady flow conditions at the end of the growing season between the lower side of the root zone and the phreatic level. Pressure profiles are used to determine the magnitude of the steady flow $\bar{q}$ for a given final depth of the water table. For instance, if at the end of the growing season w = 120 cm, the matric pressure at a height $z = w - D_r = 90$ cm equals pF 4.2 and from interpolation in Fig. 5c it is found that $\bar{q} = 0.125$ cm·d^{-1}. The area between the initial and final moisture distribution in the region below the root zone may be integrated numerically or graphically to yield $\Delta S_s = 4.6$ cm, which is the maximum amount available during the

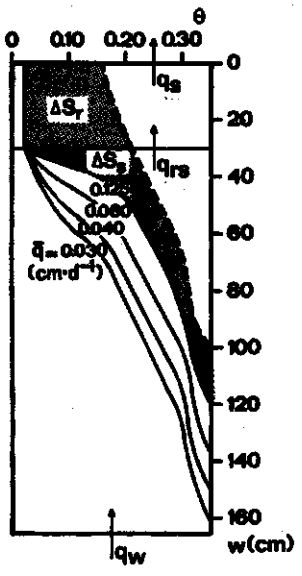

Fig. 7. Initial (broken line) and final moisture distributions for different depths of the water table w at the end of the growing season.

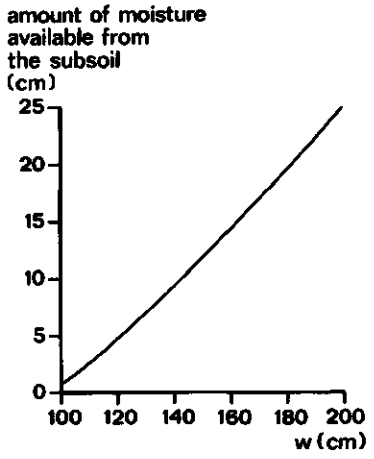

Fig. 8. Relation between the amount of moisture available from the subsoil and the depth of the water table w at the end of the growing season.

growing season by capillary rise from the subsoil. If this procedure is applied to a number of water-table depths (as shown in Fig. 7) a relation is found between the final depth of the water table w and the maximum amount of water available from the subsoil ΔS_s, which relation $\Delta S_s(w)$ is shown in Fig. 8. Instead of one relation, Wesseling (1957) computed a family of curves each of which applies to a different initial water-table depth. Integrating the area between the initial and final moisture distributions in the root zone yields ΔS_r. The total maximum amount of soil water ΔS_u available for the crop during the growing season for a given depth w of the water table at the end of the season is found as $\Delta S_u = \Delta S_r + \Delta S_s(w)$. Wesseling (1957) did not mention the flux across the lower boundary q_w, but from the procedure above it is obvious that he assumed q_w to be equal to zero.

Similar calculations were carried out by Rijtema (1965) to characterize the drought sensitivity of three types of soil in relation to the depth of the water table. In order to calculate maximum amounts of moisture available for crop growth during periods of 30, 60, 90 and 120 days assumptions were made about rates of capillary rise. A steady flux q_w from below the stationary water-table was taken into account.

Feitsma (1969) used essentially the model proposed by Wesseling (1957) except that, instead of a given depth of the water table at the end of the growing season, he introduced a time scale to calculate the maximum amount of soil moisture available for crop growth during a period of 100 days. At the beginning of the growing season at time $t = 0$ equilibrium conditions are assumed. The boundary conditions may be formulated as follows. The matric pressure at the lower side of the root zone changes instantaneously at time $t = 0$ to pF 3 and remains constant afterwards. The flux across the lower boundary $q_w = 0$ and the moisture distribution in the root zone at the end of the growing season is uniform and corresponds to pF 4.2, except for the lower 10 cm where pF 3 is assumed. A succession of steady-state flow situations is used to compute, step by step, the maximum amount of soil moisture available from the subsoil as a function of time. The amount of water released between two successive steady-states, ΔS_s is found by integrating the area between the respective moisture profiles after which the time it takes for this amount to

be transported, Δt is found from the continuity equation applied to the subsoil

$$\Delta S_s = \Delta t(q_{rs} - q_w) \tag{75}$$

Disregarding the fact that the boundary conditions differ slightly from the conditions applied by Wesseling (1957), Fig. 7 is used to elucidate the calculation procedure. For the first step ΔS_s is found by integrating the area between the initial equilibrium curve and the moisture profile for $\bar{q} = 0.125$ cm·d^{-1} which yields $\Delta S_s = 4.6$ cm. Since q_w equals zero, the total amount ΔS_s is transported to the root zone with a rate of at least 0.125 cm·d^{-1}. If it is assumed that $q_{rs} = 0.2$ cm·d^{-1}, it follows from Eqn 75 that $\Delta t = 23$ d. Hence, the amount available from the subsoil after 23 d equals $q_{rs} \times \Delta t = 4.6$ cm. Integration of the area in Fig. 7 enclosed by the moisture profiles for $\bar{q} = 0.125$ and 0.06 cm·d^{-1} yields $\Delta S_s = 3.9$ cm for which step an average flux $q_{rs} = 0.0925$ cm·d^{-1} applies. Next the length of this step is calculated from Eqn 75 which yields $\Delta t = 42$ d. It follows that after $t = 23 + 42 = 65$ d an amount equal to $4.6 + 42 \times 0.0925 = 8.5$ cm has become available for the crop from the subsoil. Continuation of the calculation yields a relation between the amount available from the subsoil as a function of time. In Fig. 9 the result is shown for a more detailed calculation, using smaller steps. Interpolation for $t = 100$ d and adding the amount available from the root zone gives the total amount available for the crop during hundred days. Although a constant matric pressure is assumed at the lower side of the root zone and the flux across the lower boundary is not considered, the calculation procedure may be regarded as a first pseudo steady-state solution to capillary rise, yielding the drawdown of the water table and the change in moisture distribution in the subsoil as a function of time.

Feddes (1971) assumed a sudden drop in matric pressure at the lower side of the root zone from the initial equilibrium value to pF 4.2 and used the method developed by Wesseling (1957) to compute $\Delta S_s(w)$, similar to Fig. 8. The procedure to calculate the

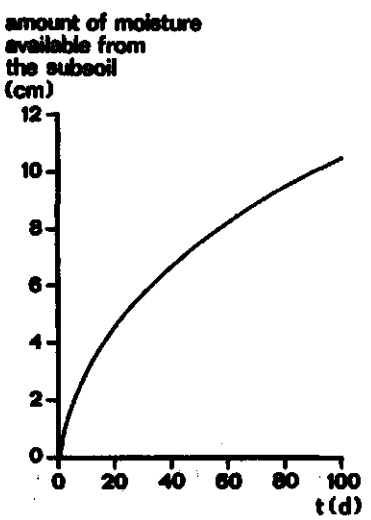

Fig. 9. Amount of moisture available from the subsoil as a function of time.

drawdown of the water table due to capillary rise as a function of time allows the phreatic level to be lowered by small steps. For each step Δw the amount released from the subsoil is obtained from the relation $\Delta S_s(w)$ and the corresponding average flux $\bar{q}$ is interpolated in Fig. 5c for z equal to the average depth of the water table below the root zone and the corresponding matric pressure equal to pF 4.2. The amount released divided by the average flux yields the time for a drawdown of Δw cm.

Instead of a fixed matric pressure at the lower side of the root zone, Rijtema (1971) used a calculation procedure for which q_{rs} is held constant as long as possible. It is assumed that flow in the root zone is governed by water uptake of the roots and that the moisture distribution in the root zone equals at all times the equilibrium distribution ($d\phi/dz = 0$). Water may be extracted from the root zone until pF 4.2 is reached. The calculation procedure is based on the principle that for the assumed equilibrium conditions in the root zone and steady flow conditions in the subsoil, the moisture distribution is fully determined for any given set of values for $\bar{q}$ and w. This is shown for the root zone extending to a depth D_r = 30 cm, $\bar{q}$ = 0.1 cm·d^{-1} and w = 120 cm as follows. The moisture distribution between the water table and the root zone equals the moisture profile for $\bar{q}$ = 0.1 cm·d^{-1}. At a height z = 90 cm above the water table and $\bar{q}$ = 0.1 cm·d^{-1} it follows from Fig. 5c that the matric pressure equals -500 mbar, which is the pressure at the lower side of the root zone p_{rs}. As a result of the assumption that in the root zone $d\phi/dz = 0$, the matric pressure at the surface equals -530 mbar and the moisture distribution corresponds to the equilibrium moisture profile for p ranging from -500 to -530 mbar. Figure 10 shows the moisture distribution for $\bar{q}$ = 0.1 cm·d^{-1} and w = 120 cm together with an equilibrium distribution for w = 100 cm. With this calculation procedure the water table can be lowered step by step. If at time t = 0 equilibrium conditions are assumed for w = 100 cm and for the first step Δw = 20 cm while $q_{rs} = \bar{q}$ = 0.1 cm·d^{-1}, the situation as depicted in Fig. 10 occurs. Integrating the increase of saturation deficits in the root zone and the subsoil yields ΔS_r = 3.6 cm and ΔS_s = 4.1 cm. If for convenience q_w is assumed constant and equal to -0.05 cm·d^{-1} it follows from Eqn 75 that $\Delta t = \Delta S_s/(q_{rs} - q_w) = 4.1/(0.1 + 0.05) = 27.3$ d and the amount available for the crop may be

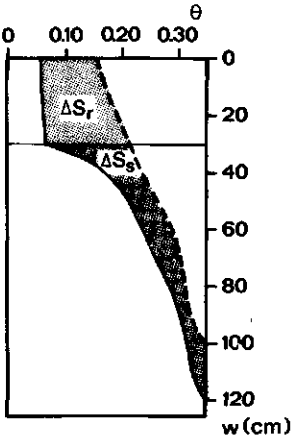

Fig. 10. Equilibrium soil moisture distribution (broken line) and the steady-state situation for $\bar{q}$ = 0.1 cm·d^{-1} after a drawdown of the water table of 20 cm.

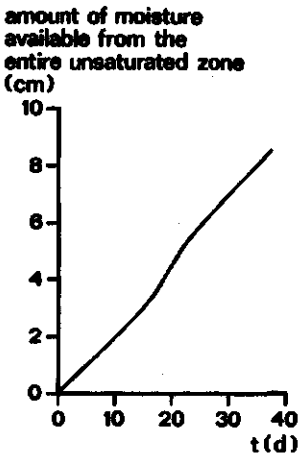

Fig. 11. Total amount of moisture available from the entire unsaturated zone as a function of time assuming $q_{rs} = \bar{q} = 0.1$ cm·d^{-1}.

calculated as $\Delta S_r + q_{rs} \times \Delta t = 3.6 + 0.1 \times 27.3 = 6.3$ cm. Continuation of the calculations for successive steps during which the water table is lowered by Δw cm yields the total amount (root zone and subsoil) available for the crop as a function of time as shown in Fig. 11. After the water table has been lowered to a depth w = 125 cm, the maximum height of capillary rise (z = 95 cm) is reached for $\bar{q} = 0.1$ cm·d^{-1} (as may be seen from Fig. 5c) and the matric pressure at the lower side of the root zone has dropped to pF 4.2. From this stage onwards the calculations are continued similar to the procedure described by Feddes (1971). Rijtema (1971) used an empirical relation between the depth of the water table and the flux across the lower boundary to determine the average flux q_w for each step Δw.

The above calculation procedure yields the flux across the surface q_s as a function of time for a given initial value for $\bar{q}$ and the assumption that $\bar{q}$ is constant until the pressure at the lower side of the root zone equals pF 4.2. A trial and error procedure is used to find the initial value for $\bar{q}$ such that the computed value for q_s equals a given extraction rate from the root zone. As initially there is no moisture deficit this extraction rate equals potential evapotranspiration minus rainfall.

De Laat (1976) used a constant value for the length of the time increment Δt and applied the continuity equation for the subsoil (75) in combination with the continuity equation for the root zone, written as

$$\Delta S = \Delta t(q_s - q_{rs}) \tag{76}$$

to solve the steady-state situation of capillary rise for given values of the flux across the upper and lower boundaries. After Rijtema (1971), equilibrium conditions are assumed in the root zone at all times ($d\phi/dz = 0$ so that $dp = -\rho g dz$). This assumption allows the expression for S_r given by Eqn 74b to be written in terms of p. At a height $z = z_{rs}$ the pressure $p = p_{rs}$, so that the saturation deficit S_r may be calculated as

$$S_r = -\frac{1}{\rho g} \int_{p_{rs}}^{p_{rs}-\rho g D_r} [n - \theta(p)]dp \qquad (77)$$

To facilitate the calculation procedure, S_r is computed for a number of values for p_{rs} to yield the saturation deficit curve for the root zone, $S_r(p_{rs})$. This relation is shown in Fig. 5g (lower curve) for the soil moisture characteristic $\theta(p)$ given in Fig. 5b and a depth of the root zone D_r = 30 cm. The saturation deficit of the subsoil S_s for a particular steady flux $\bar{q}$ is found from

$$S_s = \int_0^{z_{rs}} [n - \theta(z,\bar{q})]dz \qquad (78)$$

where the level z = 0 is chosen at the phreatic level which is situated at a depth z_{rs} below the root zone. The moving z co-ordinate system is used to calculate S_s for a number of water-table depths z_{rs} to set up a relation between S_s and z_{rs}. This procedure may be carried out for any value of the flux $\bar{q}$ to yield a relation $S_s(z_{rs},\bar{q})$ which is shown in Fig. 5e. With the aid of pressure profiles $z(p,\bar{q})$, the relation $S_s(z_{rs},\bar{q})$ is transformed into saturation deficit curves for the subsoil $S_s(p_{rs},\bar{q})$ which are presented in Fig. 5f. It shows that for the vertical part of the percolation profiles where z is not defined for given values of p and $\bar{q}$, the saturation deficit S_s is also undefined. A numerical approach to the computation of saturation deficit curves for a (heterogeneous) subsoil is discussed in Appendix A.

Since both S_r and S_s can be written as a function of p_{rs}, the saturation deficit of the entire unsaturated zone S_u is for any steady flux $\bar{q}$ computed from

$$S_u(p_{rs},\bar{q}) = S_r(p_{rs}) + S_s(p_{rs},\bar{q}) \qquad (79)$$

Saturation deficit curves for the entire unsaturated zone $S_u(p_{rs},\bar{q})$ including a depth of the root zone D_r = 30 cm are shown in Fig. 5g. Finally the saturation deficit curves $S_u(p_{rs},\bar{q})$ are combined with the pressure profiles $z(p,\bar{q})$ to yield the relation $S_u(z_{rs},\bar{q})$ which is presented in Fig. 5h.

The transient process of capillary rise due to water extraction from the root zone is approached by a sequence of steady-state situations. The calculation procedure solves for each time step Δt the steady-state profiles for a given flux across the upper and lower boundary. Since $S_u(p_{rs},\bar{q})$ and $S_r(p_{rs})$ are related by the pressure p_{rs}, Fig. 5g provides a relation between S_u, S_r and $\bar{q}$ so that, given values for S_u and S_r, the steady-state is fully determined. For example, for S_u = 18.8 cm and S_r = 7.5 cm it may be seen from Fig. 5g that $\bar{q}$ = 0.020 cm·d^{-1} and p_{rs} = -150 mbar. Interpolation in Fig. 5h for S_u = 18.8 cm and $\bar{q}$ = 0.02 cm·d^{-1} yields the depth of the water table below the root zone as z_{rs} = 106 cm.

For the calculation of the steady-state situation for capillary rise at time $n+\frac{1}{2}$ for given initial values S_r^n and S_u^n, and boundary conditions $q_s^{n+\frac{1}{2}}$ and $q_w^{n+\frac{1}{2}}$ that apply over the length of the time increment Δt, the following scheme is used.

1. Calculate S_u^{n+1} for the given boundary flux conditions from the water balance equation

$$S_u^{n+1} = S_u^n + \Delta t(q_s^{n+\frac{1}{2}} - q_w^{n+\frac{1}{2}}) \tag{80}$$

2. The relations $S_u(p_{rs},\bar{q})$ and $S_r(p_{rs})$ may be combined to give $S_r(\bar{q},S_u)$, so that for $S_u = S_u^{n+1}$ there exists a unique relation between S_r^{n+1} and $\bar{q}^{n+1}$.
3. The water balance equation for the root zone is written as

$$S_r^{n+1} = S_r^n + \Delta t(q_s^{n+\frac{1}{2}} - q_{rs}^{n+\frac{1}{2}}) \tag{81}$$

Assuming that $q_{rs}^{n+\frac{1}{2}} = \bar{q}^{n+1}$ Eqn 81 provides another relation between S_r^{n+1} and $\bar{q}^{n+1}$. Both relations are used to solve graphically or by numerical iteration S_r^{n+1} and $\bar{q}^{n+1}$.
4. The water-table depth z_{rs} is found from interpolation in $S_s(z_{rs},\bar{q})$ for $\bar{q} = \bar{q}^{n+1}$ and $S_s = S_u^{n+1} - S_r^{n+1}$.

In the original scheme (de Laat, 1976) the saturation deficit S_u at time $n+\frac{1}{2}$ is used to compute from the steady-state profiles the relation between $S_r^{n+\frac{1}{2}}$ and $\bar{q}^{n+\frac{1}{2}}$. The relation from the water balance equation is written as $S_r^{n+\frac{1}{2}} = S_r^n + \frac{1}{2}\Delta t(q_s^{n+\frac{1}{2}} - q_{rs}^{n+\frac{1}{2}})$. Assuming that the average flux during the time increment across the interface root zone - subsoil equals the flux corresponding to the average steady-state situation ($q_{rs}^{n+\frac{1}{2}} = \bar{q}^{n+\frac{1}{2}}$), the solution applies from a numerical point of view correctly at time $n+\frac{1}{2}$. The use of average values for the saturation deficits S_u and S_r will only yield an average value for $\bar{q}$ or q_{rs} if the system is linear. The unsaturated flow process, however, is non-linear and it is found that this approach may cause the solution to be inconsistent. For example the solution for $S_r^{n+\frac{1}{2}}$ and $q_{rs}^{n+\frac{1}{2}}$ may result in a value for S_r^{n+1} which is larger than the maximum possible saturation deficit in the root zone. Therefore the relation between S_r and $\bar{q}$ is in the above scheme evaluated from the steady-state profiles for S_u at time n+1. It may easily be shown by decreasing the length of the time increment that this approach does not significantly affect the simulation results. The assumption in the above scheme that $q_{rs}^{n+\frac{1}{2}} = \bar{q}^{n+1}$ introduces uncertainty about the time at which the calculated steady-state applies. Therefore the calculated saturation deficits are defined to apply at time n+1 as well as the corresponding flux $\bar{q}$. The calculated value for q_{rs} applies at time $n+\frac{1}{2}$ and other parameters, such as z_{rs} and p_{rs} may be taken at time $n+\frac{1}{2}$ or at time n+1 depending on the time at which the initial value is specified ($n-\frac{1}{2}$ or n, respectively).

As a numerical example the following initial situation is assumed: $S_u^n = 15.8$ cm and $S_r^n = 7.4$ cm. Other parameters corresponding to the initial steady-state situation may be obtained from Fig. 5. Interpolation in Fig. 5g for the given value of the saturation deficits yields $\bar{q}^n = 0.06$ cm·d^{-1} and $p_{rs}^n = -140$ mbar. The initial depth of the water table below the root zone is interpolated from Fig. 5h for $S_u = 15.8$ cm and $\bar{q} = 0.06$ cm·d^{-1} to yield $z_{rs}^n = 91.5$ cm. Consequently $w^n = z_{rs}^n + D_r = 91.5 + 30 = 121.5$ cm. The boundary conditions that apply for the next time increment $\Delta t = 10$ d are $q_s^{n+\frac{1}{2}} = 0.24$ cm·d^{-1} and $q_w^{n+\frac{1}{2}} = -0.06$ cm·d^{-1}. For a solution the above scheme is applied as follows.
1. The saturation deficit of the entire unsaturated zone is calculated from the water balance equation (80) to yield $S_u^{n+1} = 15.8 + 10 \times (0.24 + 0.06) = 18.8$ cm.
2. Figure 5g is used to compute the relation $S_r(\bar{q},S_u)$ for $S_u = 18.8$ cm. To elucidate the

construction of the relation between S_r and $\bar{q}$ an example is given in Fig. 5g. It shows for S_u = 18.8 cm that S_r = 7.5 cm for $\bar{q}$ = 0.02 cm·d^{-1}.

3. The relation between S_r and $\bar{q}$ resulting from the water balance equation (81) may be written as $S_r = 7.4 + 10 \times (0.24 - \bar{q})$. Both relations between S_r and $\bar{q}$ are shown in Fig. 12 and it appears graphically that S_r^{n+1} = 9.0 cm and $\bar{q}^{n+1}$ = 0.08 cm·d^{-1}.

4. Interpolation in Fig. 5e for $S_s = S_u^{n+1} - S_r^{n+1}$ = 18.8 - 9.0 = 9.8 cm and $\bar{q}$ = 0.08 cm·d^{-1} yields z_{rs}^{n+1} = 95.5 cm. It follows that the water table during this time step dropped from 121.5 cm to 125.5 cm below surface. The pressure at the lower side of the root zone is found from Fig. 5g for S_r = 9.0 cm as p_{rs}^{n+1} = -900 mbar. The soil moisture distributions at the beginning and at the end of the time increment are given in Fig. 13.

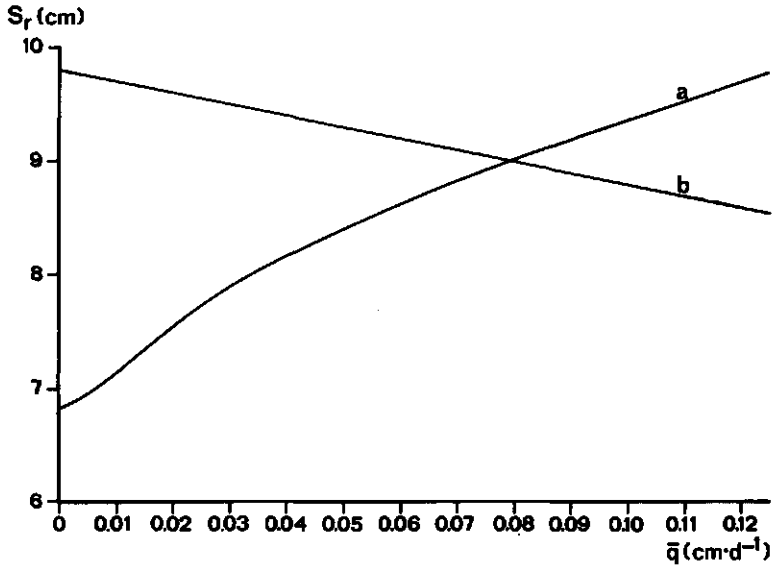

Fig. 12. The relations between S_r and $\bar{q}$ for capillary rise.
Curve a: $S_r(\bar{q},S_u)$ for S_u = 18.8 cm. Curve b: $S_r = 7.4 + 10 \times (0.24 - \bar{q})$.

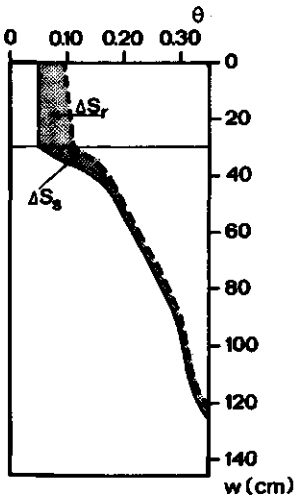

Fig. 13. The initial (broken line) and final soil moisture distribution for the example given in the text.

If the same boundary conditions apply for subsequent time steps, the situation arises that the amount of water available from the root zone is exhausted and the rate of capillary rise from the subsoil is not sufficient to maintain the upper boundary flux condition. Consequently the flux q_s must be reduced. The calculation procedure to compute the reduced or real surface flux q_s^{re} is similar to that described by Feddes (1971). Assume at time n the following initial situation: S_u^n = 18.8 cm and S_r^n = 9.0 cm. Figure 5g shows that this situation corresponds with $\bar{q}$ = 0.08 cm·d^{-1} and p_{rs} = -900 mbar. For Δt = 10 d and the same boundary conditions as used above ($q_s^{n+\frac{1}{2}}$ = 0.24 and $q_w^{n+\frac{1}{2}}$ = -0.06 cm·d^{-1}) it follows that S_u^{n+1} = 18.8 + 10 × (0.24 + 0.06) = 21.8 cm. From Fig. 5g it is seen that for S_u = 21.8 cm and for the maximum value for the matric pressure (pF 4.2) the maximum possible rate of capillary rise equals 0.07 cm·d^{-1}. The relations $S_r(\bar{q},S_u)$ for S_u = 21.8 cm and S_r = 9.0 + 10 × (0.24 - $\bar{q}$) resulting from the water balance equation (81) are plotted in Fig. 14, which shows that a solution cannot be found for $\bar{q} \leq$ 0.07 cm·d^{-1}. The maximum amount to be extracted across the upper boundary during time step n+1 equals the amount available from the root zone ($S_r^{max} - S_r^n$ = 9.8 - 9.0 = 0.8 cm) and the amount that is made available by capillary rise from the subsoil. The initial saturation deficit of the subsoil $S_s^n = S_u^n - S_r^n$ = 18.8 - 9.0 = 9.8 cm. To compute the amount that is made available from the subsoil by capillary rise for 10 days, the initial value for S_s is increased by small steps. The calculations carried out for the present numerical example are presented in Table 2. For each step the maximum rate of capillary rise $\bar{q}^{max}$ is found from Fig. 5f and the time required for each step (Column 6) is found from the water balance equation for the subsoil as $\Delta S_s/(q_{rs} - q_w)$ with

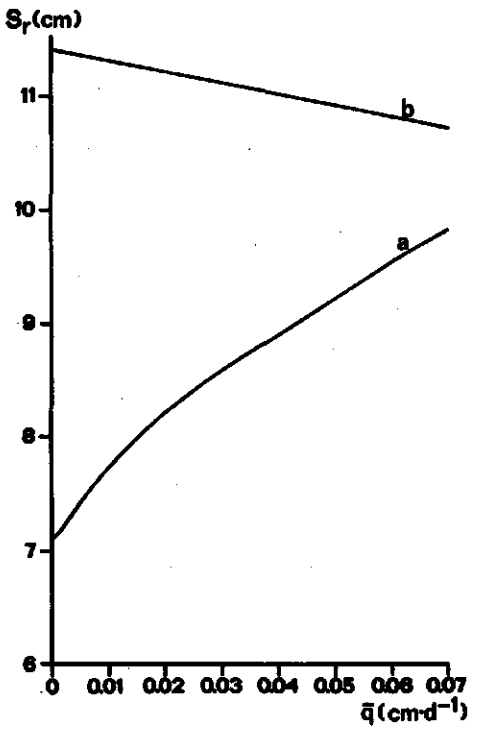

Fig. 14. Relations between S_r and $\bar{q}$ for $q_s^{re} < q_s$.

Curve a: $S_r(\bar{q},S_u)$ for S_u = 21.8 cm.
Curve b: S_r = 9.0 + 10 × (0.24 - $\bar{q}$).

Table 2. An example for the calculation of the reduced upper boundary flux q_s^{re} (see text).

(1)	(2)	(3)	(4)	(5)	(6)	(7)	(8)
step number	S_s (cm)	ΔS_s (cm)	$\bar{q}^{max}$ ($cm \cdot d^{-1}$)	$\bar{q}^{max} - q_w$ ($cm \cdot d^{-1}$)	time (d)	total time (d)	amount available from subsoil (cm)
	9.80					0.0	
1	10.12	0.32	0.10	0.16	2.0	2.0	0.20
2	10.85	0.73	0.09	0.15	4.9	6.9	0.44
3	11.29	0.44	0.08	0.14	3.1	10.0	0.25

$q_{rs} = \bar{q}^{max}$. The amount that is made available by capillary rise from the subsoil (Column 8) is found by multiplying the required time for each step (Column 6) by the maximum rate of capillary rise (Column 4). Addition of the values in Column 8 yields 0.89 cm, which amount together with the 0.80 cm available from the root zone comprises $q_s^{re} \times \Delta t$. Hence, the reduced boundary flux for this time increment, $q_s^{re} = (0.89 + 0.80)/10 = 0.17$ $cm \cdot d^{-1}$. The saturation deficit of the unsaturated zone is recalculated as $S^{n+1} = 18.8 + 10 \times (0.17 + 0.06) = 21.1$ cm and the saturation deficit of the root zone S_r^{n+1} is set equal to its maximum value.

4.3 ANALYSIS OF THE PSEUDO STEADY-STATE APPROACH

A true steady-state can only be obtained after an infinitely long time when both fluxes across the upper and lower boundary of the considered soil column are of the same magnitude and in the same direction. Consequently a succession of steady-state situations is an apparently useless concept for modelling transport in the unsaturated zone, since it requires the length of the time increment to be infinitely long and it does not allow a change in storage (see the condition stated in Eqn 67). The validity of the pseudo steady-state approach depends on the magnitude and direction of the boundary flux conditions, the initial situation and the length of the time increment.

Consider an initial equilibrium situation with a depth of the water table, $z_{rs} = 90$ cm, followed by a time increment $\Delta t = 9$d during which $q_w = 0$ and $q_{rs} = 0.1$ $cm \cdot d^{-1}$. The soil moisture distribution at the end of the time increment resulting from the pseudo steady-state approach is presented in Fig. 15a. The solution is based on the concept that the actual moisture content distribution can be approached by a moisture profile corresponding to a steady flow situation for which $\bar{q} = q_{rs}$. The actual situation is unsteady since the flux ranges from essentially zero at the water table to 0.1 $cm \cdot d^{-1}$ at the upper boundary. Rather than a steady moisture profile for $\bar{q} = 0.1$ $cm \cdot d^{-1}$, the actual situation is more properly approached by a combination of an infinite number of moisture profiles corresponding to fluxes which range from 0.1 $cm \cdot d^{-1}$ at the top to zero flux at the lower boundary. However the moisture profile corresponding to the upper boundary flux is a fair approximation of the non-steady situation because the differences between moisture profiles are largest near the upper boundary where the flux approaches the true steady-state. In downward direction the actual flux increasingly deviates from the assumed steady flux

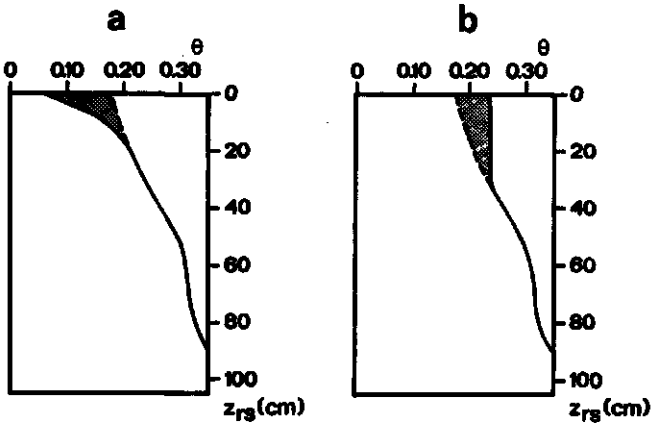

Fig. 15. Steady-state soil moisture distributions, showing the difference in saturation deficit (shaded area) for an equilibrium situation (broken line) and (a) steady capillary rise ($\bar{q}$ = 0.1 cm·d^{-1}), (b) steady percolation ($\bar{q}$ = -1.0 cm·d^{-1}).

$\bar{q}$ but the difference between the steady moisture profile and the non-steady soil moisture distribution decreases continuously and ultimately vanishes completely at the water table. It is this phenomenon which enables the use of the concept of a succession of steady-states to approach the non-steady process of capillary rise. The validity of the concept improves if (i) the length of the time increment is large, (ii) q_{rs} changes slowly in time and (iii) the difference in magnitude of the boundary flux conditions is small.

(i) Length of time increment

Unlike the numerical approach to Richards' equation for solving one-dimensional transient unsaturated flow (Freeze, 1969), the pseudo steady-state approach requires large values for Δt. The solution may even become inconsistent if the length of the time increment is taken smaller than the characteristic time τ. The characteristic time is the approximate lag between the instantaneous change in the upper boundary flux condition and the response of the water table. Given a change in the upper boundary flux from q_{rs}^{n} to q_{rs}^{n+1}, the characteristic time equals the ratio of the amount of water to be removed to reach the steady-state soil moisture distribution corresponding to q_{rs}^{n+1} (assuming a stationary position of the water table) and Δq_{rs}. For the example used above, the shaded area in Fig. 15a is the amount of water to be removed to reach the steady-state resulting from Δq_{rs} = 0.1 cm·d^{-1} while the position of the water table remains unchanged. This amount equals 0.9 cm, hence τ = 0.9/0.1 = 9 days. The response of the water table found with the pseudo steady-state approach in relation to the length of the time increment (Fig. 16a) shows a rise of the phreatic level for $\Delta t < \tau$. This is physically impossible for capillary rise in combination with a lower boundary flux equal to zero. The figure further shows that the response to an instantaneous change ($\Delta t \to 0$) is limited to a rise of 3.3 cm.

A similar inconsistency in the solution of the water-table depth arises with percolation when $\Delta t < \tau$. The area shaded in Fig. 15b shows the amount of water to be refilled (ΔS_g = -1.2 cm) if the initial equilibrium situation is followed by steady percolation

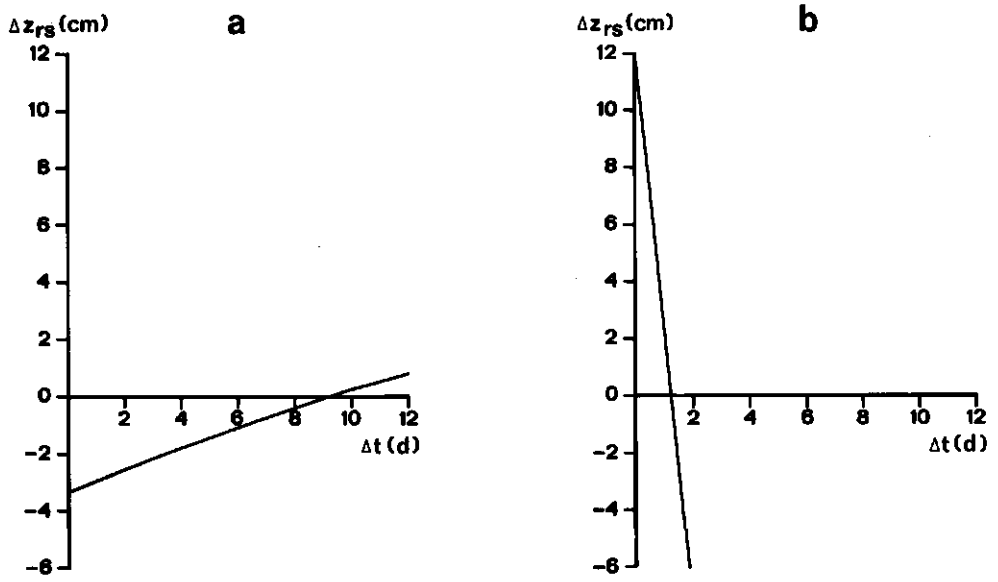

Fig. 16. Response of the water-table depth Δz_{rs} in relation to the length of the time increment Δt resulting from the pseudo steady-state approach for the corresponding situations in Fig. 15. Negative values of Δz_{rs} indicate a rise in the water table.

(q_{rs} = -1.0 cm·d^{-1}). Figure 16b shows that the use of the pseudo steady-state approach for a situation with $\Delta t < \tau$ = -1.2/-1.0 = 1.2 d yields a drawdown of the water table (assuming q_w = 0). The relations shown in Fig. 16 depend very much on the initial situation. This may be seen from Fig. 5e, which has been used to derive these relations.

(ii) Rate of change in q_{rs}

Application of the pseudo steady-state approach to situations for which $|q_{rs}|$ decreases is questionable as the characteristic time τ is negative. A decrease in the rate of capillary rise definitely yields a drawdown of the water table (assuming q_w = 0) even for very small values of Δt. However during periods with evaporation excess ($q_s > 0$), the change in q_{rs} is small as the maximum value of q_s is limited to the maximum evaporation rate. Moreover the root zone acts as a buffer while the value of q_{rs} is restricted by the depth of the falling water-table. If a period with capillary rise is followed by rainfall excess ($q_s < 0$), the change in the value of q_{rs} may be large as q_s is now limited only to the maximum infiltration rate while q_{rs} becomes independent of the water-table depth. Moreover the buffering effect of the root zone decreases due to hysteresis. Therefore a relatively large drawdown may be calculated if the pseudo steady-state procedure is applied to flow situations where, due to rainfall excess, a positive value for q_{rs} drops to zero or even becomes negative (Fig. 5e). Obviously the actual flow situation is highly non-steady and the present pseudo steady-state procedure is not suitable to solve this type of flow problem.

(iii) Influence of boundary conditions

The approximate nature of the pseudo steady-state approach (as explained earlier for the situation that $q_w = 0$) improves if the lower boundary flux q_w is positive, even with steady percolation ($q_{rs} < 0$). For the latter situation the upward flux across the lower boundary affects the characteristic time favourably while the zero flow conditions occurring somewhere between the upper boundary and the water table coincide with the lower (equilibrium) part of the percolation profile. However for relatively large negative values of the flux across the lower boundary the position of the water table is dominated by the shape of the percolation profile prevailing in the lower part of the subsoil rather than the moisture profile for capillary rise. Assuming zero flux conditions at the upper boundary the pseudo steady-state procedure yields an equilibrium soil moisture distribution regardless of the magnitude of the flux across the lower boundary. For deep water-tables the solution is equivalent to the situation shown in Fig. 2. Consequently the same objections raised against the use of a constant storage coefficient to solve saturated groundwater flow problems apply to the use of the pseudo steady-state procedure when there are large negative values of the flux across the lower boundary.

In conclusion, the pseudo steady-state procedure may only be applied to periods with evaporation excess (the inconsistency as discussed under (i) is usually small for capillary rise) and in combination with a lower boundary flux condition which is either positive or small in the downward direction. In order to adapt the pseudo steady-state procedure for general use, new concepts have to be introduced to remove the existing inconsistencies and to treat periods with rainfall excess after a situation with capillary rise. For a relatively large lower boundary flux in the downward direction, a solution of the position of the water table cannot be found with the aid of a moisture profile corresponding to the flux across the upper boundary. Therefore it is proposed that the pseudo steady-state approach is applied to both boundary flux conditions separately. The solutions for the upper and lower boundary flux condition (termed upper or lower boundary solution) finally result in a combined pseudo steady-state procedure.

4.4 UPPER BOUNDARY SOLUTION

4.4.1 Percolation

The calculation scheme for capillary rise (page 55) reduces the pseudo steady-state procedure to a problem of two relations and two unknowns (Fig. 12). The first relation $S_r(\bar{q},S_u)$ derived from the steady-state profiles, is in fact based on Darcy's law and the second relation between S_r and $\bar{q}$ is merely an equation of continuity, based on the water balance for the root zone (Eqn 81). As both relations are equally well set up for negative values of $\bar{q}$ the scheme may also be used for percolation. When computing the relation $S_r(\bar{q},S_u)$ for a given S_u value, it should be noted, however, that as a result of the schematization of the pressure profiles (Fig. 5c) into a strictly vertical part and into a part that coincides with the equilibrium profile, S_r does not change over a certain range of negative $\bar{q}$ values. For example, if $S_u = 16.1$ cm it may be seen from Fig. 5g that

for $-0.03 \leq \bar{q} \leq 0$ cm·d^{-1} the value of p_{rs} and hence of S_r is constant and equal to 6.5 cm (see PQ in Fig. 17). Outside this range of $\bar{q}$ values for which S_r is constant the relation between S_r and $\bar{q}$ is, unlike for the situation of capillary rise, independent of S_u. The entire (independent) relation (the Curve OPR in Fig. 17) is computed from a combination of $S_r(p_{rs})$ and $\bar{q}(p)$ with $p = p_{rs}$. The latter relation is equal to $-K(p)$, as for steady percolation it follows from Eqn 71 that $\bar{q} = -K$ for large water-table depths ($z \to \infty$, and thus $S_u \to \infty$).

For a numerical example consider the following initial equilibrium situation at time n: $S_u^n = 18.5$ cm, $S_r^n = 6.8$ cm and $z_{rs}^n = 110$ cm. If for the next time increment ($\Delta t = 1$ d) the following boundary conditions apply: $q_s^{n+\frac{1}{2}} = -2.4$ cm·d^{-1} and $q_w^{n+\frac{1}{2}} = 0$ cm·d^{-1}, the total saturation deficit $S_u^{n+1} = 18.5 - 2.4 = 16.1$ cm. For this S_u value $S_r(\bar{q},S_u)$ is presented in Fig. 17, Curve a (OPQ). The other relation between S_r and $\bar{q}$ may be written as $S_r = S_r^n + \Delta t(q_s^{n+\frac{1}{2}} - \bar{q}) = 4.4 - \bar{q}$ and the solution, obtained graphically from Fig. 17 yields $\bar{q}^{n+1} = -0.5$ cm·d^{-1} and $S_r^{n+1} = 4.9$ cm. As explained earlier, the solution to the position of the water table is inconsistent if $\Delta t < \tau$. The characteristic time may be found from Fig. 5e. For $z_{rs} = 110$ cm, the change in saturation deficit for $\bar{q}$ changing from 0.0 to -0.5 cm·d^{-1} is read as $\Delta S_s = -1.9$ cm. Consequently $\tau = \Delta S_s/\Delta q_{rs} = -1.9/-0.5 = 3.8$ d. Since the length of the time step used is one day only, the solution to the position of the water table yields a large drawdown (for $S_s = S_u^{n+1} - S_r^{n+1} = 16.1 - 4.9 = 11.2$ cm and $\bar{q} = -0.5$ cm·d^{-1} it is found from Fig. 5e that $z_{rs} = 121$ cm).

From a computational point of view, the best procedure to remove this inconsistency in the solution of the phreatic level is the assumption of an equilibrium profile in the

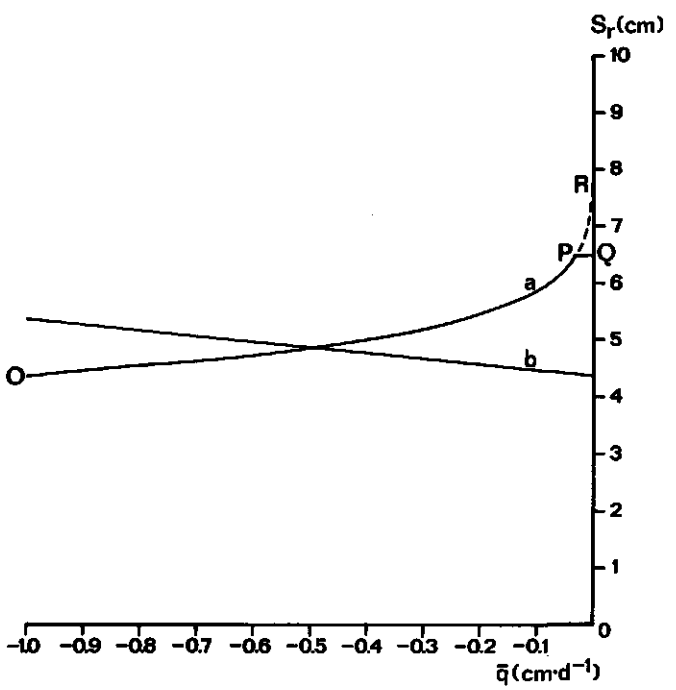

Fig. 17. Relation between S_r and $\bar{q}$ for percolation.
Curve a: $S_r(\bar{q},S_u)$ for $S_u = 16.1$ cm (OPQ) and $S_u \to \infty$ (OPR). Curve b: $S_r = 4.4 - \bar{q}$.

subsoil. Thus with percolation the curve for $\bar{q} = 0$ in Fig. 5e is always used to solve z_{rs} for a given S_s value. It may be seen from Fig. 5e that this assumption is approximately correct for shallow water-tables or low percolation rates. For deep water-tables the results are expected to be poor. However, it was found in this study that deep water-tables are usually computed by the model for the lower boundary solution (Section 4.5). Therefore, the water-table depth is, with percolation, always solved from the equilibrium curve in Fig. 5e. For the above example it is found for $S_s^{n+1} = 11.2$ cm and $\bar{q} = 0$ that $z_{rs}^{n+1} = 108$ cm.

It should be noted that the value found for the percolation rate should not exceed the saturated hydraulic conductivity. For the permeable 'medium fine sandy soil' used here to illustrate calculation procedures the problem does not arise but for soils with a lower saturated hydraulic conductivity such a situation might occur. Then $|\bar{q}^{n+1}|$ equals the saturated hydraulic conductivity as a result of which ponding of water on the upper boundary of the subsoil may occur. Serious ponding may result in a situation where the root zone becomes waterlogged ($S_r \leq 0$) while there is still a saturation deficit in the subsoil ($S_s > 0$). Generally ponding occurs when the water level has reached the soil surface in which case the water balance equations yield $S_u = S_r \leq 0$. These negative values serve as the initial saturation deficits for the next time increment in the absence of surface drainage. In the presence of a surface drainage system the saturation deficits are increased by the amount that is discharged overland during the time increment.

If the subsoil is not homogeneous with respect to the K(p) relation (Appendix A), the percolation rate at the upper boundary of the subsoil may exceed the saturated hydraulic conductivity in one of the lower layers. This causes the formation of a perched water-table due to which a steady-state situation may not exist. To avoid computational difficulties with percolation in a heterogeneous soil, one ('average') K(p) relation must be used.

4.4.2 Capillary rise

As explained earlier, the pseudo steady-state procedure may cause a rise in the phreatic level for $q_{rs} > 0$ and $q_w = 0$. This inconsistency with capillary rise, resulting from $\Delta t < \tau$, is usually small compared with that for percolation. If the situation occurs it is assumed that the position of the water table is not affected by the upper boundary flux condition but that the change in the phreatic level is governed by q_w only. The water-table depth z_{rs}^* at the end of the time increment resulting from q_w alone is computed for equilibrium conditions in the subsoil. The curve in Fig. 5e for $\bar{q} = 0$ represents the relation between z_{rs} and the equilibrium saturation deficit in the subsoil S_e. Denoting this curve by $z_{rs}(S_e)$ the solution of z_{rs}^* follows from

$$z_{rs}^* = z_{rs}^n + \frac{dz_{rs}}{dS_e} \Delta S_e \qquad (82)$$

where the change in S_e results from q_w alone, so that $\Delta S_e = -\Delta t \cdot q_w^{n+\frac{1}{2}}$. This procedure

yields a stationary position of the phreatic level for $\Delta t < \tau$ and $q_w = 0$. For a changing lower boundary flux condition the characteristic time was not defined. It is, however, assumed that the solution is consistent if the computed value for z_{rs}^{n+1} is larger than z_{rs}^*. If this condition is not valid the final water-table depth is taken equal to z_{rs}^*. For example, for an initial situation at time n with $S_s^n = 6.2$ cm and $z_{rs}^n = 80$ cm followed by a time increment of one day during which $q_{rs}^{n+\frac{1}{2}} = 0.2$ cm·d^{-1} and $q_w^{n+\frac{1}{2}} = 0.1$ cm·d^{-1}, the saturation deficit $S_s^{n+1} = 6.3$ cm and Fig. 5e yields $z_{rs}^{n+1} = 78.1$ cm, hence a rise of the phreatic level. A first interpolation in Fig. 5e for $z_{rs}^n = 80$ cm and $\bar{q} = 0$ yields $S_s^* = 6.0$ cm and a second interpolation for $S_s = S_s^* - \Delta t \times q_w^{n+\frac{1}{2}} = 6.0 - 0.1 = 5.9$ cm and $\bar{q} = 0$ gives $z_{rs}^* = 79.4$ cm. Thus $z_{rs}^{n+1} = \max(z_{rs}^{n+1}, z_{rs}^*) = \max(78.1, 79.4) = 79.4$ cm. Without the corrective procedure the rise of the water level would have been 1.9 cm. The calculated rise of 0.6 cm is caused by the lower boundary flux condition which is positive in an upward direction.

4.4.3 Rainfall excess following capillary rise

A situation with capillary rise followed by rainfall excess represents the most extreme case of a changing upper boundary flux condition; the flux does not only change in magnitude but also in direction. If the root zone is dry and the amount of water infiltrating through the soil surface is relatively small, the situation at the end of the time increment may be highly non-steady. As the pseudo steady-state approach is not likely to perform well, the following procedure is proposed. Given an initial situation at time n, the computation of the situation at time n+1 consists of two steps. In the first step, prior to the solution of $\bar{q}$, the total saturation deficit is redistributed to a steady-state situation corresponding to the initial water-table depth, taking into account the rainfall excess. Thus for z_{rs}^n and $S_u^* = S_u^n - q_s^{n+\frac{1}{2}} \times \Delta t$ the steady-state soil moisture distribution is solved. For this purpose Fig. 5h may be used to yield the corresponding flux $\bar{q}^*$. From Fig. 5e the saturation deficit S_s^* for $\bar{q}^*$ and z_{rs}^n is found, where it should be noted that if $\bar{q}^* < 0$ the curve for $\bar{q} = 0$ must be used as an equilibrium moisture distribution in the subsoil is assumed when there is percolation. The saturation deficit in the root zone is computed as $S_r^* = S_u^* - S_s^*$. If the actual z_{rs}^n value does not correspond with the initial steady-state situation due to the corrective procedure discussed in Section 4.4.2, S_r^* may be greater than S_r^n. Then S_r^* is set equal to S_r^n.

In the second step the pseudo steady-state procedure is applied with $S_u^n = S_u^*$, $S_r^n = S_r^*$, $q_s^{n+\frac{1}{2}} = 0$ and the given lower boundary condition $q_w^{n+\frac{1}{2}}$. The advantage of this procedure is that it does not give rise to inconsistencies. But more important is the phenomenon that it allows for a transport of water from the root zone to the subsoil even when the computed steady-state yields a situation with capillary rise. In this way redistribution accounts for the usual discrepancy between the actual duration of the rain shower and the length of the time increment used in the model. The procedure is elucidated by the following example.

Given at time n: $S_u^n = 21.1$ cm, $S_r^n = 9.8$ cm and $z_{rs}^n = 100$ cm. For the next time increment ($\Delta t = 10$ d) the following boundary conditions apply: $q_s^{n+\frac{1}{2}} = -0.37$ cm·d^{-1} and $q_w^{n+\frac{1}{2}} = 0$ cm·d^{-1}. The redistribution of soil moisture in the first step of the procedure

is calculated as follows. For $z_{rs}^{n} = 100$ cm and $S_u^* = S_u^n + q_s^{n+\frac{1}{2}} \times \Delta t = 21.1 - 0.37 \times 10 = 17.4$ cm it is found from Fig. 5h that $\bar{q}^* = 0.03$ cm·d^{-1}. Interpolation in Fig. 5e for $z_{rs}^{n} = 100$ cm and $\bar{q}^* = 0.03$ cm·d^{-1} yields $S_s^* = 10.0$ cm, so that $S_r^* = S_u^* - S_s^* = 17.4 - 10.0 = 7.4$ cm. For the second step the pseudo steady-state procedure is applied with $S_u^n = S_u^* = 17.4$ cm, $S_r^n = S_r^* = 7.4$ cm, $q_s^{n+\frac{1}{2}} = 0$ and the lower boundary condition $q_w^{n+\frac{1}{2}}$ which has been given equal to zero. It follows from the water balance (Eqn 80) that $S_u^{n+1} = 17.4$ cm for which value the relation $S_r(\bar{q},S_u)$ is computed. From this relation and $S_r = S_r^n - \bar{q} \times \Delta t$ it may be found that $\bar{q}^{n+1} = 0.022$ cm·d^{-1} and $S_r^{n+1} = 7.2$ cm. Interpolation in Fig. 5e for $S_s^{n+1} = 10.2$ cm and $\bar{q}^{n+1} = 0.022$ cm·d^{-1} yields $z_{rs}^{n+1} = 102$ cm. The example shows that almost one third of the rainfall excess has entered the subsoil ($\Delta S_s = -1.1$ cm), while there is still capillary rise resulting in a drawdown of the water table by 2 cm.

4.4.4 Flow chart for the upper boundary solution

The flow chart in Fig. 18 shows the calculation scheme of the pseudo steady-state solution for the upper boundary flux condition. To simplify the diagram those situations for which the phreatic level rises into the root zone are not considered. Before application a number of relations have to be computed. The saturation deficit in the root zone is integrated for 13 values of p_{rs} mentioned in Appendix A, yielding $S_r(p_{rs})$. The computation of $S_s(z_{rs},\bar{q})$ and $S_s(p_{rs},\bar{q})$ is discussed in Appendix A. Combining these relations with $S_r(q_{rs})$ gives $S_u(z_{rs},\bar{q})$ and $S_u(p_{rs},\bar{q})$.

The steps indicated in the flow chart are elucidated as follows.

1. Given values for S_u^n and S_r^n the initial steady-state is fully determined. As the water-table depth may not correspond to the steady-state situation, its value must be given. In this scheme it is assumed that z_{rs} applies halfway the previous time increment.
2. The length of the time increment and boundary conditions have to be specified. The flux q_s must be regarded as the maximum possible flow rate across soil surface. The real upper boundary flux q_s^{re} may be different due to desiccation or complete saturation of the root zone.
3. Interpolation in Fig. 5g is required to determine whether the initial situation corresponds to capillary rise ($\bar{q}^n > 0$) or percolation ($\bar{q}^n < 0$).
4. Check whether this is a situation with rainfall excess ($q_s^{n+\frac{1}{2}} < 0$) following a period with capillary rise ($\bar{q}^n > 0$).
5. If there is excess of rainfall following a period with capillary rise, soil moisture is redistributed as discussed in Section 4.4.3.
6. Compute S_u^{n+1} from the water balance equation.
7. The computation of the relation between S_r^{n+1} and $\bar{q}^{n+1}$ for S_u^{n+1} is discussed in Section 4.4.1 for $\bar{q} < 0$, while for $\bar{q} > 0$ an example is shown in Fig. 5g. The relation based on the water balance may be written as $S_r^{n+1} = S_r^n + \Delta t(q_s^{n+\frac{1}{2}} - \bar{q}^{n+1})$. The relation $S_r(\bar{q},S_u)$ is defined for $-K_{sat} \leq \bar{q} \leq \bar{q}_{max}$ where K_{sat} is the saturated hydraulic conductivity and $\bar{q}_{max}$ is the maximum possible rate of capillary rise. If $\bar{q}^{n+1}$ is outside this range of $\bar{q}$ values a solution cannot be obtained.
8. Check the upper constraint of $\bar{q}^{n+1}$.
9. Apply the scheme explained in Table 2 to compute the reduced upper boundary flux q_s^{re}.

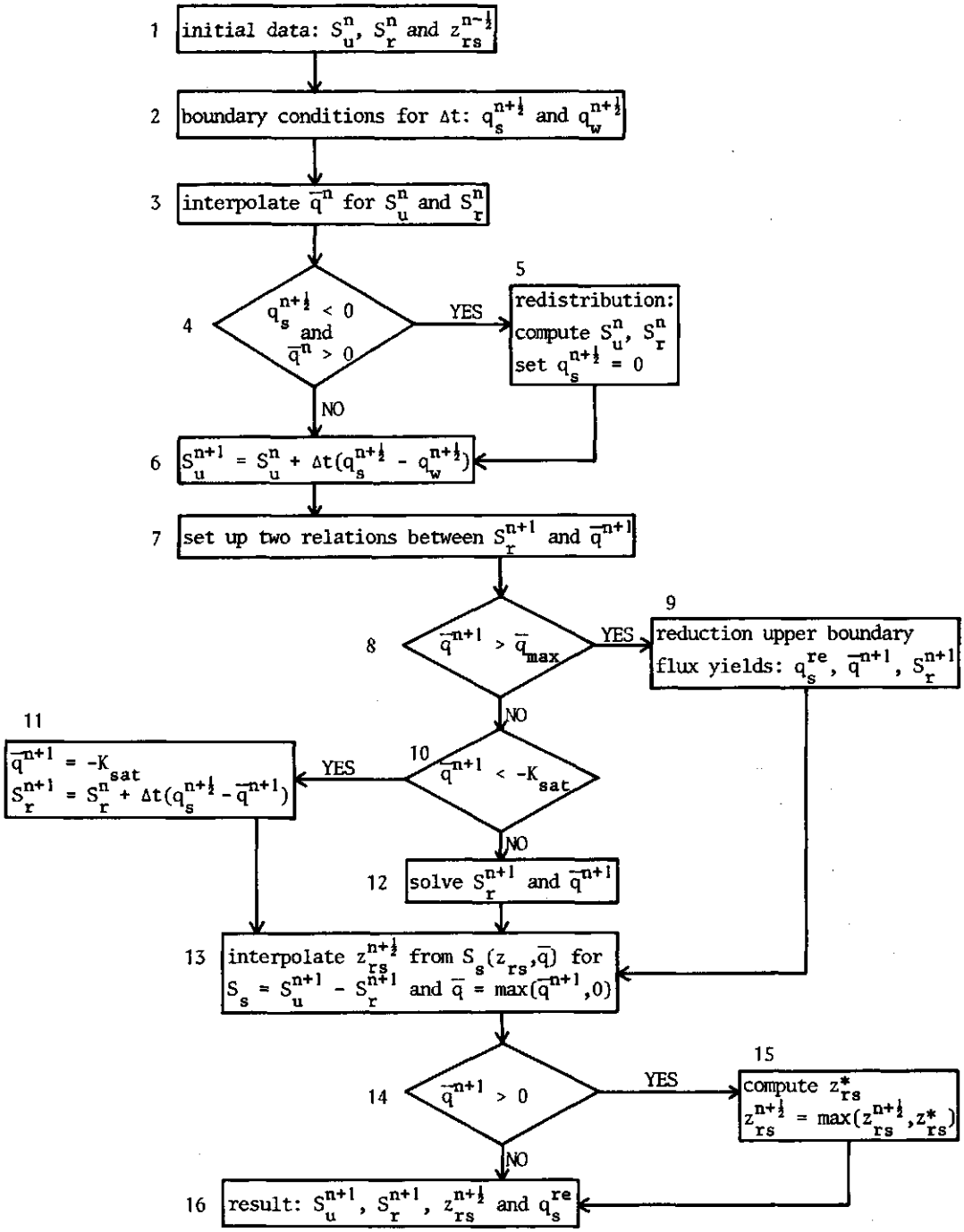

Fig. 18. Simplified flow chart of the solution for the upper boundary flux condition. For explanation see the text.

This scheme yields $\bar{q}^{n+1}$, while S_r^{n+1} is set equal to its maximum value (corresponding to pF 4.2).

10. Check the lower constraint of $\bar{q}^{n+1}$.
11. The value for $\bar{q}^{n+1}$ equals $-K_{sat}$ and S_r^{n+1} follows from the water balance.
12. Solve $\bar{q}^{n+1}$ and S_r^{n+1} from the relations set up in Step 7.
13. When interpolating the water-table depth, $\bar{q} = 0$ must be used if $\bar{q}^{n+1} < 0$ to avoid the inconsistency as discussed in Section 4.4.1.
14. Check for a situation of capillary rise ($\bar{q}^{n+1} > 0$).
15. Use the procedure discussed in Section 4.4.2 to correct for a possible inconsistency in the computed water-table depth.
16. The scheme yields initial values for the following time increment and the real upper boundary flux q_s^{re}. If required other values, such as p_{rs} and q_{rs} are easily derived.

4.5 LOWER BOUNDARY SOLUTION

The solution for the lower boundary flux condition is based on the concept that the soil moisture distribution may be approached by a sequence of steady-state situations corresponding to the lower boundary flux q_w. The solution applies to the lower part of the subsoil and the situations for which the storage coefficient is independent of the water-table depth.

For steady flow conditions the storage coefficient is defined as

$$\mu = \Delta S_s / \Delta z_{rs} \tag{83}$$

where μ is a function of z_{rs} and $\bar{q}$. The relation $\mu(z_{rs},\bar{q})$ derived from $S_s(z_{rs},\bar{q})$ is presented in Fig. 19 for $\bar{q} \leq 0$. As a result of the schematization of the pressure profiles (Fig. 5c), the storage coefficient for a particular percolation rate is either

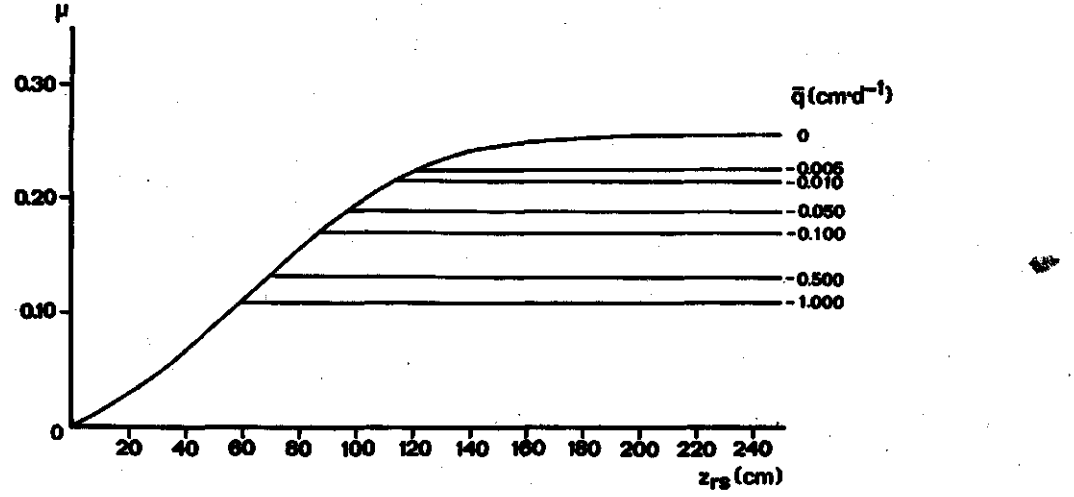

Fig. 19. Storage coefficient μ as a function of the water-table depth z_{rs} for a number of steady flow situations $\bar{q}$.

constant or equal to the μ value for the equilibrium profile. For situations that μ is independent of the water-table depth the storage coefficient is denoted by μ_q. The relation between μ_q and $\bar{q}$ is easily derived, as for steady percolation $\bar{q} = -K$. With the aid of the soil moisture characteristic the relation $K(p)$ is transformed into $K(\theta)$. Using the relation $\bar{q}(\theta) = -K(\theta)$ as its inverse $\theta(\bar{q})$, it follows (Fig. 20) that $\mu_q = n - \theta(\bar{q}) = \mu_q(q_w)$ where $q_w = \bar{q}$. For the most relevant values for q_w (say $-1.0 < q_w < -0.01$ cm·d^{-1}) the relation $\mu_q(q_w)$ may often be approximated by

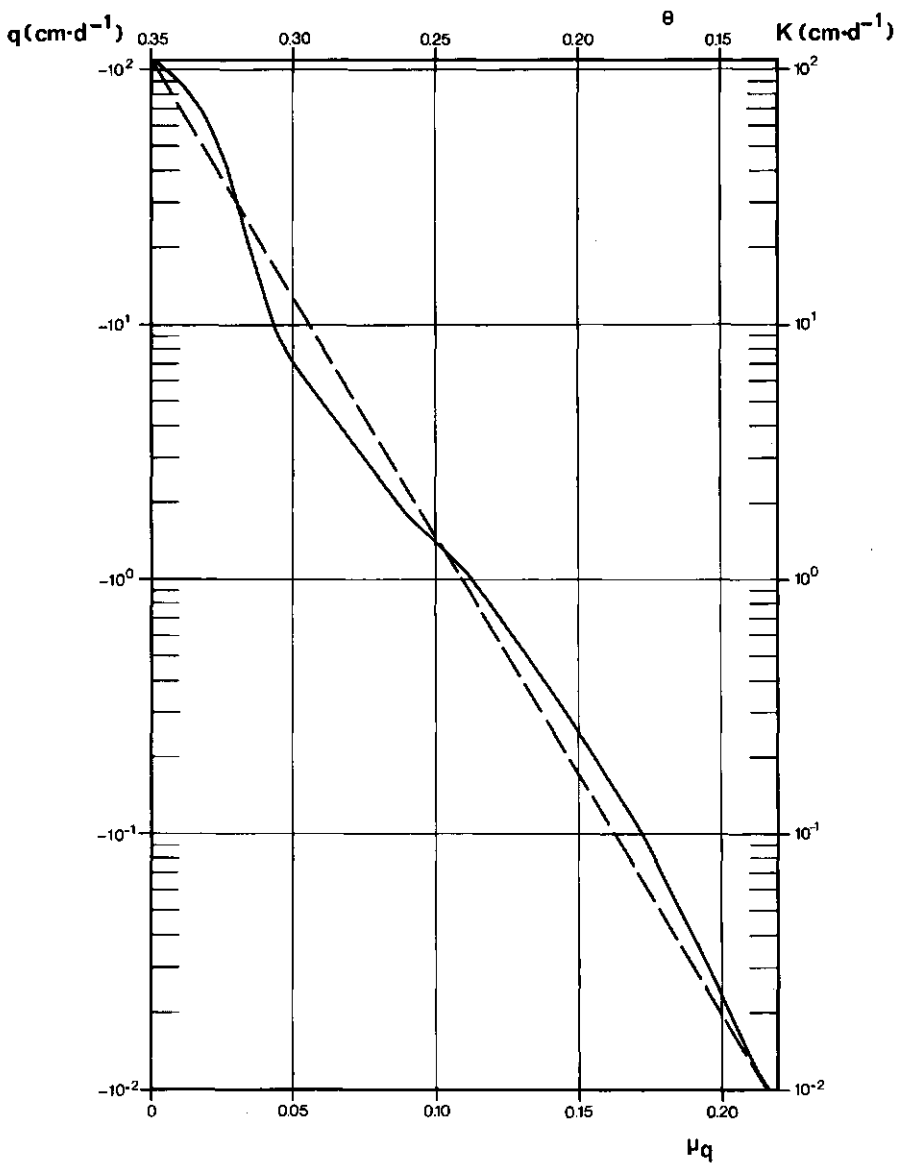

Fig. 20. Relation between the hydraulic conductivity K and the moisture content θ used as a relation between the steady flux $\bar{q}$ and the storage coefficient μ_q. The approximate relation (broken line) is given by Eqn 84.

$$\mu_q = A + B \lg(-q_w) \tag{84}$$

where the constants A and B depend on the soil physical properties. For the medium fine sandy soil used here A = 0.110 and B = -0.054 yield the broken line in Fig. 20.

The model for the lower boundary solution does not consider flow in the upper part of the subsoil. The initial equilibrium moisture profile serves as the upper boundary of the model. For example, consider an initial situation for z_{rs} = 85 cm and $\bar{q}$ = 0, followed by a time increment Δt = 5 d during which q_w = -1.0 cm·d^{-1}. Superposition of the moisture profile for $\bar{q}$ = -1.0 cm·d^{-1} on the initial equilibrium curve yields the soil moisture distribution as shown in Fig. 21a. The moisture profile corresponding to the downward flux across the lower boundary is termed 'percolation profile'. Since the percolation profile is at the upper and lower side bounded by the same curve it may be schematized to a rectangle (Fig. 21b). The upper boundary of the model is situated at a height $\zeta_p = \zeta_{rs} - z_{rs}$, where z_{rs} is the initial water-table depth (z_{rs} = 85 cm). The shaded area equals the saturation deficit of the percolation profile S_p. The rectangular shape results from the restriction that the lower boundary solution only applies to situations for which $\mu = \mu_q$ and therefore is independent of z_{rs}. It allows the saturation deficit to be expressed as

$$S_p = \mu_q(\zeta_p - \zeta) \tag{85}$$

where ζ is the actual height of the water table, the level for which p = 0. The water balance of the lower boundary model may be written as

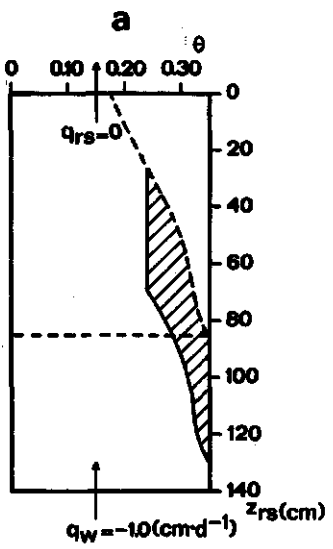

Fig. 21a. Moisture profile for $\bar{q}$ = -1.0 cm·d^{-1} superimposed on the initial equilibrium soil moisture distribution (broken line), where the shaded area equals the saturation deficit S_p of the percolation profile (S_p = 5 cm).

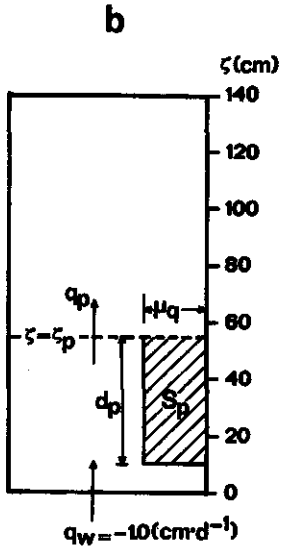

Fig. 21b. Schematization of the percolation profile used for the lower boundary solution.

$$S_p^{n+1} = S_p^n + \Delta t(q_p^{n+\frac{1}{2}} - q_w^{n+\frac{1}{2}}) \qquad (86)$$

where q_p is the flux (positive upwards) across the level ζ_p. When solving ζ from Eqn 85 the same difficulties arise as for the upper boundary solution. The saturation deficit and boundary flux condition which determine the steady-state solution do not apply at the same time. In view of the approximate nature of the analysis little of its generality is lost when $\zeta^{n+\frac{1}{2}}$ is solved from Eqn 85 with $S_p^{n+\frac{1}{2}}$ replaced by S_p^{n+1}. Hence, the solution for ζ at time $n+\frac{1}{2}$ follows from

$$\zeta^{n+\frac{1}{2}} = \zeta_p - \frac{S_p^{n+1}}{\mu_q(q_w^{n+\frac{1}{2}})} \qquad (87)$$

The flow chart in Fig. 22 shows the calculation scheme of the pseudo steady-state solution for the lower boundary flux condition. When flow in the upper part of the unsaturated zone can be neglected, q_p equals zero and ζ_p corresponds to the phreatic level at the onset of the calculations. This situation applies shortly after a sudden lowering of the level in open water courses or during the early stages of a pumping test. In general ζ_p and q_p depend on flow in the upper part of the unsaturated zone. A solution of these variables is obtained in combination with the model for the upper boundary solution, as discussed in the next section.

For a numerical example, consider the situation of Fig. 21 to apply at time n, so that $S_p^n = 5.0$ cm. For the next time increment ($\Delta t = 5$ d) the following boundary conditions are assumed: $q_p^{n+\frac{1}{2}} = 0$ and $q_w^{n+\frac{1}{2}} = -0.1$ cm·d^{-1}. It follows from the water balance (Eqn 86) that $S_p^{n+1} = 5.5$ cm. Calculating the storage coefficient from Eqn 84 gives

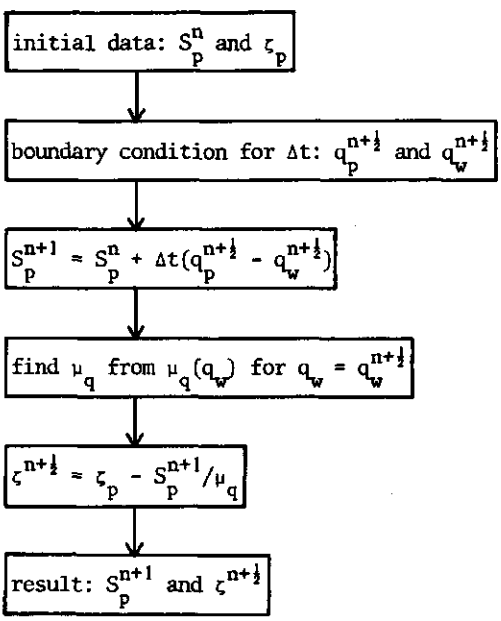

Fig. 22. Flow chart for the lower boundary solution. For explanation see the text.

$\mu_q = 0.110 - 0.054 \lg(0.1) = 0.164$. Noting $\zeta_p = 55$ cm, it follows from Eqn 87 that $\zeta^{n+\frac{1}{2}} = 55 - 5.5/0.164 = 21.5$ cm. Since $\zeta^{n-\frac{1}{2}} = 9.5$ cm this corresponds to a rise of the phreatic level with 12 cm. The rise is caused by the decrease in flow rate across the lower boundary from $q_w^{n-\frac{1}{2}} = -1.0$ cm·d^{-1} to $q_w^{n+\frac{1}{2}} = -0.1$ cm·d^{-1}. This effect (a rise without recharge ($q_p = 0$) from above) is similar to the phenomenon of delayed yield (Section 3.1).

4.6 COMBINED PSEUDO STEADY-STATE SOLUTION

Transient unsaturated flow is approached by a sequence of steady-state situations corresponding to the upper boundary flux of the subsoil q_{rs}. For capillary rise the assumption of steady flow is seriously violated if the flux across the lower boundary is large in the downward direction so that the actual soil moisture profile has a more elongated shape than the assumed steady-state profile. Therefore the drawdown of the water table is recalculated assuming steady flow in the lower part of the subsoil corresponding to the lower boundary flux q_w. If the lower boundary solution yields a water-table depth below the level that is found with the steady-state solution for $\overline{q}^{n+1}$, a percolation profile develops. The upper boundary of the percolation profile ζ_p equals the phreatic level at the time it starts to develop and remains unchanged during the period the percolation profile exists. The difference in the calculated phreatic levels is an indication to what extent the steady-state profile for $\overline{q}^{n+1}$ is elongated.

Below the upper boundary of the percolation profile the flow is always downwards. For a solution of the flux q_p across this level the following conditions can be formulated. The flux q_p must be

1. downwards in order to satisfy flow conditions in the lower boundary model,
2. equal to $\overline{q}^{n+1}$ for steady percolation in the upper boundary model,
3. approaching zero when the pF in the root zone reaches its maximum value,
4. independent of flow conditions in the lower boundary model in order to avoid an iterative solution.

These properties are obtained if $q_p^{n+\frac{1}{2}}$ is taken equal to the steady flux solved with the scheme in Fig. 18 for the situation that the water table is at infinite depth. The solution uses the relation $S_r(\overline{q},S_u)$ for $S_u \to \infty$ (Curve a (OPR) in Fig. 17) so that $q_p^{n+\frac{1}{2}} < 0$ and $q_p^{n+\frac{1}{2}} \leq \overline{q}^{n+1}$.

For the combined model to be consistent it is necessary that for $S_p \to 0$ the water-table depth z_{rs} found with the upper boundary solution is below the level ζ found with the lower boundary solution. Since $\zeta = \zeta_p$ for $S_p = 0$ (Eqn 87) the condition for consistency may be formulated as

$$z_{rs} > \zeta_{rs} - \zeta_p \qquad \text{for} \qquad S_p \to 0 \tag{88}$$

The validity of this condition is demonstrated with the use of the relation $z_{rs}(S_e)$ introduced in Section 4.4.2. If ΔS_e is the increase of the S_e value since the time the percolation profile started to develop, a positive value of ΔS_e necessarily yields a water-table depth z_{rs} below the level ζ_p. Thus Eqn 88 may be replaced by the condition $\Delta S_e > S_p$ for $S_p \to 0$. As a result of the corrective procedure introduced to avoid incon-

sistency with capillary rise (Section 4.4.2) $dS_e \geq -q_w dt$. Since $q_p < 0$ and $dS_p = (q_p - q_w)dt$, it follows that $dS_e/dt > dS_p/dt$. Hence, if a percolation profile exists ($S_p > 0$ and $q_w < 0$) the condition $\Delta S_e > S_p$ is valid during periods with capillary rise. For rainfall excess redistribution causes the saturation deficit in the subsoil S_s to be equal to S_e at the beginning of the percolation period. During percolation the equilibrium profile applies in the subsoil so that $S_e = S_s$ and thus $dS_e = (\bar{q} - q_w)dt$. Since $\bar{q} \geq \bar{q}_p$ it follows that $dS_e/dt \geq dS_p/dt$. Hence the condition $\Delta S_e > S_p$ is always valid.

Soil moisture characteristics and K(p) relations are subject to hysteresis. Though the effects may be considerable, it was mentioned that they may often be neglected when both relations are combined (e.g. into a K(θ) relation). When computing the saturation deficit curves for the subsoil, both relations have indeed been used. Therefore hysteresis effects are only considered for the root zone. The use of a hysteretic soil moisture

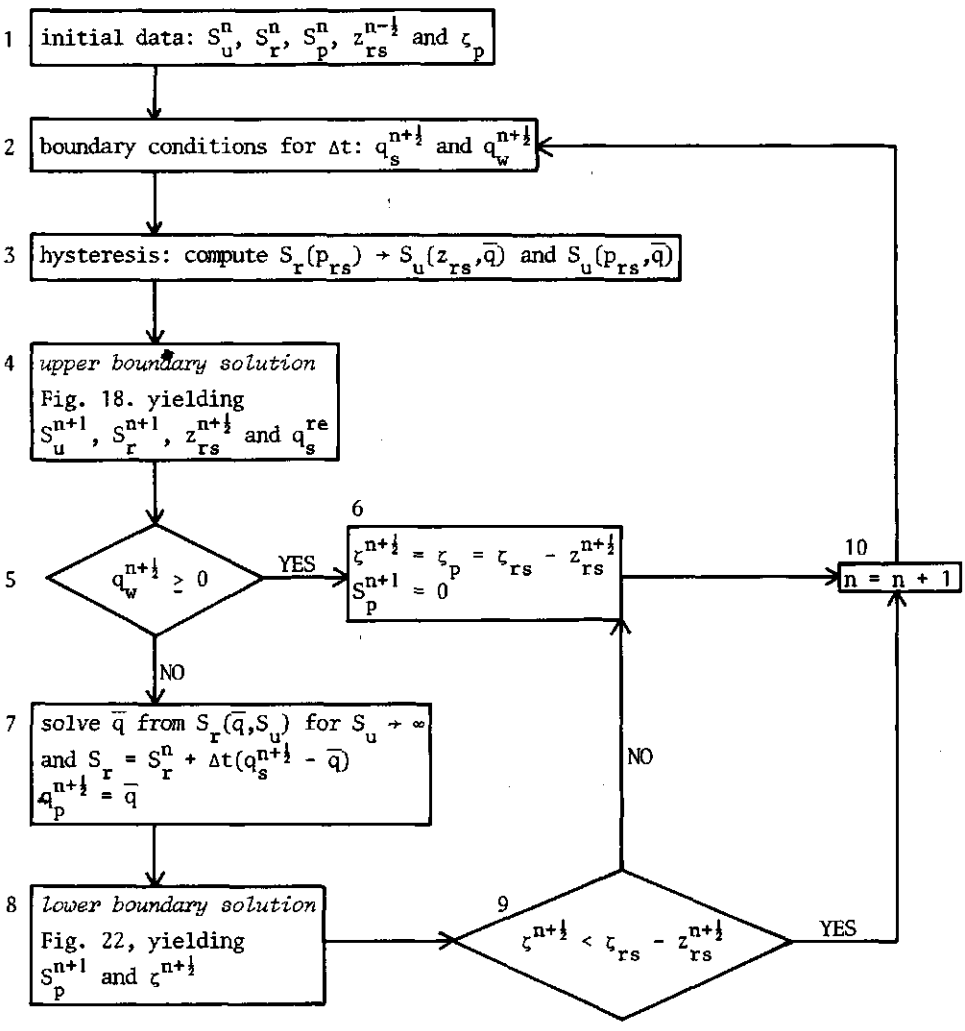

Fig. 23. Simplified flow chart of the combined model for unsaturated flow. For explanation see the text.

characteristic to compute $S_r(p_{rs})$ causes this relation to become time-variant and consequently relations for S_u will also change in time. The effect of hysteresis on the $S_r(p_{rs})$ relation is discussed in Appendix B.

The flow chart of the combined model for unsaturated flow is given in Fig. 23. To obtain a surveyable diagram, situations for which the water level rises into the root zone are not considered. The steps indicated in the flow chart are elucidated as follows.

1. Calculations are preferably started for a situation that $S_p = 0$. This situation can be expected in shallow water-table aquifers after a long wet period (with $q_p < q_w$). Initial values for S_u and S_r are found from Fig. 5 for a given water-table depth and a $\bar{q}$ value corresponding to the rainfall excess in the preceding period. For situations that S_p cannot be neglected, initial values for S_p and ζ_p have to be estimated.
2. For a given length of the time increment a constant flux at the upper and lower boundary must be specified.
3. The computation of $S_r(p_{rs})$ is discussed in Appendix B. It should be noted that as a consequence of a changing $S_r(p_{rs})$ relation, the relations for S_u are also time-variant.
4. The upper boundary solution is given in Fig. 18.
5. Check for the sign of the lower boundary flux condition.
6. A percolation profile does not exist.
7. The flux $q_p^{n+\frac{1}{2}}$ equals the steady flux $\bar{q}$ for the situation that $S_u \rightarrow \infty$.
8. The lower boundary solution is given in Fig. 22.
9. Check whether the lower boundary solution yields a level ($\zeta^{n+\frac{1}{2}}$) below the phreatic level that is found with the upper boundary solution ($\zeta_{rs} - z_{rs}^{n+\frac{1}{2}}$).
10. The time index may be increased if required.

5 A quasi three-dimensional approach

For the solution of saturated-unsaturated sub-surface flow in shallow water-table aquifers, it is assumed that the Dupuit-Forchheimer assumptions are approximately valid. The three-dimensional flow system may then be schematized into horizontal flow in the saturated part and vertical flow in the unsaturated region. If the fluctuations of the water table are small as compared with the total saturated thickness D of the aquifer, the latter may be taken as a constant. The value of D is chosen such that the upper boundary of the saturated zone is just beneath the lowest phreatic level occurring in the period considered. Since water and soil are assumed incompressible, storage changes are restricted to the unsaturated zone. Taking into account recharge from the overlying partly saturated region, unconfined saturated flow is described by Eqn 45, rewritten here for convenience as

$$\frac{\partial}{\partial x}\left(T(x,y)\,\frac{\partial h}{\partial x}\right) + \frac{\partial}{\partial y}\left(T(x,y)\,\frac{\partial h}{\partial y}\right) = q_w(x,y,h,t) \qquad (89)$$

where the transmissivity $T = \bar{K}D$. If R is the region for which Eqn 89 holds and S_1 and S_2 constitute the boundary of R, the conditions valid at the boundary may be formulated as

$$\text{on } S_1: \qquad h = h^*(x,y,t) \qquad (90a)$$

$$\text{on } S_2: \qquad \frac{\partial h}{\partial n} = 0 \qquad (90b)$$

where the phreatic level h^* on S_1 is supposed to be given and n is the direction normal to the boundary.

Figure 24 is the schematization of the saturated-unsaturated sub-surface flow system in the vertical plane. It shows a cross section of an unconfined aquifer bounded by a stream and a groundwater divide (no-flow boundary). The model for unsaturated flow is presented at one particular location only. The lower boundary of this model ($\zeta = 0$) is taken at a height D above the impermeable base of the aquifer. At the soil surface the upper boundary flux condition q_s is supposed to be given as a function of x, y and t.

For the simulation of transient sub-surface flow the time is discretized to small steps. During a time increment Δt, extending from time n to n+1, flow is assumed to be steady. The Dirichlet conditions at the boundary on S_1 and the Neumann conditions at the soil surface apply halfway the time increment. The solution of the steady-state saturated-unsaturated flow situation is then obtained at time $n+\frac{1}{2}$ and yields the internal boundary flux q_w. The procedure comprises three steps: (i) computation of a relation between q_w and h, (ii) solution of the steady-state saturated flow situation, and (iii) solution of

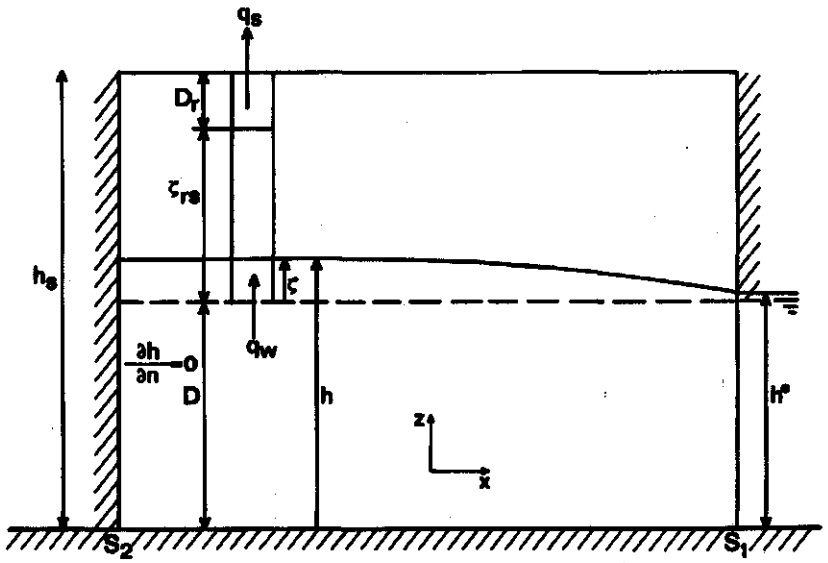

Fig. 24. Schematic presentation in the vertical plane and boundary conditions of the quasi three-dimensional approach to saturated-unsaturated flow.

the steady-state unsaturated flow situation.

(i) relation between q_w and h

Application of the model for unsaturated flow for $q_s^{n+\frac{1}{2}}$ and for different values of $q_w^{n+\frac{1}{2}}$ yields a relation between the change in the position of the water table $\Delta\zeta = \zeta^{n+\frac{1}{2}} - \zeta^{n-\frac{1}{2}}$ and $q_w^{n+\frac{1}{2}}$. Since $\zeta = h - D$, it follows that $\Delta\zeta = \Delta h$. If q_w is either positive or small in the downward direction, the relation between the lower boundary flux and the change in the phreatic level is approximately linear:

$$q_w^{n+\frac{1}{2}} = a \cdot \Delta h + b \qquad (91)$$

where a and b are constants to be determined for each time step. The approximate linearity stems from the relation between S_u and z_{rs} in Fig. 5h. This relation governs the water-table depth in the absence of a percolation profile. The equilibrium curve used when $\bar{q} \leq 0$ shows that for a small change in the water-table depth dS_u/dz_{rs} is approximately constant. For capillary rise the solved value of $\bar{q}$ decreases slightly if S_u increases due to q_w alone, so that (see Fig. 5h) dS_u/dz_{rs} approaches a constant value. Since dS_u/dz_{rs} is proportional to dq_w/dh, it follows for a small change in the phreatic level during the time increment that Eqn 91 is approximately valid.

Large changes in h usually involve large negative q_w values in which case the phreatic level is governed by Eqn 87. Introducing d_p as the depth of the water table below the upper boundary of the percolation profile (Fig. 21b) gives

$$\zeta_p = d_p + \zeta \qquad (92)$$

Substituting Eqn 92 for time $n-\frac{1}{2}$ into Eqn 87 yields

$$\zeta^{n+\frac{1}{2}} = \zeta^{n-\frac{1}{2}} - \frac{S_p^{n+1}}{\mu_q(q_w^{n+\frac{1}{2}})} + d_p^{n-\frac{1}{2}} \qquad (93)$$

Replacing S_p^{n+1} by Eqn 86, $\mu_q(q_w^{n+\frac{1}{2}})$ by Eqn 84 and introducing $\Delta h = \zeta^{n+\frac{1}{2}} - \zeta^{n-\frac{1}{2}}$ into Eqn 93 gives

$$\Delta h = \frac{q_w^{n+\frac{1}{2}} \cdot \Delta t - q_p^{n+\frac{1}{2}} \cdot \Delta t - S_p^n}{A + B \lg(-q_w^{n+\frac{1}{2}})} + d_p^{n-\frac{1}{2}} \qquad (94)$$

Equation 94 is valid for $q_w^{n+\frac{1}{2}} < 0$ and $S_p^{n+1} > 0$. It follows from Eqn 86 that the condition $S_p^{n+1} > 0$ may be written as $q_w^{n+\frac{1}{2}} < q_p^{n+\frac{1}{2}} + S_p^n/\Delta t$. Hence, Eqn 94 applies for $q_w^{n+\frac{1}{2}} < \min(0, q_p^{n+\frac{1}{2}} + S_p^n/\Delta t)$.

The implicit non-linear expression for q_w in Eqn 94 and the explicit one in Eqn 91 are combined as follows. The model for unsaturated flow is applied for an arbitrary negative value of $q_w^{n+\frac{1}{2}}$ to yield $q_p^{n+\frac{1}{2}}$. In order to solve the constants a and b in Eqn 91 the model for unsaturated flow is used twice to compute Δh for a small positive value of $q_w^{n+\frac{1}{2}}$ and $q_w^{n+\frac{1}{2}} = \min(0, q_p^{n+\frac{1}{2}} + S_p^n/\Delta t)$. The latter value of $q_w^{n+\frac{1}{2}}$ yields a water-table depth below or equal to ζ_p, while Eqn 94 yields $\Delta h = d_p^{n-\frac{1}{2}}$, or $\zeta^{n+\frac{1}{2}} = \zeta_p$. For decreasing values of $q_w^{n+\frac{1}{2}} < \min(0, q_p^{n+\frac{1}{2}} + S_p^n/\Delta t)$, Δh decreases linearly according to Eqn 91 and more than linearly according to Eqn 94. The point of intersection q_w^* is found by a Newton iterative procedure. An example of the time-dependent relation between q_w and Δh used to solve Eqn 89 is given in Fig. 25.

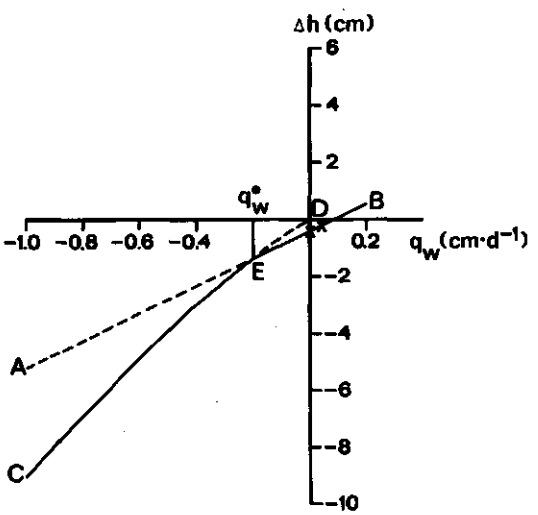

Fig. 25. The solid line (CEB) is an example of the time-variant relation between q_w and Δh used to solve Eqn 89. The linear part (AB) results from two applications of the model for unsaturated flow for $q_w = 0$ and $q_w = 0.05$ cm·d^{-1} (indicated by ×). The non-linear part (CD) is computed from Eqn 94 with $\Delta t = 1$ d, $S_p = 0$, $d_p = 0$, $q_p = 0$, $A = 0.110$ and $B = -0.054$. Both relations intersect at E for $q_w^* = -0.2$ cm·d^{-1}.

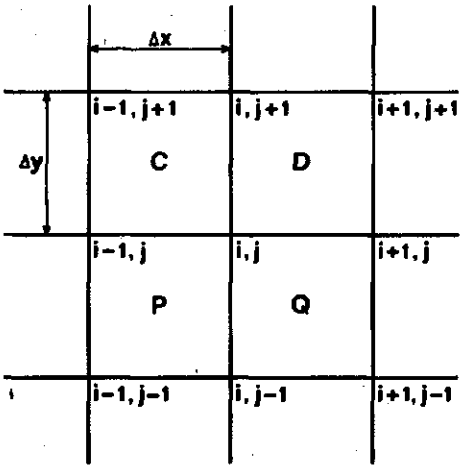

Fig. 26. Grid configuration for two-dimensional horizontal flow.

(ii) solution of saturated flow

For a numerical solution of Eqn 89 the region R is schematized to a horizontal x,y grid. If the nodes in the x direction are subscripted by i and those in the y direction by j (Fig. 26) the finite difference equation to Eqn 89 at time $n+\frac{1}{2}$ may be written as

$$\frac{(T_{i+1,j} + T_{i,j})(h_{i+1,j}^{n+\frac{1}{2}} - h_{i,j}^{n+\frac{1}{2}})}{2(\Delta x)^2} - \frac{(T_{i,j} + T_{i-1,j})(h_{i,j}^{n+\frac{1}{2}} - h_{i-1,j}^{n+\frac{1}{2}})}{2(\Delta x)^2} +$$

$$\frac{(T_{i,j+1} + T_{i,j})(h_{i,j+1}^{n+\frac{1}{2}} - h_{i,j}^{n+\frac{1}{2}})}{2(\Delta y)^2} - \frac{(T_{i,j} + T_{i,j-1})(h_{i,j}^{n+\frac{1}{2}} - h_{i,j-1}^{n+\frac{1}{2}})}{2(\Delta y)^2} = (q_w)_{i,j}^{n+\frac{1}{2}} \qquad (95)$$

Equation 95 is applied for each of the nodes for which h has to be calculated. The phreatic level is then solved with a point iterative method (Gauss-Seidel or SOR). The right side of Eqn 95 is replaced by a linear(ized) expression for q_w written (without the space index i,j) as

$$q_w^{n+\frac{1}{2}} = a(h^{n+\frac{1}{2}} - h^{n-\frac{1}{2}}) + b \qquad (96)$$

where for $q_w \geq q_w^*$ the coefficients a and b are identical to the constants in Eqn 91. For $q_w < q_w^*$ the values of a and b vary for each iteration cycle so that Eqn 96 represents the tangent to Eqn 94. The tangent for iteration cycle r is obtained for q_w^{r-1}, so that

$$\frac{1}{a^r} = \left|\frac{d(\Delta h)}{dq_w}\right|_{q_w^{r-1}} \qquad (97)$$

Differentiating Eqn 94 for q_w^{r-1}, gives the coefficient a^r (without the time subscript) as

$$a^r = \frac{(\mu_q^{r-1})^2}{\Delta t \cdot \mu_q^{r-1} - 0.43B(q_w^{r-1} \cdot \Delta t - q_p \cdot \Delta t - S_p)/q_w^{r-1}} \qquad (98)$$

so that

$$b^r = q_w^{r-1} - a^r(\Delta h)^{r-1} \qquad (99)$$

where $(\Delta h)^{r-1}$ is the change in the phreatic level calculated with Eqn 94 and μ_q^{r-1} is the storage coefficient according to Eqn 84, both for $q_w = q_w^{r-1}$.

(iii) solution of unsaturated flow

The model for unsaturated flow is applied in each node for the given upper boundary flux condition $q_s^{n+\frac{1}{2}}$ and the lower boundary flux $q_w^{n+\frac{1}{2}}$ calculated with Eqn 96. The steady-state solution yields the saturation deficit in the root zone and the subsoil, the matric pressure and the flux at the interface root zone - subsoil, and the real upper boundary flux q_s^{re}.

For the solution presented above the interface between the models for saturated and unsaturated flow has been taken at a fixed level. Equations 91 and 94 used to link both models appear to be independent of this level, provided it is located below the phreatic surface. The interface may therefore be taken just below the moving water-table, resulting in a varying reference level for ζ. The advantage of using saturation deficits instead of saturations is that such shifts in the origin of the vertical co-ordinate ζ do not involve volume transfers across the fluctuating interface, provided that the shifts remain below the water table. Therefore the model for unsaturated flow can be linked to models for saturated flow which take into account a varying thickness of the saturated flow region.

6 Application and use

6.1 EXPERIMENTAL VERIFICATION

In order to apply the quasi three-dimensional sub-surface flow model to an actual field situation, sink terms are added to the right side of Eqn 89. They involve a term q_e representing groundwater extraction from wells and a term q_o representing groundwater discharge into the open water system. Withdrawal rates from nodes in which groundwater is extracted are supposed to be specified halfway the time increment ($q_e^{n+\frac{1}{2}}$). The discharge into the surface water system is computed with the aid of a linearized relation between the flux q_o and h.

The computer program used in this study is written in FORTRAN. That part of the computer model dealing with saturated flow was developed and written by van den Akker (1972). It uses a finite element method, based on the variational principle (Zienkiewicz, 1967) to approach the solution of Eqn 89. A horizontal x,y grid is used to divide the region R into a number of sub-areas, the elements. Within each element (indicated by a letter in Fig. 26) the transmissivity is assumed constant. Using square elements, the equation for node i,j at time $n+\frac{1}{2}$ is written as (van den Akker, 1972)

$$\frac{2}{3}(T_C + T_D + T_P + T_Q)h_{i,j}^{n+\frac{1}{2}} - \frac{1}{6}[T_C(2h_{i-1,j+1}^{n+\frac{1}{2}} + h_{i,j+1}^{n+\frac{1}{2}} + h_{i-1,j}^{n+\frac{1}{2}}) +$$

$$T_D(h_{i,j+1}^{n+\frac{1}{2}} + 2h_{i+1,j+1}^{n+\frac{1}{2}} + h_{i+1,j}^{n+\frac{1}{2}}) + T_P(h_{i-1,j}^{n+\frac{1}{2}} + 2h_{i-1,j-1}^{n+\frac{1}{2}} + h_{i,j-1}^{n+\frac{1}{2}}) +$$

$$T_Q(h_{i+1,j}^{n+\frac{1}{2}} + h_{i,j-1}^{n+\frac{1}{2}} + 2h_{i+1,j-1}^{n+\frac{1}{2}})] = \ell^2(q_w)_{i,j}^{n+\frac{1}{2}} + \ell^2(q_e)_{i,j}^{n+\frac{1}{2}} + \ell^2(q_o)_{i,j}^{n+\frac{1}{2}} \qquad (100)$$

where ℓ is the mesh width ($\ell = \Delta x = \Delta y$). Application of Eqn 100 to each of the nodes for which h has to be calculated yields a set of equations which is solved by SOR. The over-relaxation parameter ω is computed according to an empirical formula

$$\omega = 2 - \pi\sqrt{\frac{2}{I^2} + \frac{2}{J^2}} \qquad (101)$$

where I and J are the number of nodes in x and y direction, respectively. The total number of iterations is controlled by the maximum local difference in the calculated value for h between two successive iteration cycles. If this difference is less than the error criterium ε for which a value is chosen at the beginning of the calculations (in this study $\varepsilon = 0.01$ cm), convergence has occurred. When testing the computer program convergence problems were encountered resulting from the discontinuity in the relation for q_w

(Fig. 25). The problem arose for the situations

$$q_w^r < q_w^* < q_w^{r-1} \tag{102a}$$

and

$$q_w^r > q_w^* > q_w^{r-1} \tag{102b}$$

The following solution to the convergence problem has been adopted. If one of the situations given by Eqn 102 occurs, Eqn 100 is recalculated for the concerning node with q_w^{r-1} set equal to q_w^*. The two relations between q_w and h now applying to q_w^{r-1} are tried until q_w^r and q_w^{r-1} both correspond to only one of these. Once the computer program proved to be internally consistent, convergent and numerically correct, it was applied to an actual field-size saturated-unsaturated flow problem.

6.1.1 Selected study area

The study area selected for simulation by the sub-surface flow model is located in the east of the Netherlands around the pumping site ''t Klooster' (Fig. 27) near Hengelo (Gld.) The area considered for simulation is 6 × 6 km^2 and is described by means of a square grid with a mesh width of 500 m (Fig. 28). The pumping station is situated exactly in the middle. Two small intermittent streams are schematized to follow the nodes. Most of the area is occupied by farmland (Fig. 29), and grass is the principal crop grown (70%). The climate is humid with moderate temperatures. The mean annual rainfall and evapotranspiration are about 75 cm and 45 cm, respectively. The region is geohydrologically characterized by a thick coarse sandy aquifer, overlying a more or less impermeable layer of fine silty sand at a depth of about 35 m, and covered on top by a few metres of aeolian loamy sand. The surface elevation taken from a detailed topographical map shows a difference between the highest and lowest grid point in the area of only 7 m.

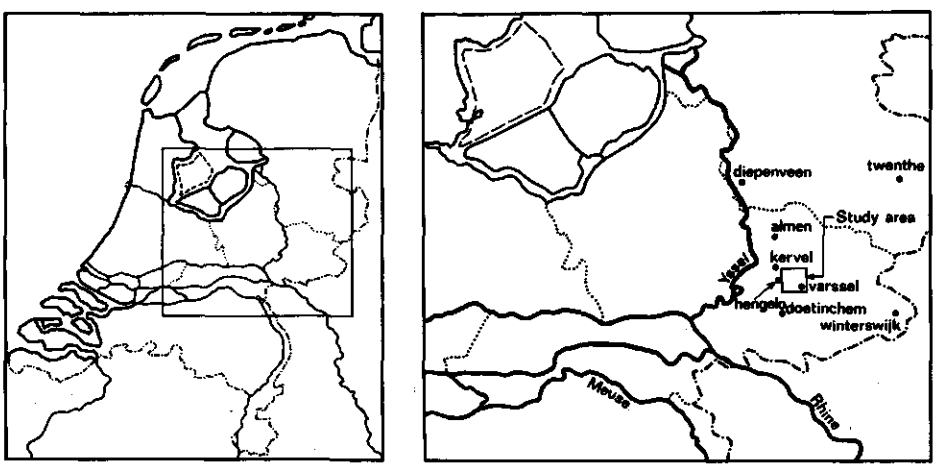

Fig. 27. Location of the study area.

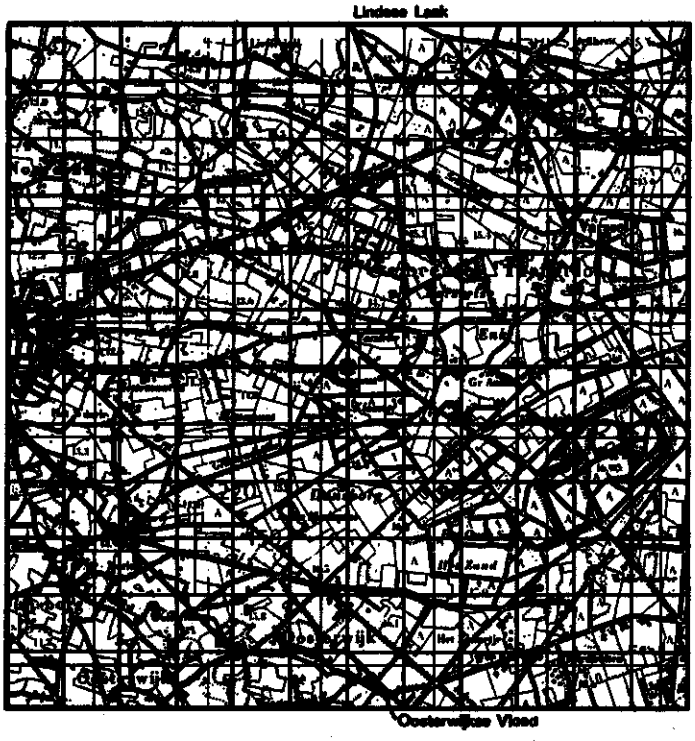

Fig. 28. Grid configuration for the study area and the schematization of both streams. × pumping site, — stream.

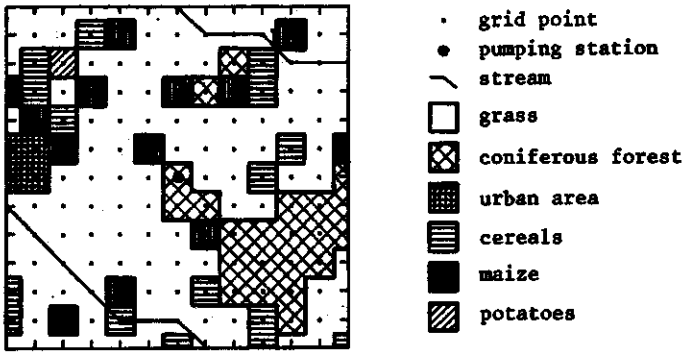

Fig. 29. Land use for the growing season of 1973 in the study area.

Water-table elevations were recorded twice a month in 28 observation wells shown in Fig. 30. The depth of the water table ranged in the period considered for simulation between zero and 4.5 m below soil surface.

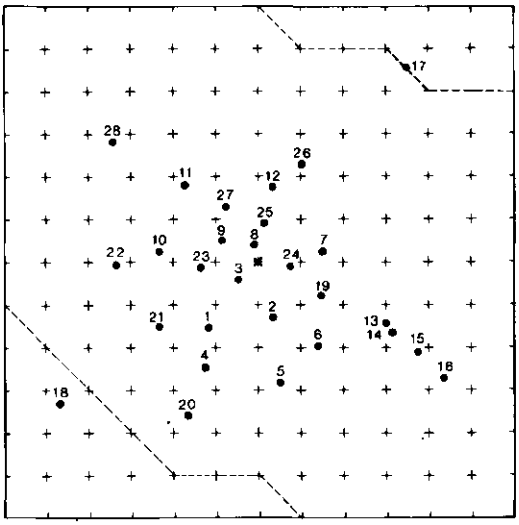

Fig. 30. Location of observation wells in the study area.

6.1.2 Saturated flow

In the eastern part of the Netherlands where the study area is located (Achterhoek) rather intensive geohydrological investigations were carried out in the past (e.g. Ernst et al., 1970). Within a radius of 6 km around the pumping site 't Klooster, the results of 13 borings are available. From the boring descriptions and grain-size data transmissivity values were estimated. These values are supported by a field pumping test carried out in 1964 by the Institute for Land and Water Management Research in Wageningen, the Netherlands. The test was held on the pumping site 't Klooster before the station came into operation. Based on results from these investigations a transmissivity map of the study area was compiled (Fig. 31). Transmissivity values used in the model range from 1700 to 3500 $m^2 \cdot d^{-1}$.

Due to the flat topography of the study area there is no surface runoff, unless the soil is completely saturated. The sub-surface discharge into the drainage system is relatively small. From investigations (Colenbrander, 1970) in a nearby experimental basin

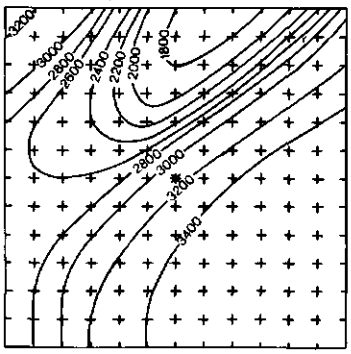

Fig. 31. Contours of transmissivity values ($m^2 \cdot d^{-1}$) in the study area.

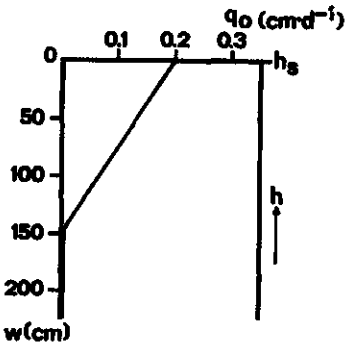

Fig. 32. Linearized empirical relation between the water-table elevation h (= h_s - w) and the groundwater discharge q_o given by Eqn 103 used in the study area.

(Leerinkbeek area) a linear relation was derived between the discharge into the surface water system q_o and the water-table depth w (Fig. 32). Since $w = h_s - h$, the groundwater discharge may be formulated as

$$q_o = \begin{cases} 0.2 & \text{for} \quad h_s - h \leq 0 \quad (103a) \\ -0.0013(h_s - h) + 0.2 & \text{for} \quad 0 < h_s - h < 150 \quad (103b) \\ 0 & \text{for} \quad h_s - h \geq 150 \quad (103c) \end{cases}$$

The relation given by Eqn 103 applies for every node. More recently Ernst (1978) showed that for the eastern part of the Netherlands an (approximate) exponentional relation applies between q_o and w. If the required data for this relation can be obtained it could be used instead of Eqn 103 without appreciable difficulties. However, it is to be expected that the simulation results are not noticeably affected as the total open water discharge from the model area and thus the groundwater discharge into the open water courses are relatively unimportant.

For the discharge of groundwater into the open water courses, schematized in nearby nodes, the drainage resistance resulting from a silt layer at the river bed and convergence of stream lines can be taken into account (de Laat & Awater, 1978). However, for the study area this approach was not considered necessary, as the two rivers are very small and only carry water during wet periods (mostly in winter time). For the nodes in which both streams were schematized, the phreatic level was taken equal to the observed open water level.

Dirichlet conditions apply for all nodes at the model boundary. The prescribed phreatic levels for each successive time step were derived from six observation wells just outside the model area.

Groundwater withdrawal from wells is restricted to the pumping site located in the centre. The extracted water is almost entirely used for domestic supply outside the study area. Extraction rates Q are available in $m^3 \cdot d^{-1}$. The flux q_e is obtained for each time step from

$$q_e = \frac{\sum_{t}^{t+\Delta t} Q(t)}{\Delta t} \quad \frac{100}{500 \cdot 500} \quad cm \cdot d^{-1} \qquad (104)$$

6.1.3 Unsaturated flow

Soil physical data were collected by the Soil Survey Institute, Wageningen, the Netherlands, in 1973 (van Holst et al., 1974). Most important soils in the study area are podzol soils (about 50%), sandy hydro-earth soils (about 20%) and very old arable fields, known as 'Enk' earth soils (about 20%). At, or near each node the soil profile was described from borings. The depth of the borings was 30 cm below the lowest water-table but not deeper than 200 cm below soil surface. The upper layer of the soil containing 80% of the roots was taken as the root zone. Values of D_r ranged between 20 and 100 cm and were rounded (for computational reasons) to decimetres. Based on the described texture the borings were compared with a large series of soil profiles of which $\theta(p)$ and $K(p)$ relations are available. This comparison resulted in eleven different soil moisture characteristics to be distinguished for the root zone. For the subsoil ten different pF-curves and three $K(p)$ relations were used. The root zone was taken as homogeneous. A typical soil moisture characteristic, used in about 25% of the nodes, is given in Fig. 33a, Curve a. With regard to their capillary properties, the selected $K(p)$ relations may be characterized as poor, medium and good (Fig. 33c). For each node one of these $K(p)$ relations was used to compute the pressure profiles. These profiles were combined with two different soil moisture characteristics to obtain the saturation deficit curves. For the upper 50 cm of the subsoil one of the ten selected pF-curves was used. Figure 33a, Curve b, shows a typical soil moisture characteristic applied for the upper part of the subsoil in about 45% of the nodes. At greater depth one $\theta(p)$ relation was used for the entire area. This relation (Fig. 33b) was actually measured in the field at a depth between 1.5 and 2 m.

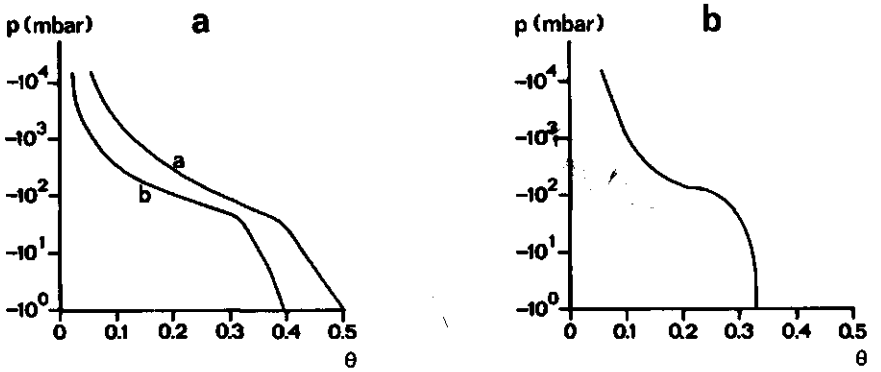

Fig. 33. Soil physical data used in the study area.
(a) Typical soil moisture characteristics used for the root zone (Curve a) and the upper part of the subsoil (Curve b).
(b) Soil moisture characteristic used for the lower part of the subsoil.

The measurements were carried out in 1977 to obtain a relation between K and θ. From this relation the parameters were derived for the lower boundary solution. The K(θ) relation was established by Bouma (1977) using the crust test in combination with an instantaneous profile method (Arya et al., 1975). Investigations at different locations do not justify a variation in the K(θ) relation within the study area. As values for q_w during the summer period range from -0.01 to -0.05 cm·d^{-1} the corresponding range of the K(θ) relation is used to derive the parameters of the $\mu_q(q_w)$ relation (84) as shown in Fig. 33d, yielding A = -0.01 and B = -0.06.

6.1.4 Surface flux

In the absence of irrigation in the study area and neglecting surface runoff, the surface flux at time n+½ follows from

$$q_s^{n+\frac{1}{2}} = E_{re}^{n+\frac{1}{2}} - P^{n+\frac{1}{2}} \qquad (105)$$

where $E_{re}^{n+\frac{1}{2}}$ is the real or actual evapotranspiration flux and $P^{n+\frac{1}{2}}$ is the precipitation flux, both taken as an average over the time increment Δt.

Precipitation was assumed to be uniformly distributed. Daily rainfall data were obtained from three different gauging stations outside and in the study area (Fig. 27): Doetinchem (1×), Kervel (1×) and Varssel (2×). The value between brackets indicates the

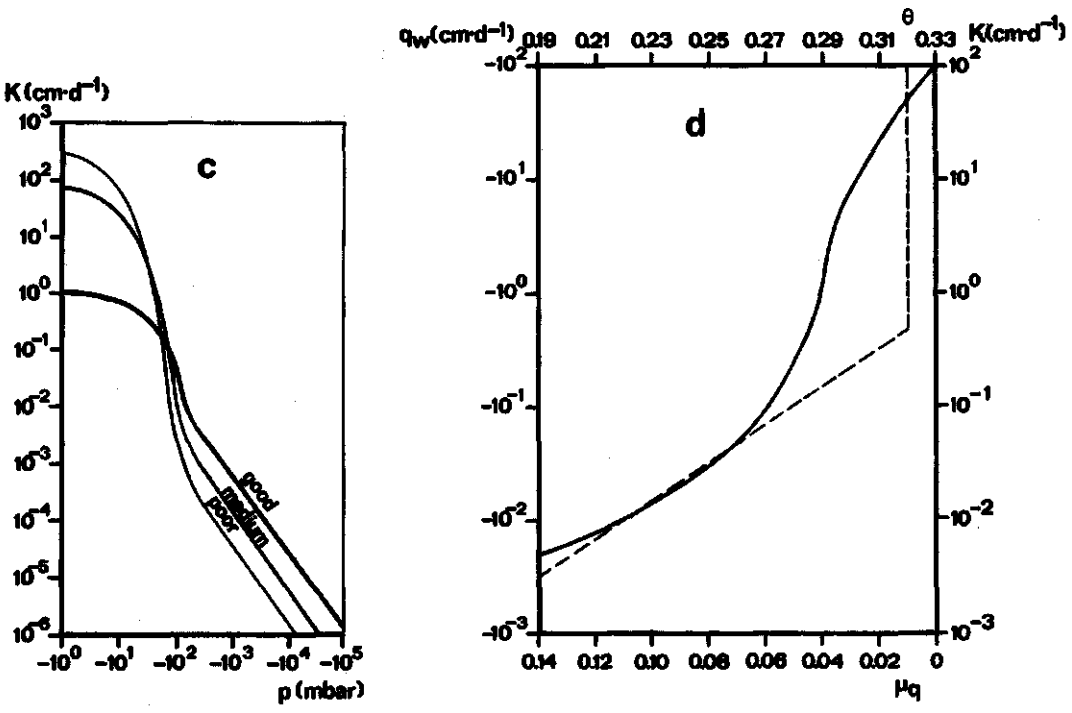

(c) K(p) relations used for the subsoil.
(d) The measured K(θ) relation and the derived relation (broken line) between μ_q and q_w.

weight factor used for the calculation of P. During the period considered precipitation was in the form of rain. In view of the flat topography of the area, the low intensities of the rainfall and the high permeability of the soil, surface runoff was not considered except when the root zone was fully saturated ($S_r < 0$). Then the water remaining on the surface was assumed to run off overland during the same time increment.

Evapotranspiration rates were computed for each node individually. Neglecting the storage of heat in the soil, the formula of Penman (1948) for the calculation of evaporation of a wet surface E_{wet} may be written as

$$E_{wet} = \frac{\frac{sR_n}{L} + \gamma E_a}{s + \gamma} \tag{106}$$

where s is the slope of the temperature-saturated vapour pressure curve, R_n is the net radiation, L is the latent heat of vaporization, γ is the psychrometric constant and E_a is the aerodynamic evaporation. Using turbulent transport theories, the original empirical expression for E_a, proposed by Penman, was later improved, to include the geometry of the evaporating surface (see Feddes, 1971)

$$E_a = \frac{\varepsilon \rho_a}{p_a} \frac{(e_s - e_a)}{r_a} \tag{107}$$

where ε is the ratio of molecular weight of water vapour and dry air, ρ_a is the density of the air, p_a is the atmospheric pressure, e_s is the saturated vapour pressure for the air temperature at 2 m height, e_a is the actual vapour pressure at 2 m height and r_a is the diffusion resistance to water vapour in the air. Values for r_a in relation to crop height and wind velocity were tabulated by Feddes (1971). Standard meteorological data were used to calculate E_{wet} from Eqn 106. They comprise wind velocity, relative humidity, temperature and relative sunshine duration. The daily values (24 hours means) were provided by the Royal Dutch Meteorological Institute and obtained from the following stastions: Almen, Diepenveen, Twenthe and Winterswijk (see Fig. 27).

Taking into account the diffusion resistance r_s of both crop and soil and neglecting evaporation of intercepted water, the real evapotranspiration E_{re} of a cropped surface with limited water supply may be written as (Monteith, 1965; Rijtema, 1965)

$$E_{re} = \frac{s + \gamma}{s + \gamma(1 + r_s/r_a)} \tag{108}$$

After Rijtema (1965), the diffusion resistance r_s is expressed as

$$r_s = r_c + S_c(r_\ell + r_p) \tag{109}$$

where r_c is the diffusion resistance depending on the fraction of soil covered, r_ℓ is the resistance depending on light intensity, r_p is the resistance depending on soil moisture conditions and flow in the plant while S_c is the fraction of the soil covered by the crop.

For a crop with ample water supply $r_p = 0$ and it follows for the potential evapotranspiration

$$E_{pot} = \frac{s + \gamma}{s + \gamma(1 + (r_c + S_c r_\ell)/r_a)} E_{wet} \quad (110)$$

The expression proposed by Rijtema (1965) for the resistance r_p of the soil plant system and values for r_c and r_ℓ as functions of S_c and mean short-wave radiation, respectively, can be found from van Bakel (1979).

The linking of the models for evapotranspiration and unsaturated flow requires that evapotranspiration rates, here expressed in $kg \cdot m^{-2} \cdot s^{-1}$ are converted to $cm \cdot d^{-1}$. The real evapotranspiration E_{re} depends on soil moisture conditions through the resistance r_p while unsaturated flow depends on E_{re} through the upper boundary flux q_s. Therefore few iterations of the calculation of both models are necessary to solve $q_s^{n+\frac{1}{2}}$ and $E_{re}^{n+\frac{1}{2}}$.

There has been little change in the cropping pattern (Fig. 29) during the years considered for simulation. The small urban area in the region is treated by the model as if it were grass.

6.1.5 Simulation results

The ability of the model to correctly simulate water-table elevations for an actual field-size sub-surface flow problem was tested in the study area over a time period of almost 6 years. The simulation started at the beginning of April 1971 and ended in December 1976, using a time increment of 10 days. As compared with average weather conditions, the summer of 1972 was extremely wet and the growing season (the period from April to September) of the years 1971, 1973 and 1975 was dry. Extremely dry was the year 1976, while the winter of 1974/1975 was very wet.

The initial steady-state situation was calculated several times for different percolation rates in the unsaturated region. For q_w ($= \bar{q}$) $= -0.1$ $cm \cdot d^{-1}$ calculated phreatic levels compared favourably with observed water-table elevations at the onset of the simulation period. The years 1971, 1972 and 1973 were simulated several times during the development of the model. Results of earlier model versions are published elsewhere (de Laat et al., 1975; de Laat & van den Akker, 1976). For the calibration of the present model the growing season of 1971 was used. Calibration was necessary to estimate the hysteresis factor used for the root zone and to test the empirical relation (103) between q_o and w. The test runs did not give reasons to alter the $q_o(w)$ relation adopted originally. Furthermore it appeared from testing different hysteresis factors (0, 0.5 and 1.0) that a value of 0.5 was most suitable.

Computed water-table elevations were interpolated in time and space to be compared with observed values in the 28 wells shown in Fig. 30. From the difference between the measured and simulated water-table elevation Δh (cm), the average $\overline{\Delta h}$ and the average absolute difference $\overline{|\Delta h|}$ are calculated for the total number of observations. Values for $\overline{\Delta h}$, $\overline{|\Delta h|}$ and the standard deviation σ of Δh are presented in Table 3a. In hydrology an efficiency factor R_E is often used for the comparison of rainfall-runoff models. The efficiency factor may be defined as (Nash & Sutcliffe, 1970)

Table 3. (a) Comparison of observed and simulated water-table elevations. (b) Idem, with $\overline{\Delta h}$ set to zero.

a					b		
Well No.	$\overline{\Delta h}$	$\overline{\lvert\Delta h\rvert}$	σ	R_E	Well No.	$\overline{\lvert\Delta h\rvert}$	R_E
1	1	6	8	0.97	1	6	0.97
2	2	7	10	0.97	2	8	0.97
3	15	16	12	0.87	3	9	0.95
4	-4	7	8	0.97	4	6	0.98
5	-5	9	8	0.96	5	7	0.98
6	-2	9	10	0.96	6	8	0.97
7	-9	13	12	0.92	7	9	0.95
8	2	10	14	0.94	8	10	0.94
9	12	13	10	0.92	9	7	0.97
10	19	20	11	0.79	10	8	0.95
11	10	13	11	0.90	11	8	0.95
12	9	10	8	0.95	12	6	0.97
13	-8	13	12	0.92	13	10	0.95
14	-4	11	12	0.94	14	10	0.95
15	28	28	12	0.71	15	10	0.95
16	25	25	12	0.76	16	10	0.95
17	0	11	15	0.87	17	11	0.87
18	0	8	10	0.96	18	8	0.96
19	7	12	17	0.78	19	11	0.81
20	-10	11	6	0.95	20	5	0.99
21	6	9	10	0.94	21	7	0.96
22	14	16	12	0.82	22	9	0.92
23	16	19	15	0.83	23	8	0.92
24	-48	50	17	0.28	24	10	0.92
25	10	11	9	0.94	25	7	0.97
26	12	13	11	0.91	26	7	0.96
27	16	17	12	0.86	27	8	0.95
28	7	11	11	0.91	28	8	0.93

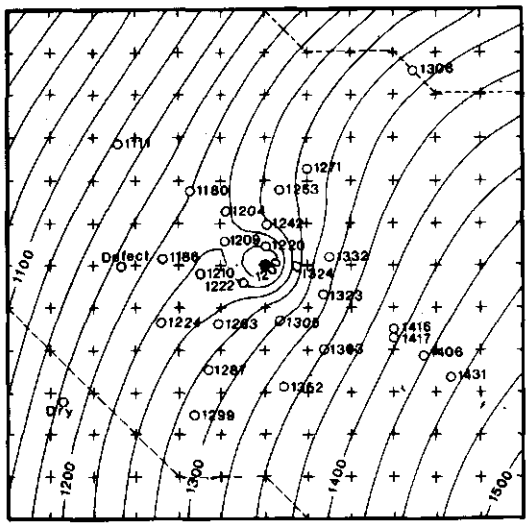

Fig. 34. Simulated water-table elevation contours and observed values at the end of August 1973 in the study area. The quantities are expressed in cm.

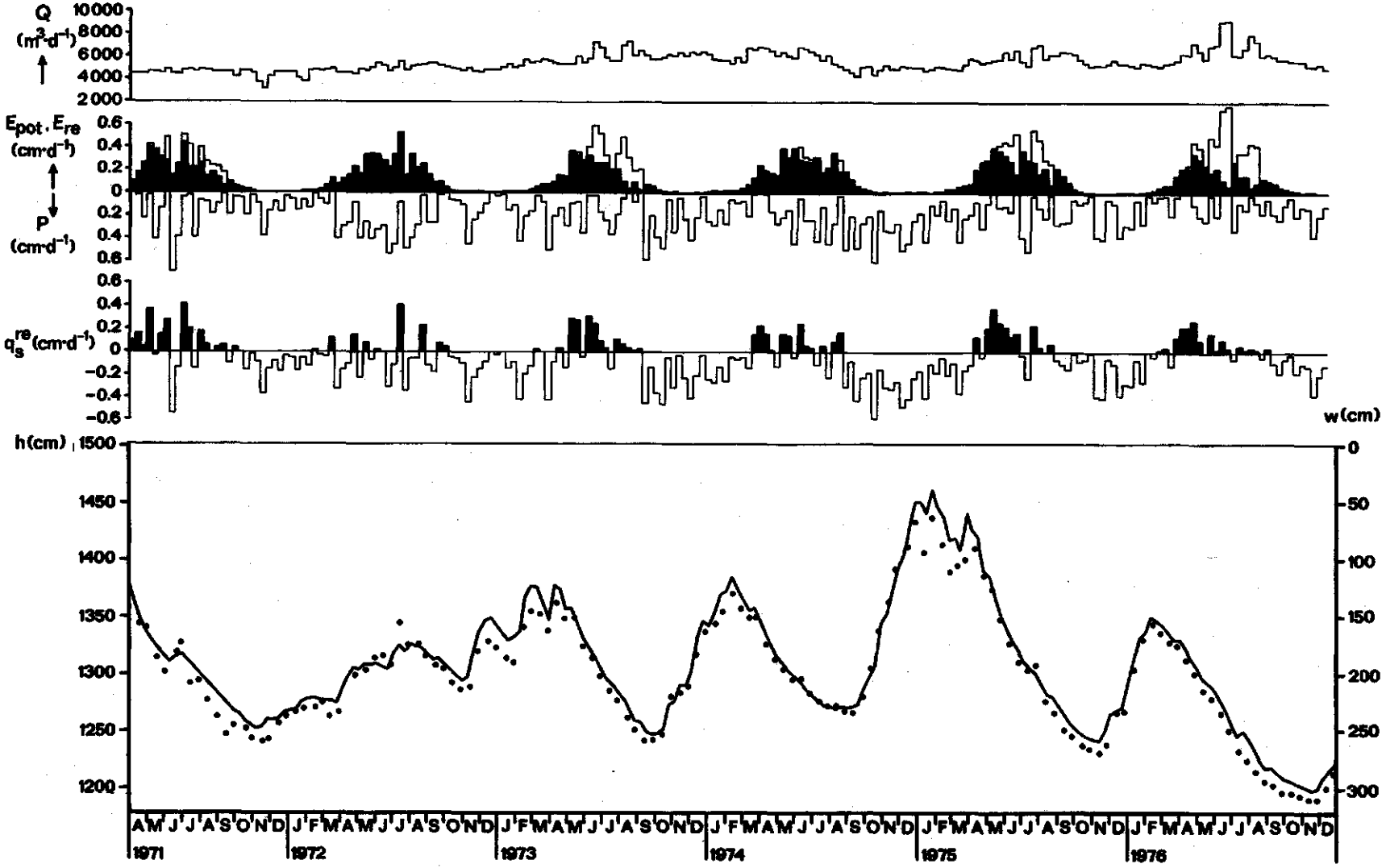

Fig. 35. The given groundwater extraction rates Q, the calculated real and potential evapotranspiration rates E_{re} and E_{pot}, the precipitation data P, the resulting surface flux q_s^{re} (= E_{re} - P) and the simulated water-table elevation h in well No. 12 compared with observed values (·).

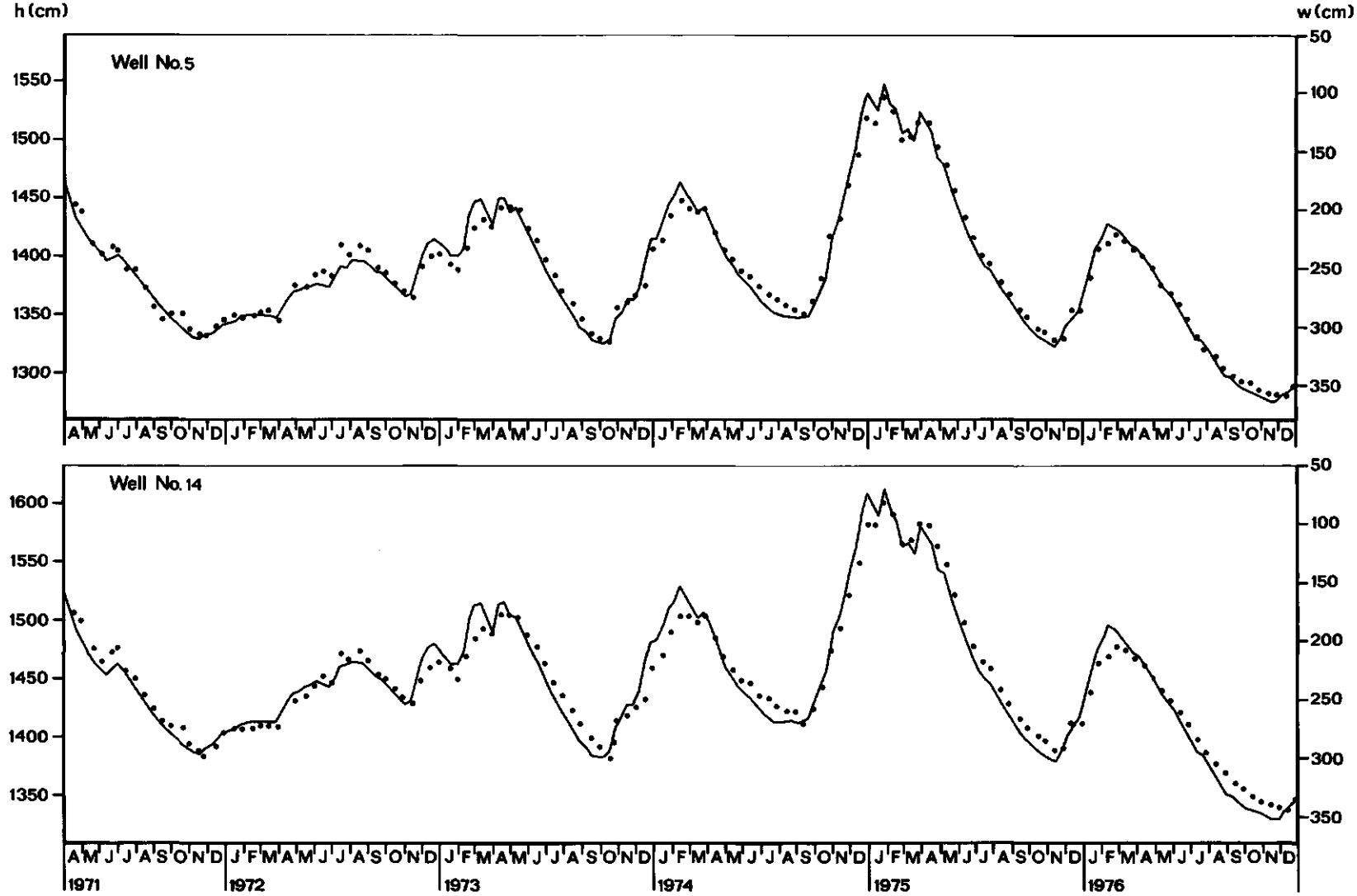

Fig. 36a. Comparison of simulated water-table elevations with observed values (·).

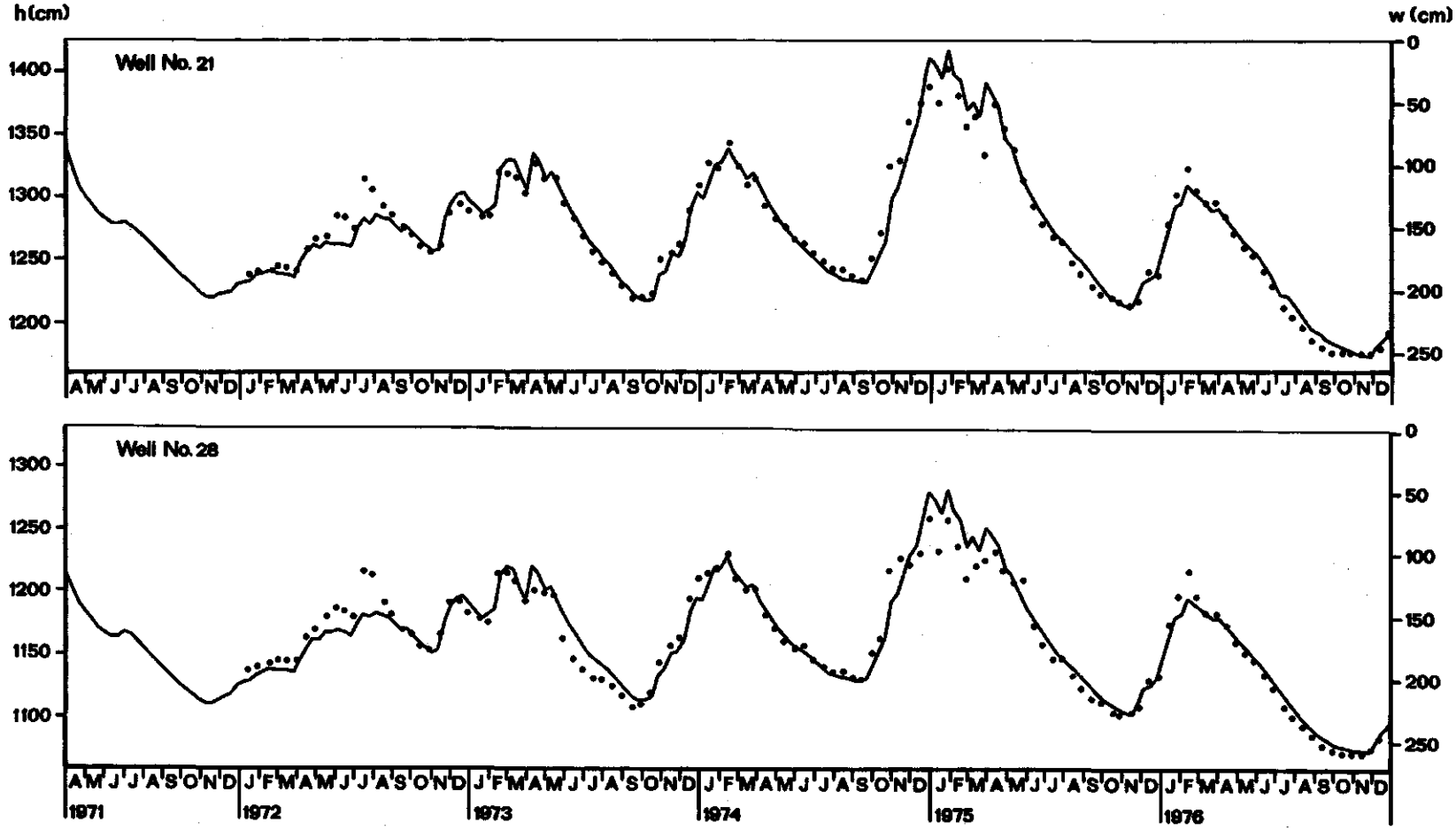

Fig. 36b. Comparison of simulated water-table elevations with observed values (·).

$$R_E = 1 - \frac{\Sigma(F - F')^2}{\Sigma(F - \overline{F})^2} \qquad (111)$$

where F represents the measured water-table elevations, F' the simulated values and $\overline{F}$ the mean of the observed data. If simulated and observed data fully agree $R_E = 1$, while $R_E = 0$ if the simulated values equal the mean of the observed values. The efficiency factor for each of the observation wells is presented in Table 3a. The value for $\overline{\Delta h}$ is largely governed by the difference between actual and model surface elevation at the observation well. In order to eliminate the effect of $\overline{\Delta h}$ on the comparison of the simulated and observed fluctuation of the phreatic level, values for $\overline{|\Delta h|}$ and R_E were computed for observed data which were 'corrected' for $\overline{\Delta h}$ (Table 3b).

Simulated water-table elevation contours and observed values at the end of August 1973 are shown in Fig. 34. To illustrate the goodness of fit, observed and simulated water-table elevations for observation well No. 12 are plotted in Fig. 35. Also given in the same figure are the groundwater extraction rates, precipitation data, calculated potential and real evapotranspiration rates and the resulting actual flux across the soil surface. Simulated water-table elevations in four observation wells (Nos 5, 14, 21 and 28) are compared in Fig. 36 with observed values, which are 'corrected' for $\overline{\Delta h}$.

Due to the nature of the model for unsaturated flow, least accurate results are obtained if a period with capillary rise is followed by rainfall excess. This situation occurs frequently during the growing season of 1972. In an attempt to improve the result by decreasing Δt, it appeared that reducing the length of the time increment does not affect the simulated water-table elevation significantly. The effect of non-steady saturated flow conditions resulting from a large variation in the extraction rate is shown in Figs 35 and 36 by the calculated phreatic level in the summer of 1976.

6.2 SENSITIVITY ANALYSIS

A comprehensive sensitivity analysis was carried out with respect to input data. Part of the analysis considers vertical flow in one node only and covers the entire simulation period (van Bakel, 1979). An approximate relation between q_w and h, derived from the quasi three-dimensional simulation results, serves as the lower boundary condition of the unsaturated flow model. The analysis is, therefore, limited primarily to the effect on calculated real and potential evapotranspiration rates.

Another part of the sensitivity analysis considers flow in the entire study area, but only for the years 1973 and 1974 (Awater & de Laat, 1979). Bouma & van Heesen (1979) used the same period to study the effect of the different ways of collecting soil physical data on the simulation results. Their investigations are important, as the costs of simulating regional, saturated-unsaturated flow problems largely depend on the degree of detail to which soil physical data need to be measured.

In this study the sensitivity of the results of simulation to a variation in the values of seven parameters was investigated. The parameters were selected for different reasons. The hysteresis factor was chosen as its value had to be estimated. Variations in the relations K(p) and $q_o(h)$ were analyzed as no actual measurements of these rela-

tions were conducted in the study area. The transmissivity, the prescribed phreatic levels for the nodes at the boundary and the relation $\mu_q(q_w)$ were chosen because comprehensive data were not available. Finally the depth of the 'effective root zone' was included in the analysis as its value is not well defined. The parameter D_r results from the schematization of the unsaturated region into a root zone and a subsoil. In the root zone upward flow is governed by the water uptake of the roots and moisture is available for the crop until pF 4.2 applies over the entire depth. The root zone may, therefore, be considered as a reservoir, the size of which depends on D_r. Although rooting depths were extensively measured in the study area, the effective rooting depth D_r, which is assumed to comprise 80% of the roots, had to be estimated.

The sensitivity analysis for the seven parameters is restricted to results obtained for a period of one year (37 time increments of 10 days each) starting at the beginning of April 1973. First a run of the model was made with the parameters set equal to the values used for the six-year simulation period. This run was then repeated with nothing changed except the value of the parameter under consideration. The effect of parameter variation was investigated for the simulated water-table elevations and the calculated real evapotranspirations. A global impression of the sensitivity may be obtained by comparing average values. To reduce the effect of the prescribed levels at the boundary, simulated water-table elevations and real evapotranspiration values were averaged over the interior of the model area. The interior comprises 49 nodes located in the centre at a distance of more than 1000 m from the model boundary.

Average water-table elevations resulting from simulation runs with the original and changed parameter value were plotted. Figure 37 shows, as an example, the effect of a variation in the hysteresis factor on the average water-table elevation in the interior

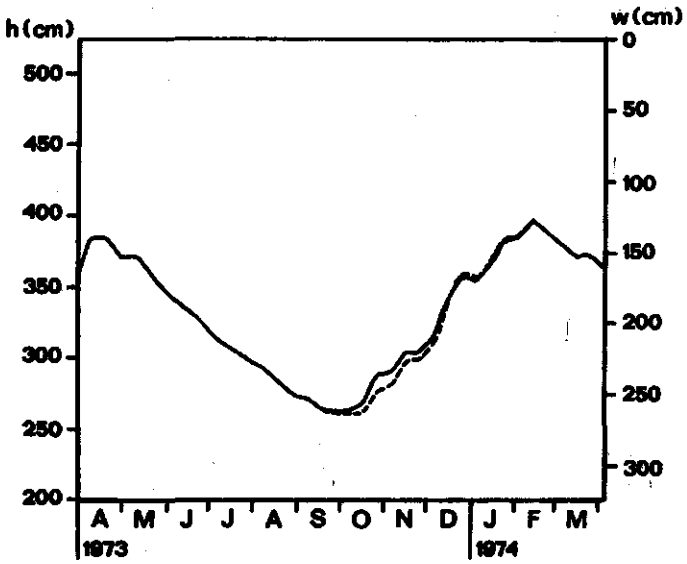

Fig. 37. Comparison of calculated water-table elevations in the interior of the study area for sensitivity to a change in the hysteresis factor from its original value 0.5 (—) to zero (---).

Table 4. Summary of sensitivity analysis results.

Parameter	Change	Effect of changing parameter value on	
		water-table elevation	real evapotranspiration
Hysteresis factor	Set to zero	At the beginning of the second half year 12 cm lower, thereafter 2 cm higher.	Overestimated by 0.3 cm, but locally more than 1 cm.
Hydraulic conductivity relation K(p)	'good' → 'medium' 'medium' → 'poor' (Fig. 33c)	In the first half year 2 cm higher. In the second half year, at first more than 10 cm higher, later decreasing to no change.	Underestimated by 1.8 cm, but locally more than 5 cm.
Groundwater discharge relation $q_o(h)$	See Fig. 38	Varying from 20 cm lower for the highest levels to 2 cm lower for the lowest levels.	Underestimated by 0.6 cm, but locally more than 4 cm.
Transmissivity T	Increased by 25%	High levels 2 cm lower. Local effect (except for the well site) ranges from +3 to -8 cm.	Underestimated by 0.1 cm.
Prescribed phreatic levels at the boundary	Raised by 5 cm	High levels 2 cm and low levels 4 cm higher.	Overestimated by 0.1 cm, but locally almost 1 cm.
Storage coefficient relation $\mu_q(q_w)$	See Fig. 39	Up to 10 cm higher in summer and 10 cm lower in winter.	Underestimated by 0.4 cm (at some locations by 1 cm but also overestimated by 1 cm).
Depth of root zone D_r	Decreased by 10 cm	In the second half year (when the water table is rising) 10 to 15 cm higher.	Underestimated by almost 2.8 cm. (The local effect ranges from 2 to 5 cm.)

of the study area. The results for all seven parameters are summarized in Table 4. This table also gives the effect of parameter variation on the total real evapotranspiration calculated for the considered period of one year. The effect applies to the average value for the nodes in the interior. The results of the sensitivity analysis are discussed below.

Hysteresis factor Neglecting hysteresis results in a delayed response of the water table to rainfall excess at the end of the summer as may be seen in Fig. 37. Since more of the rainfall excess during the growing season is kept in the root zone, the calculated evapotranspiration rates are higher.

Hydraulic conductivity The capillary properties of the subsoil in the study area are described by three different K(p) relations (Fig. 33c). The K(p) relation characterized as 'poor' applies to only eight nodes. For the sensitivity analysis these nodes were

left unchanged. Nodes initially characterized as 'good' became 'medium' and the capillary properties of nodes initially 'medium' were changed to 'poor'. The calculated real evapotranspiration proves sensitive to a variation in the K(p) relation. At places where the water-table depth may be considered as 'critical', the calculated values are largely reduced. As a result of the poor capillary properties, less water becomes available for the crop due to a decrease in capillary rise and an increase of the pF value in the root zone. Consequently, the saturation deficit at the end of the summer is smaller, resulting in higher levels when rainfall excess causes the water table to rise.

Groundwater discharge The relation between groundwater discharge and water-table depth was drastically changed (Fig. 38). The change represents an 'improvement' of the drainage system affecting primarily the most shallow water-tables. The effect on water tables deeper than 200 cm is almost negligible. Calculated real evapotranspiration values are lower as the drawdown of the water table hampers the process of capillary rise and reduces (at some places considerably) the amount of moisture available in the root zone at the beginning of the growing season.

Transmissivity A large change in the transmissivity values has negligible effect on the simulated water-table elevations and calculated real evapotranspiration rates.

Prescribed phreatic levels at the boundary The prescribed phreatic levels were derived from the same data in two different ways, independent of each other. Both series obtained for 1973 were compared for two arbitrarily selected nodes. The 95% confidence limits of the average value appeared to be 4 and 2 cm, respectively. Based on these results the prescribed levels were raised by 5 cm. The change also applies for the initial situation. As the water table in the study area is relatively deep (the average depth for 1973 in the interior is 190 cm) the calculated real evapotranspiration is not very sensitive to a change in the prescribed levels at the boundary.

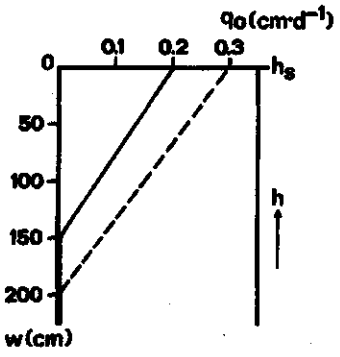

Fig. 38. The original (—) and changed (---) relation between q_o and h used for the sensitivity analysis.

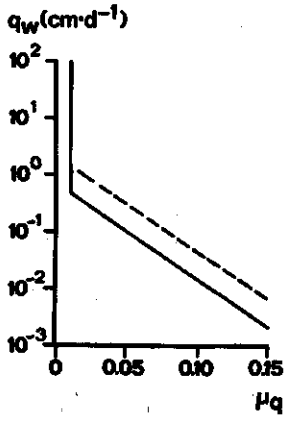

Fig. 39. The original (—) and changed (---) relation between μ_q and h used for the sensitivity analysis.

Storage coefficient The change in the relation between μ_q and q_w (Fig. 39) effectively increases the storage coefficient by 0.03. As a result of the larger μ_q value the fluctuation of the water table in 1973 is reduced by 20 cm. The change has two effects which act in opposite directions on the calculated real evapotranspiration. On the one hand capillary rise benefits from the higher phreatic levels in the growing season, while on the other hand less moisture is available in the subsoil due to a larger downward flux across the lower boundary of the model for unsaturated flow.

Depth of the root zone A decrease of D_r results in an underestimation of E_{re} for three reasons: (i) less water is available in the root zone at the beginning of the growing season, (ii) less water is kept in the root zone during periods with rainfall excess, and (iii) the supply by capillary rise is hampered due to larger z_{rs} values. The calculated lower real evapotranspiration values result in smaller saturation deficits at the end of the summer yielding higher phreatic levels during the time the water table is rising.

The sensitivity was, apart from the seven input parameters, also investigated for a change in the calculation procedure. The upper boundary condition given by Eqn 105 requires an iterative solution of the models for evapotranspiration and unsaturated flow to calculate $E_{re}^{n+\frac{1}{2}}$. Instead of solving $E_{re}^{n+\frac{1}{2}}$ by iteration, $E_{pot}^{n+\frac{1}{2}}$ is used to compute the surface flux as

$$q_s^{n+\frac{1}{2}} = E_{pot}^{n+\frac{1}{2}} - P^{n+\frac{1}{2}} \tag{112}$$

The actual surface flux q_s^{re} computed by the model for unsaturated flow is then used to calculate the real evapotranspiration rate

$$E_{re}^{n+\frac{1}{2}} = (q_s^{re})^{n+\frac{1}{2}} + P^{n+\frac{1}{2}} \tag{113}$$

As a result of the change in the model, the calculated real evapotranspiration rate equals its potential value until the pressure in the root zone reaches wilting point, because $q_s^{re} = q_s$ for pF values less than 4.2. The use of Eqn 112 instead of Eqn 105 and the calculation of E_{re} with Eqn 113 rather than by iteration did not have any effect on the simulated water-table elevations. The calculated real evapotranspiration for the interior of the model area was overestimated by only 0.1 cm, but after 130 days when pF 4.2 is reached in most parts of the region by 0.5 cm. Local effects largely depend on the type of land use. Potatoes appeared to be very sensitive while the calculated real evapotranspiration of grass was hardly affected.

The results of the sensitivity analysis may be summarized as follows. The fluctuation of the simulated water-table elevation depends largely on the relation between μ_q and q_w which is derived from the $K(\theta)$ relation applying to the lower part of the subsoil. The average water-table height in summer is predominantly governed by the prescribed phreatic levels at the boundary, while in winter the empirical relation (103) between

q_o and h appears to prevail.

The calculated real evapotranspiration is sensitive to the water-table elevation at the beginning of the growing season, the hydraulic conductivity relation K(p) and the depth of the effective root zone D_r. The sensitivity to the parameter D_r is most pronounced as it directly affects the amount of water available for the crop. A similar sensitivity was noticed by Feddes et al. (1978) using a sink term function to describe water uptake by roots. They reported that a relatively small change in the sink term function affects the system.

A final run of the model showed that the difference between the real and potential evapotranspiration of grass is not governed by the diffusion resistance r_p (see Section 6.1.4) but results from a deficiency of available water in the root zone.

When evaluating the sensitivity analysis, it should be realized that the results apply for one particular situation. In another period or region for which conditions differ significantly from those in the study area in 1973, the foregoing conclusions may not be applicable.

6.3 CONSEQUENCES OF GROUNDWATER EXTRACTION

The model has been used in the study area to predict consequences of the implemented groundwater extraction. Since the model was verified only with respect to water-table elevations, in the absence of other possibilities, an investigation of these consequences should be restricted to the prediction of the drawdown of the phreatic level. Nevertheless tentative conclusions will be drawn with respect to other hydrological consequences for the following reason. Assuming that the geohydrological data, the groundwater extraction rates and the prescribed phreatic levels at the boundary are correct, the simulated water-table elevation is governed by q_w and q_o. Because the discharge q_o is very small, in particular during the last 1½ year of the simulated time period, the flux q_w is correctly simulated considering the excellent agreement of computed and observed water-table elevations. The recharge of the saturated zone from the overlying unsaturated region depends (in particular at the end of the growing season) very much on the saturation deficit and thus the surface flux q_s. Assuming that rainfall rates were accurately measured the real evapotranspiration during the growing season must have been approached properly. Potential evapotranspiration rates are independent of soil moisture conditions and verified for lysimeter experiments (Rijtema, 1965) and field experiments (Feddes, 1971).

The simulation model was applied in the study area in exactly the same way as for verification but without groundwater extraction from the wells in the centre. A condition for this application is that the effect of the change in the actual situation on the boundary conditions is either negligible or predictable. With regard to the study area, the boundary of the model was chosen at such a distance from the pumping site that the prescribed phreatic levels are not appreciably affected by the implemented extraction, while the effect on the water levels in both streams is assumed insignificant.

The water balances resulting from simulation of the actual situation and the situation without extraction are presented in Table 5. The quantities are expressed in cm and refer to a period of approximately one year (except for 1976) starting at the begin-

Table 5a. Water balances (quantities in cm) for the actual situation.

IN	1971	1972	1973	1974	1975	1976	OUT	1971	1972	1973	1974	1975	1976
Precipitation	50.8	73.6	67.5	91.5	60.9	33.1	Evapotranspiration	45.5	46.8	39.2	46.7	47.1	32.2
Storage change	8.6	-6.3	0.2	-8.6	9.5	11.6	Surface water discharge	1.4	4.2	8.1	10.1	3.3	0.1
							Groundwater discharge	7.8	11.2	14.1	20.6	14.1	7.6
							Extraction	4.7	5.1	6.3	5.5	5.9	4.8
	59.4	67.3	67.7	82.9	70.4	44.7		59.4	67.3	67.7	82.9	70.4	44.7

Table 5b. Water balances (quantities in cm) for the situation without extraction.

IN	1971	1972	1973	1974	1975	1976	OUT	1971	1972	1973	1974	1975	1976
Precipitation	50.8	73.6	67.5	91.5	60.9	33.1	Evapotranspiration	46.0	46.8	39.9	47.1	48.3	32.7
Storage change	8.1	-6.2	0.1	-9.0	9.7	11.3	Surface water discharge	1.9	5.8	10.0	11.9	4.4	0.3
							Groundwater discharge	11.0	14.8	17.7	23.5	17.9	11.4
							Extraction	0	0	0	0	0	0
	58.9	67.4	67.6	82.5	70.6	44.4		58.9	67.4	67.6	82.5	70.6	44.4

Table 6a. Water balances (quantities in cm) for the actual situation (summer half year).

IN	1971	1972	1973	1974	1975	1976	OUT	1971	1972	1973	1974	1975	1976
Precipitation	27.7	50.1	25.5	36.7	28.1	16.5	Evapotranspiration	39.4	42.5	33.2	42.2	40.7	29.7
Storage change	19.6	-2.0	19.7	12.4	25.5	22.1	Surface water discharge	1.4	0.7	3.2	0.2	2.5	0.1
							Groundwater discharge	4.3	2.5	5.9	3.8	7.6	5.5
							Extraction	2.2	2.4	2.9	2.9	2.8	3.3
	47.3	48.1	45.2	49.1	53.6	38.6		47.3	48.1	45.2	49.1	53.6	38.6

Table 6b. Water balances (quantities in cm) for the situation without extraction (summer half year).

IN	1971	1972	1973	1974	1975	1976	OUT	1971	1972	1973	1974	1975	1976
Precipitation	27.7	50.1	25.5	36.7	28.1	16.5	Evapotranspiration	39.9	42.5	33.8	42.6	41.9	30.2
Storage change	19.5	-2.0	19.7	12.2	26.0	21.9	Surface water discharge	1.8	1.3	3.9	0.5	3.1	0.3
							Groundwater discharge	5.5	4.3	7.5	5.8	9.1	7.9
							Extraction	0	0	0	0	0	0
	47.2	48.1	45.2	48.9	54.1	38.4		47.2	48.1	45.2	48.9	54.1	38.4

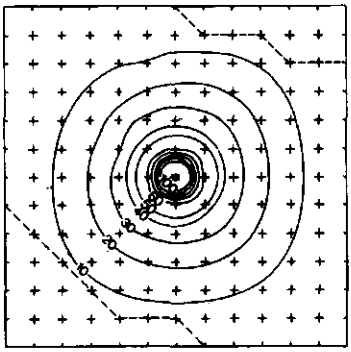

a

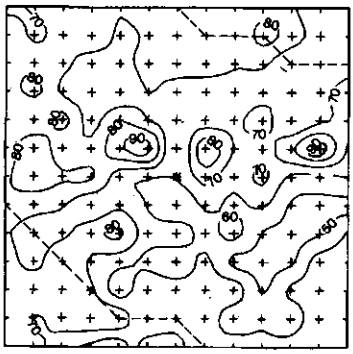

b

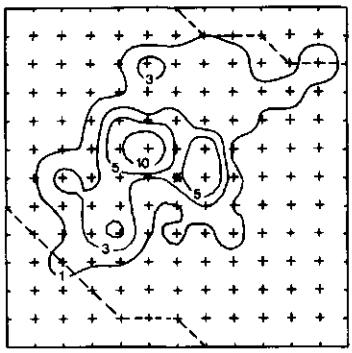

c

Fig. 40. Contours for the simulated situation in the study area at the end of August 1973.
(a) Difference in water-table elevation (cm) for the situations with and without the implemented extraction.
(b) Relative evapotranspiration (%) contours.
(c) Difference in relative evapotranspiration between the situations with and without extraction.

ning of April. The water balances for the summer half year (170 days) are given in Table 6. This table shows that the total amount of groundwater, leaving the region during the growing season as surface water ('Surface water discharge') is relatively small. Most of the rainfall excess in the study area is discharged across the model boundary as groundwater ('Groundwater discharge').

The difference in the calculated water-table elevation for the situations with and without groundwater extraction at the end of August 1973 is shown in Fig. 40a. As a result of the drawdown less water becomes available for the crop by capillary rise, which may result in a reduction of the evapotranspiration. Most of the reductions occur during the summer half year. The relative contribution to the supply of the implemented groundwater extraction of each of the terms of the water balance during the summer half year is presented in Fig. 41. The results show that a simple relation between reduction of evapotranspiration due to groundwater extraction and the prevailing climatological conditions during the growing season does not exist. Other important factors must be considered, such as water-table depth and soil moisture conditions at the beginning of the growing season (which are very favourable in 1975) and the distribution of precipitation over the season.

If crop production is not restricted by water supply, the total actual evapotranspiration at the end of the growing season ΣE_{re} equals the total potential evapotranspiration ΣE_{pot}. The production capacity of the crop is often expressed in terms of

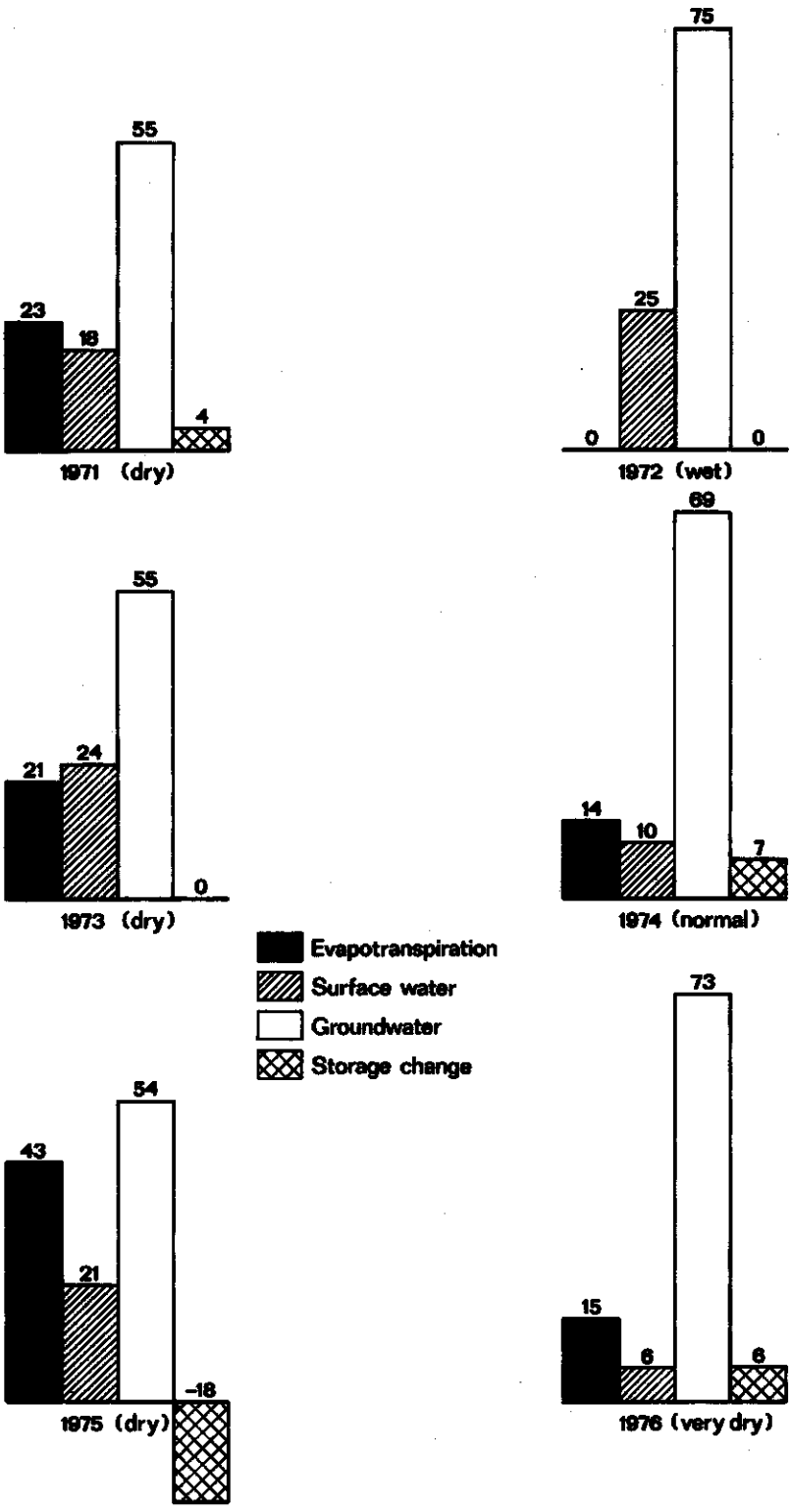

Fig. 41. Relative contribution (%) of the different sources to groundwater extraction during the growing season (170 days).

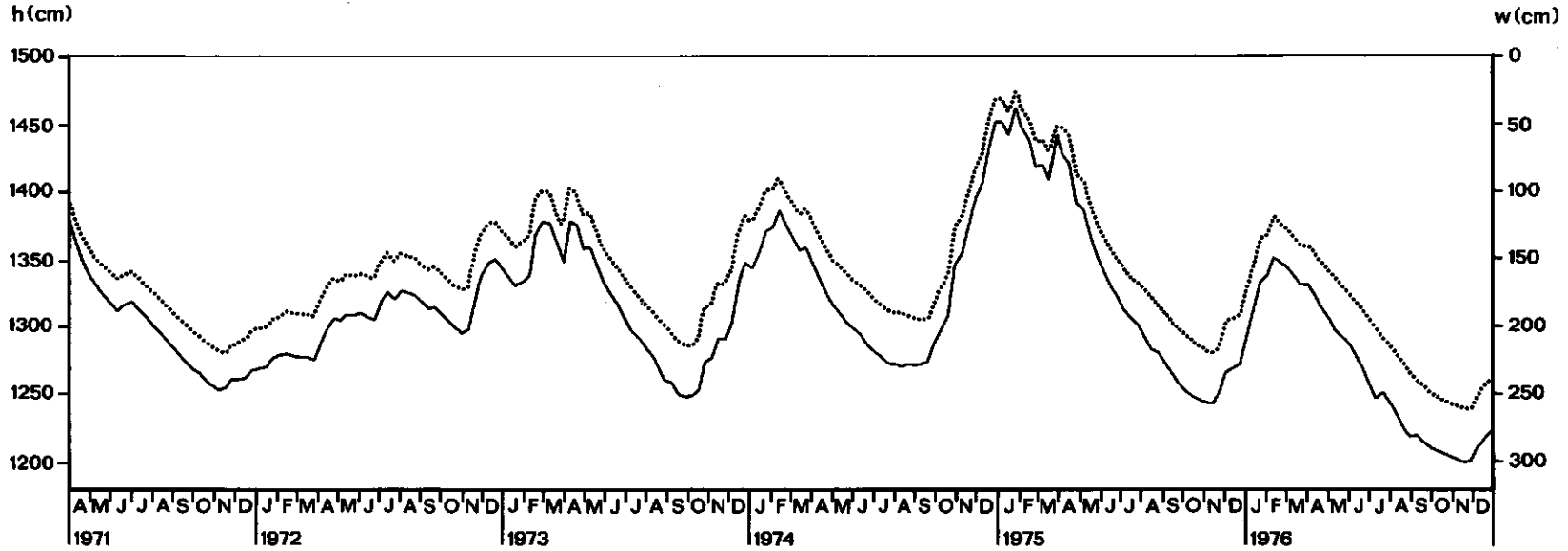

Fig. 42. Comparison of simulated phreatic levels in observation well No. 12 for the situations with (—) and without (•••) the implemented groundwater extraction.

relative evapotranspiration (Feddes & van Wijk, 1976), defined as $(\Sigma E_{re}/\Sigma E_{pot})\cdot 100\%$. Relative evapotranspiration calculated from simulation results for the situation without extraction is presented in Fig. 40b. Reductions in relative evapotranspiration and consequently in crop production are likely to occur in areas showing high evapotranspiration rates and situated not too far from the pumping site as may be seen from Figs 40b and 40c.

The effect of groundwater extraction on the calculated phreatic level in well No. 12 is shown in Fig. 42.

Applications of the quasi three-dimensional approach to saturated-unsaturated flow as described in this study were reported for the following regions.

- Leerinkbeek area (141 km^2). De Laat & van den Akker (1976) studied consequences of groundwater extraction on the water-table elevation and crop production for a three-year period.
- Dinxperlo area (57.5 km^2). Awater (1976) investigated possibilities to reduce the drawdown resulting from pumpage by means of surface water infiltration. The simulation period covered 4½ years.
- Glindhorst area (156 km^2). The 'Werkgroep Wateronttrekking Gelderse Vallei' (1979) studied hydrological consequences for different groundwater extraction rates for a three-year period.
- Achterhoek area (701 km^2). Awater & de Laat (1979) investigated for a three-year period the effect of sprinkling and different extraction patterns on the water-table elevation and real evapotranspiration.

For each of the above mentioned applications the length of the time step used was ten days and the mesh width of the two-dimensional horizontal grid 1000 m, except for the Dinxperlo area where the distance between the nodes was 500 m.

Summary

The most important driving forces for transport of water in soil are differences in elevation and pressure. These forces are usually combined into the hydraulic potential gradient. Darcy's law relates this gradient to the flux density or specific discharge. The proportionality factor of both quantities is the hydraulic conductivity K. Combination of Darcy's law and the principle of continuity leads to a general equation (13) with two dependent variables (θ and p). In this study the generality is restricted to isothermal flow of an incompressible homogeneous liquid in an isotropic rigid soil.

The particular forms of the general equation applying to simplified flow problems are essentially different for a situation of complete saturation and for a partly saturated flow system. For complete saturation the number of dependent variables reduces to one, and the hydraulic conductivity is a function of the independent variables alone. The solution of differential equations governing flow in unsaturated porous media requires the soil moisture characteristic, the relation between θ and p, to be specified. Moreover, the hydraulic conductivity is a function of θ or p. Since both empirical relations {θ(p) and K(p) or K(θ)} are difficult to measure and subject to hysteresis, solutions of partial differential equations governing saturated flow are often more easily obtained than of those governing unsaturated flow.

The algebraic formulation of the flow problem results in an abstract simulation system, or mathematical model. Real simulation systems comprise physical and analogue models. A viscous fluid analogue model for simulating vertical unsaturated flow was developed by Wind (1972) and a special purpose electrical analogue by Wind & Mazee (1979). The most versatile models for saturated flow are the resistance-capacitance analogues. Although these direct simulation methods are capable of solving complex flow problems, mathematical models are, due to recent advances in the field of computer technology, considered superior in many ways.

The numerical solution of the governing partial differential equations may be obtained by finite element or finite difference methods. The use of finite element methods is advantageous if the flow domain is to be described by an irregular grid or when complicated saturated-unsaturated flow problems are to be solved. Finite element techniques are a recent development in the field of sub-surface hydrology. Most of the available solutions of groundwater flow problems indeed use a finite difference method. Some current finite difference techniques are discussed towards the end of Chapter 2.

For historical reasons and in view of the above mentioned differences in the nature of the partial differential equations governing flow in completely saturated and partly saturated porous media, flow above and below the water table was traditionally treated separately. As it is often sufficient to consider flow in the unsaturated region vertically and, in the saturated part in horizontal direction only, the separate approach

largely reduces the complexity of the flow problem. However, serious objections are raised if water tables are shallow or rapidly fluctuate, as the effect of unsaturated flow on the saturated system may be considerable.

A unified approach to saturated-unsaturated flow was first reported by Rubin (1968). In Chapter 3 a review is given of a number of papers using a single equation to model flow in partly saturated flow systems. The problems solved by this rigorous approach deal with pumping tests and flow in shallow water-table aquifers. For these flow problems the effect of the unsaturated system on unconfined groundwater flow is most pronounced.

The use of a single equation to solve saturated-unsaturated flow problems introduces numerical difficulties. The governing equation is parabolic in the unsaturated zone and of an elliptical type in the saturated part, while the position of the phreatic surface separating both regions is a priori unknown. The numerical solution requires a small mesh size in the region above the water table and in the vicinity of the well, because the value of the dependent variable may change drastically over a short distance. Moreover, the non-linearity of the coefficients in the unsaturated part of the flow domain requires for reasons of stability and convergence that time is discretized to small steps. Due to the limited capacity of the core memory of the computer and the extremely high running costs, applications to regional problems have not been reported.

An alternative solution proposed by Pikul et al. (1974) links Richards' equation for vertical unsaturated flow to the equation of Boussinesq for horizontal saturated flow. The efficiency of the resulting quasi three-dimensional approach for solving saturated-unsaturated flow problems does not improve significantly, mainly because of the time step restriction for the solution of the equation for unsaturated flow, which is imposed upon the entire system.

A model for vertical unsaturated flow being more efficient in terms of computer costs is developed in Chapter 4. The model simulates transient flow by a succession of steady-state situations. Steady upward flow in a soil column extending to a height of one metre above the water table was first computed by Richards (1931). A systematic computation of steady-state relations was carried out by Wind (1955) and used by others to compute for various water-table depths the maximum amount of soil moisture available for the crop. Feitsma (1969) used a succession of steady-state situations to simulate the transient process of capillary rise and the drawdown of the water table.

In this study the pseudo steady-state approach to capillary rise is analyzed. Its approximate value depends on the length of the time increment used for simulation in relation to the characteristic time of the unsaturated flow system. With a shallow water-table in a sandy aquifer, the characteristic time is of the order of days. The results of the pseudo steady-state approach become inconsistent if the length of the time increment used is smaller than the characteristic time. Similar difficulties arise for a decreasing flux across the upper boundary and for the situation that capillary rise is followed by percolation. Furthermore the position of the water table may not be simulated properly if the flux across the lower boundary is large and downwards.

In this study the unsaturated zone extends from just below the phreatic level to the soil surface. The region is schematized into a root zone and a subsoil. As flow in the root zone is largely governed by the water uptake of the roots, the gradient of the

hydraulic potential in the root zone is assumed equal to zero. It is shown that the steady-state situation is fully determined by only two parameters (e.g. the saturation deficit of the root zone S_r and the steady flux in the subsoil $\bar{q}$). The use of saturation deficits reduces the solution of the steady-state situation to a problem of two relations with two unknowns (S_r and $\bar{q}$). The steady-state solution corresponding to the upper boundary flux of the subsoil is termed upper boundary solution. Procedures are developed to account for the above mentioned inconsistencies and to treat periods with rainfall excess following capillary rise. If the root zone desiccates to wilting point the calculation procedure yields furthermore the actual flux across the soil surface. When there is a large downward flux across the lower boundary, the upper boundary solution is unsuitable for computing the water-table depth. For a downward lower boundary flux condition the position of the phreatic level is therefore simulated by a pseudo steady-state approach to percolation applying to the lower part of the unsaturated zone. The steady-state solution corresponding to the lower boundary flux of the subsoil is termed lower boundary solution. The upper and lower boundary solutions are combined into one simulation model, taking into account hysteresis and heterogeneity. However, with percolation capillary properties are assumed homogeneous, so that the model does not allow for the formation of perched water-tables.

A quasi three-dimensional approach for simulating transient sub-surface flow in shallow water-table aquifers is outlined in Chapter 5. The solution uses a two-dimensional horizontal grid to describe saturated flow. A special procedure is developed to link in each node of the grid the unsaturated flow model with the saturated system.

An area of 36 km^2 in the east of the Netherlands was chosen for experimental verification of the quasi three-dimensional model. The area was described by a rectangular grid with a mesh size of 500 m. The length of the time increment used was ten days and the simulation period covered almost six years. Simulated water-table elevations compared favourably with observed values. Less accurate results were obtained in periods with an alternating evapotranspiration and rainfall excess. The sensitivity of the simulated water-table elevations and calculated real evapotranspiration rates to a variation in the value of several parameters was investigated. The results discussed in Chapter 6 show that the calculated real evapotranspiration is most sensitive to the conceptual approach for water uptake by the roots. For the approach to evapotranspiration as used in this study, it appeared furthermore that the difference between the calculated actual and potential evapotranspiration of grass depends on the amount of soil moisture available in the root zone rather than upon the empirical diffusion resistance for soil and crop (r_p).

An application of the model for saturated-unsaturated flow is given. Consequences of the implemented groundwater extraction in the study area on the calculated phreatic levels and water balances are predicted for the same period used for the verification of the model.

Samenvatting

De belangrijkste drijvende krachten voor de beweging van water in de grond zijn verschillen in hoogte en druk. Het is gebruikelijk deze krachten te combineren in de gradiënt van de hydraulische potentiaal. Het verband tussen deze gradiënt en de fluxdichtheid of het specifieke debiet staat bekend als de wet van Darcy. Hierin is de hydraulische doorlatendheid K de evenredigheidsconstante van beide grootheden. Combinatie van de wet van Darcy en het continuïteitsbeginsel leidt tot een algemene stromingsvergelijking (13) met twee afhankelijke variabelen (θ en p). In deze studie is de algemeenheid beperkt tot isotherme stroming van een onsamendrukbare homogene vloeistof in een isotrope rigide grond.

Van de algemene formulering afgeleide vergelijkingen voor vereenvoudigde stromingsproblemen vertonen wezenlijke verschillen voor zover zij betrekking hebben op een geheel of een gedeeltelijk verzadigd systeem. Bij volledige verzadiging is er nog slechts sprake van één afhankelijke variabele die niet van invloed is op de hydraulische doorlatendheid K. Voor het oplossen van differentiaalvergelijkingen voor stroming in een gedeeltelijk verzadigd systeem moet het verband tussen θ en p worden gespecificeerd. Bovendien is de hydraulische doorlatendheid een functie van θ of p. Beide empirische relaties {θ(p) en K(p) of K(θ)} zijn moeilijk te bepalen en onderhevig aan hysteresis. Vandaar dat oplossingen van partiële differentiaalvergelijkingen in het algemeen eenvoudiger worden verkregen voor stroming in een volledig verzadigd systeem dan voor stroming in een gedeeltelijk verzadigd medium.

De algebraïsche formulering van het stromingsprobleem resulteert in een abstract simulatiesysteem of mathematisch model. Daarnaast bestaan er ook fysische en analoge modellen. Wind (1972) ontwikkelde een hydraulisch analogon en Wind & Mazee (1979) een elektrisch analogon voor de simulatie van verticale stroming in de onverzadigde zone. De meest veelzijdige electrische analogons voor de simulatie van verzadigde grondwaterstroming bestaan uit een netwerk van weerstanden en condensatoren. Ofschoon met deze directe simulatietechnieken gecompliceerde stromingsproblemen zijn op te lossen, worden mathematische modellen in velerlei opzicht als superieur beschouwd. Hieraan heeft vooral de recente ontwikkeling op het gebied van de digitale computertechniek bijgedragen.

Voor het numeriek oplossen van stromingsvergelijkingen worden eindige elementen- en eindige differentiemethoden gebruikt. De eindige elementenmethode biedt voordelen bij het oplossen van gecompliceerde verzadigde-onverzadigde stromingsproblemen en in gevallen waarbij het gebruik van een onregelmatig netwerk wenselijk is. De methode wordt pas sinds kort toegepast voor het oplossen van stromingsproblemen in poreuze media. Van de bestaande numerieke oplossingen is dan ook het grootste deel verkregen met behulp van eindige differenties. Een aantal gangbare eindige differentietechnieken wordt besproken aan het einde van hoofdstuk 2.

Om historische redenen, maar ook vanwege de genoemde verschillen tussen stromingsvergelijkingen voor volledig verzadigde en gedeeltelijk verzadigde systemen, werd de waterbeweging boven en beneden het freatisch vlak vanouds gescheiden behandeld. Deze benadering vereenvoudigt de oplossing van het stromingsprobleem aanmerkelijk, omdat in de onverzadigde zone veelal volstaan kan worden met het in beschouwing nemen van stroming in verticale richting en in de verzadigde zone met stroming in het horizontale vlak. Maar in het geval van ondiepe of snel fluctuerende grondwaterstanden bestaan er ernstige bezwaren tegen deze aanpak vanwege het effect van de onverzadigde stroming op het verzadigde systeem.

Een integrale benadering van verzadigde-onverzadigde stroming werd voor het eerst gerapporteerd door Rubin (1968). In hoofdstuk 3 wordt een overzicht gegeven van modellen die gebruik maken van slechts één vergelijking voor het oplossen van stroming in een gedeeltelijk verzadigd medium. De toepassingen van deze rigoureuze benadering hebben betrekking op de simulatie van pompproeven en stroming in watervoerende pakketten met een ondiepe grondwaterstand. Voor deze stromingssituaties is het effect van het onverzadigde systeem op de stroming in het verzadigde freatische pakket het meest geprononceerd.

Het gebruik van slechts één vergelijking voor het simuleren van verzadigde-onverzadigde stroming introduceert numerieke problemen. De stromingsvergelijking is namelijk parabolisch in de onverzadigde zone en van een elliptisch type in het verzadigde deel, terwijl de ligging van het freatisch vlak tussen beide gebieden a priori onbekend is. Omdat de afhankelijke variabele in de onverzadigde zone en in de buurt van de put aanzienlijk kan variëren over een geringe afstand, moet gebruik gemaakt worden van een netwerk met een kleine maaswijdte. Bovendien vereist de niet-lineariteit van de coëfficienten die betrekking hebben op het onverzadigde deel van het stromingsgebied dat om redenen van stabiliteit en convergentie de tijdstappen tot een kleine grootte worden teruggebracht. Voor stromingsgebieden van enige omvang leidt dit tot exorbitante rekentijden en een tekort aan beschikbare geheugencapaciteit van de computer. Vandaar dat tot op heden geen toepassingen op regionale schaal bekend zijn.

Een alternatieve oplossing (Pikul et al., 1974) is de koppeling van Richards' vergelijking voor verticale onverzadigde stroming aan de vergelijking van Boussinesq voor horizontale verzadigde stroming. De resulterende quasi drie-dimensionale aanpak blijkt niet tot een significant grotere doelmatigheid te leiden bij het oplossen van verzadigde-onverzadigde stromingsproblemen. De belangrijkste oorzaak hiervan is dat de beperkingen die gelden ten aanzien van de lengte van de tijdstap voor onverzadigde stroming, worden opgelegd aan het gehele systeem.

In hoofdstuk 4 wordt de ontwikkeling beschreven van een model voor verticale onverzadigde stroming waarvoor de rekenkosten aanmerkelijk lager zijn. Niet-stationaire stroming wordt door het model gesimuleerd met een opeenvolging van stationaire toestanden. Opwaartse stationaire stroming in een grondkolom met een hoogte van een meter boven het freatisch vlak werd voor het eerst berekend door Richards (1931). Een systematische berekening van stationaire relaties werd uitgevoerd door Wind (1955) en later door anderen toegepast bij de bepaling van de voor het gewas maximaal beschikbare hoeveelheid vocht in relatie tot de diepte van de grondwaterstand. Feitsma (1969) gebruikte hierbij een opeenvolging van stationaire toestanden om het niet-stationaire proces van capillaire

opstijging en grondwaterstandsdaling te simuleren.

In deze studie is de pseudo stationaire benadering van capillaire opstijging geanalyseerd. De resultaten die met deze aanpak worden verkregen, blijken afhankelijk te zijn van de lengte van de gebruikte tijdstap in relatie tot de karakteristieke tijd van het onverzadigde systeem. In het geval van een ondiepe grondwaterstand in een zandige grond ligt de waarde van de karakteristieke tijd in de orde van grootte van dagen. Indien de lengte van de gebruikte tijdstap kleiner is dan de karakteristieke tijd, worden met de pseudo stationaire benadering resultaten verkregen die fysisch gezien onjuist zijn. Hetzelfde geldt in geval van een afnemende flux door de bovenrand van het model en voor de situatie waarbij capillaire opstijging wordt gevolgd door percolatie. Bovendien is gebleken dat voor een grote neerwaartse flux door de onderrand de positie van het freatisch vlak niet goed gesimuleerd kan worden.

In deze studie strekt de onverzadigde zone zich uit van juist beneden het freatisch vlak tot aan maaiveld. Het gebied is schematisch verdeeld in een wortelzone en een ondergrond. Omdat stroming in de wortelzone in hoge mate wordt bepaald door de wateropname van de wortels, is de gradiënt van de hydraulische potentiaal in de wortelzone gelijk gesteld aan nul. Er is aangetoond dat de stationaire stromingstoestand volledig is bepaald door slechts twee parameters (b.v. het verzadigingstekort van de wortelzone S_r en de stationaire flux in de ondergrond $\bar{q}$). Door gebruik te maken van verzadigingstekorten wordt de oplossing van een stationaire situatie teruggebracht tot een probleem van twee relaties met twee onbekenden (S_r en $\bar{q}$). De oplossing van de stationaire situatie overeenkomend met de flux door de bovenrand van de ondergrond wordt bovenrandoplossing genoemd. Procedures zijn ontwikkeld om de hierboven genoemde onjuistheden te corrigeren en om perioden met neerslagoverschot volgend op een situatie met capillaire opstijging te kunnen simuleren. Indien de wortelzone uitdroogt tot verwelkingspunt, berekent het model bovendien de werkelijke flux door de bovenrand. In het geval van een grote neerwaartse flux door de onderrand is de bovenrandoplossing ongeschikt voor de berekening van de grondwaterstand. Vandaar dat voor een neerwaartse flux door de onderrand de grondwaterstand wordt gesimuleerd met behulp van een pseudo stationaire benadering van de stroming in het deel van de ondergrond dat juist boven het freatisch vlak gelegen is. De oplossing van de stationaire situatie overeenkomend met de flux door de onderrand van de onverzadigde zone wordt onderrandoplossing genoemd. De boven- en onderrandoplossingen zijn gecombineerd in één simulatiemodel waarbij rekening is gehouden met hysteresis en heterogeniteit. In geval van percolatie worden de capillaire eigenschappen echter homogeen verondersteld, zodat met het model geen schijngrondwaterspiegels gesimuleerd kunnen worden.

In hoofdstuk 5 wordt een uiteenzetting gegeven van een quasi drie-dimensionale benadering voor de simulatie van niet-stationaire verzadigde-onverzadigde stroming in watervoerende pakketten met een ondiepe grondwaterstand. Bij de oplossing wordt gebruik gemaakt van een twee-dimensionaal horizontaal netwerk voor de beschrijving van de verzadigde grondwaterstroming. Een speciale procedure is ontwikkeld om in ieder knooppunt van dit netwerk het model voor stroming in de onverzadigde zone te koppelen aan het verzadigde systeem.

Teneinde het quasi drie-dimensionale model experimenteel te verifiëren werd in het oosten van Nederland een gebied gekozen ter grootte van 36 km^2. Voor een beschrijving van

het gebied is gebruik gemaakt van een rechthoekig netwerk met een maaswijdte van 500 m. Met een tijdstap van tien dagen werd een periode van bijna zes jaar gesimuleerd. De overeenkomst tussen de gesimuleerde grondwaterstanden en de waargenomen waarden is bevredigend. Minder nauwkeurige resultaten zijn verkregen in perioden met een afwisselend verdampings- en neerslagoverschot. De gevoeligheid van de gesimuleerde grondwaterstanden en de berekende evapotranspiratie ten aanzien van een variatie in de waarde van een aantal parameters werd onderzocht. Uit een bespreking van de resultaten in hoofdstuk 6 blijkt dat de berekende werkelijke verdamping in hoge mate wordt bepaald door de conceptuele benadering van de wateropname door de wortels. Voor de in deze studie gevolgde benaderingswijze van de gewasverdamping is verder gebleken dat het verschil tussen de berekende werkelijke en potentiële evapotranspiratie van gras vrijwel uitsluitend afhankelijk is van de beschikbare hoeveelheid vocht in de wortelzone en in veel mindere mate van de empirische diffusieweerstand voor bodem en gewas (r_p).

Met een toepassing van het model voor verzadigde-onverzadigde stroming werden de gevolgen van grondwateronttrekking voor de berekende grondwaterstanden en waterbalansen voorspeld. De toepassing heeft betrekking op de onttrekking in het modelgebied en de periode die ook voor de verificatie van het model is gebruikt.

List of symbols

a	Coefficient in Eqn 72	$cm \cdot d^{-1} \cdot mbar^{n}$
a	Coefficient in Eqn 91	d^{-1}
A	Coefficient in Eqn 15	-
A	Coefficient in Eqn 84	-
b	Coefficient in Eqn 91	$cm \cdot d^{-1}$
B	Coefficient in Eqn 84	-
c	Hydraulic resistance of confining layer	s
c_f	Compressibility of the soil matrix	Pa^{-1}
c_w	Compressibility of water	Pa^{-1}
C	Specific moisture capacity	Pa^{-1}, $mbar^{-1}$
∂	Partial differential operator	-
d_p	Depth of water table below upper boundary of percolation profile	cm
D	Thickness of (saturated part of) aquifer	m, cm
D	Diffusivity as defined by Eqn 29	$m^2 \cdot s^{-1}$
D'	Thickness of confining layer	m
D_r	Thickness of 'effective' root zone	cm
e_a	Actual vapour pressure at 2 m height	bar
e_s	Saturated vapour pressure for the air at 2 m height	bar
E_a	Aerodynamic evaporation	$kg \cdot m^{-2} \cdot s^{-1}$
E_{pot}	Potential evapotranspiration	$kg \cdot m^{-2} \cdot s^{-1}$, $cm \cdot d^{-1}$
E_{re}	Real evapotranspiration	$kg \cdot m^{-2} \cdot s^{-1}$, $cm \cdot d^{-1}$
E_{wet}	Evaporation of a wet surface	$kg \cdot m^{-2} \cdot s^{-1}$
F	Observed water-table elevation	cm
$\bar{F}$	Mean of observed water-table elevations	cm
F'	Simulated water-table elevation	cm
g	Acceleration due to gravity	$m \cdot s^{-2}$
h	Water-table elevation	m, cm
h*	Water-table elevation at boundary S_1	cm
h_s	Soil surface elevation	m, cm
i	Space index in x direction	-
I	Total number of nodes in x direction	-
j	Space index in y direction	-
J	Total number of nodes in y direction	-
k	Proportionality factor in Darcy's law (Eqn 10)	$m^2 \cdot s^{-1} \cdot Pa^{-1}$
K	Hydraulic conductivity	$m \cdot s^{-1}$, $cm \cdot d^{-1}$

$\overline{K}$	Hydraulic conductivity of an aquifer taken as a constant in vertical direction	$m \cdot s^{-1}$, $cm \cdot d^{-1}$
K'	Hydraulic conductivity of confining layer	$m \cdot s^{-1}$
K_x, K_y, K_z	Principal components of the hydraulic conductivity tensor	$m \cdot s^{-1}$
K_{sat}	Saturated hydraulic conductivity in the unsaturated zone	$cm \cdot d^{-1}$
ℓ	Mesh width	cm
L	Latent heat of vaporization	$J \cdot kg^{-1}$
L	Horizontal distance used in problem (54)	m
m	Index for boundary node in x direction	-
n	Time index	-
n	Porosity	-
n	Coefficient in Eqn 72	-
n	Direction normal to the boundary	-
p	Hydraulic or matric pressure, relative to atmospheric pressure	Pa, mbar
p_a	Atmospheric pressure (p_a = 1.013)	bar
p_{rs}	Matric pressure at interface root zone - subsoil	mbar
P	Pressure equivalent of total soil water potential	Pa
P	Precipitation	$cm \cdot d^{-1}$
q	Flux density or specific discharge	$m \cdot s^{-1}$, $cm \cdot d^{-1}$
$\overline{q}$	Flux in case of steady unsaturated vertical flow	$cm \cdot d^{-1}$
q_e	Sink term due to groundwater extraction	$cm \cdot d^{-1}$
q_i	Source or sink term function	$cm \cdot d^{-1}$
q_o	Groundwater discharge into surface water system	$cm \cdot d^{-1}$
q_p	Upper boundary flux of percolation profile	$cm \cdot d^{-1}$
q_{rs}	Flux across interface root zone - subsoil	$cm \cdot d^{-1}$
q_s	Maximum possible flux across soil surface	$m \cdot s^{-1}$, $cm \cdot d^{-1}$
q_s^{re}	Real flux across soil surface	$cm \cdot d^{-1}$
q_u	Upward flux from the saturated region into the unsaturated zone	$m \cdot s^{-1}$
q_w	Vertical flux across a level just below the water table or lower boundary of the unsaturated flow model	$m \cdot s^{-1}$, $cm \cdot d^{-1}$
q_w^*	Flux for which both relations (91) and (94) apply	$cm \cdot d^{-1}$
q_x, q_y, q_z	Flux in the respective co-ordinate directions	$m \cdot s^{-1}$
Q	Groundwater extraction	$m^3 \cdot d^{-1}$
r	Iteration index	-
r	'Effective' pore radius	m
r_a	Diffusion resistance to water vapour in the air	$s \cdot m^{-1}$
r_c	Diffusion resistance depending on the fraction of soil covered	$s \cdot m^{-1}$
r_ℓ	Diffusion resistance depending on light intensity	$s \cdot m^{-1}$

r_p	Diffusion resistance depending on soil moisture conditions and flow in the plant	$s \cdot m^{-1}$
r_s	Total diffusion resistance of crop and soil	$s \cdot m^{-1}$
R_E	Efficiency factor	-
R_n	Net radiation	$J \cdot s^{-1} \cdot m^{-2}$
s	Slope of the temperature - saturation vapour pressure curve	$bar \cdot K^{-1}$
s_s	Specific storage $\{s_s = \rho g n(c_f + c_w)\}$	m^{-1}
s_w	Degree of water saturation	-
S_1, S_2	Part of boundary for horizontal saturated flow for which $h = h^*$, and the flux normal to the boundary equals zero, respectively	-
S_c	Fraction of the soil covered by the crop	-
S_e	Saturation deficit in the subsoil for $\bar{q} = 0$	cm
S_p	Saturation deficit of percolation profile	cm
S_r	Saturation deficit of root zone	cm
S_s	Saturation deficit of subsoil	cm
S_u	Saturation deficit of entire unsaturated zone $(S_u = S_r + S_s)$	cm
t	Time	s, d
T	Transmissivity	$m^2 \cdot s^{-1}$, $cm^2 \cdot d^{-1}$
T_A	Average transmissivity of element A	$cm^2 \cdot d^{-1}$
w	Depth of water table below soil surface	m, cm
x,y,z	Cartesian co-ordinate directions or distance along the respective co-ordinate directions	m, cm
z_i, z_w, z_s	Various heights used in problem (54)	m
z_{rs}	Distance between phreatic level and interface root zone - subsoil applying to the upper boundary solution	cm
z^*_{rs}	Depth of water table resulting from the lower boundary flux alone	cm
α, β	Integration dummies	-
α	Reciprocal of delay index	s^{-1}
γ	Psychrometric constant	$bar \cdot K^{-1}$
Δ	Increment	-
ϵ	Ratio molecular weight of water vapour and dry air $(\epsilon = 0.622)$	-
ζ	Height of the water table above the lower boundary of the unsaturated flow model	cm
ζ_p	Elevation of upper boundary of percolation profile in the model for unsaturated flow	cm
ζ_{rs}	Distance between the interface root zone - subsoil and the lower boundary of the unsaturated flow model	cm
η	Fluid dynamic viscosity	$kg \cdot m^{-1} \cdot s^{-1}$

θ	Fractional volumetric moisture content	-
θ_m	Moisture content used in Eqn 64	-
κ	Intrinsic permeability	m^2
μ	Specific yield or storage coefficient	-
μ_A, μ_B	Short-term and long-term specific yield, respectively, used in Eqn 53	-
μ_q	Storage coefficient which is independent of water-table depth	-
ρ	Density of soil water	$kg \cdot m^{-3}$
ρ_a	Density of air (ρ_a = 1.2047)	$kg \cdot m^{-3}$
σ	Standard deviation of the differences between simulated and observed water-table elevations	cm
τ	Time (τ < t) used in Eqn 53	s
τ	Characteristic time	d
ϕ	Hydraulic head or total soil water potential expressed as energy per unit weight	m, cm
ϕ'	Hydraulic head in adjoining aquifer	m
$\Psi_t, \Psi_p, \Psi_o, \Psi_g$	Total, pressure, osmotic and gravitational soil water potential, respectively, expressed as energy per unit mass	$J \cdot kg^{-1}$
ω	Over-relaxation parameter	-
∇	Operator for gradient or divergence	-

Appendix A

Computation of S_s and z_{rs} as a function of p_{rs} and $\bar{q}$ for a heterogeneous soil profile

If different K(p) relations apply to different layers in the subsoil pressure profiles do not exist. Instead of $z(p,\bar{q})$, a relation can be computed between the pressure at the interface root zone - subsoil p_{rs} and the depth of the water table below this interface z_{rs} for a number of positive values for $\bar{q}$, yielding $z_{rs}(p_{rs},\bar{q})$. A numerical approach to the computation of the relations $S_s(z_{rs},\bar{q})$ and $S_s(p_{rs},\bar{q})$ for a heterogeneous subsoil is given below.

The subsoil is divided into layers with a depth of 1 cm. For each layer a soil moisture characteristic and K(p) relation must be specified. Given a water-table depth z_{rs} (integer in cm) the layer index ℓ runs from 1 to z_{rs}, where $\ell = 1$ for the layer of which the lower side is at a depth z_{rs} (Fig. A1). For a given steady flux $\bar{q}$ and water-table depth z_{rs}, the computation of S_s and p_{rs} proceeds as follows. The matric pressure distribution is numerically approached for the successive layers starting at the phreatic level in upward direction. The variables are initialized as follows: $p = 0$; $\Delta p = -1$ mbar; $S_s = 0$ and $\ell = 1$, where Δp is a first estimate for the change in p over layer ℓ.

Step 1: The average pressure $\bar{p}$ in layer ℓ is estimated as $\bar{p} = p + \frac{1}{2}\Delta p$.

Step 2: Interpolate the hydraulic conductivity K for $p = \bar{p}$ from the K(p) relation that applies for layer ℓ. (It may often be necessary to carry out this interpolation on a double logarithmic scale, due to the non-linearity of this relation.)

Step 3: Compute the increase in height Δz from Darcy's law, written as

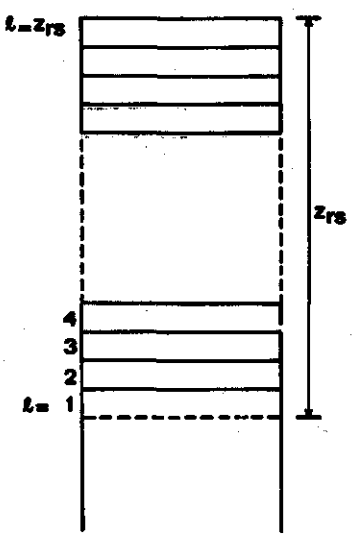

Fig. A1. The use of the layer index ℓ for a particular water-table depth z_{rs}.

$$\Delta z = -\frac{1}{\rho g}\,\frac{K}{\bar{q} + K}\,\Delta p$$

Step 4: Improve the estimate for $\bar{p}$ halfway layer ℓ to

$$\bar{p} = p + \tfrac{1}{2}\,\frac{\Delta p}{\Delta z}$$

Step 5: Interpolate K for $p = \bar{p}$ from the K(p) relation that applies for layer ℓ.

Step 6: Compute the change in p over layer ℓ (for which $\Delta z = 1$ cm) from Darcy's law, now written as

$$\Delta p = -\rho g\,\frac{K + \bar{q}}{K}\,\Delta z$$

(Comparison with analytical solutions shows no need to repeat Steps 1 to 6 to improve the solution for Δp.)

Step 7: Interpolate for $\bar{p} = p + \frac{1}{2}\Delta p$ the moisture content θ from the soil moisture characteristic for layer ℓ and increase S_s with the saturation deficit of this layer

$$S_s = S_s + n - \theta$$

where n is the porosity of layer ℓ.

Step 8: Compute the matric pressure at the upper side of layer ℓ

$$p = p + \Delta p$$

Step 9: Increase the layer index

$$\ell = \ell + 1$$

Step 10: If $\ell \leq z_{rs}$ go to Step 1. If not, the computations are completed and $p_{rs} = p$.

The above scheme is executed for values of z_{rs} increasing from zero with steps of 1 cm until the absolute value calculated for p_{rs} is greater than or equal to 16000 mbar. If the soil is homogeneous the computed relation between p and z (and between θ and z) does not change with z_{rs}. Then values for p_{rs} and S_s are easily computed for z_{rs} if the above scheme is applied with the following initial data: $\ell = z_{rs}$ and values for Δp, S_s and $p = p_{rs}$ as computed for the previous water-table depth ($z_{rs} - 1$). From the calculated relations between z_{rs}, p_{rs} and S_s values for z_{rs} and S_s are interpolated for different values of p_{rs}, yielding $S_s(p_{rs})$ and $z_{rs}(p_{rs})$.

The above procedure is carried out for a number of values for $\bar{q}$ resulting in the relations $S_s(p_{rs},\bar{q})$ and $z_{rs}(p_{rs},\bar{q})$. In this study S_s and z_{rs} are computed for the following 13 values for p_{rs}: 0, -10, -20, -31, -50, -100, -250, -500, -1000, -2500, -5000, -10000 and -16000 mbar and the following 18 values for $\bar{q}$: 0, 0.001, 0.005, 0.010, 0.015,

0.020, 0.030, 0.040, 0.060, 0.080, 0.100, 0.125, 0.150, 0.200, 0.300, 0.400, 0.500 and 1.000 $cm \cdot d^{-1}$.

As for a homogeneous profile the values computed for z as a function of p are independent of the water-table depth, the relation $z_{rs}(p_{rs},\bar{q})$ may be written as $z(p,\bar{q})$, which are the pressure profiles in Fig. 5c. The saturation deficit curves $S_s(p_{rs},\bar{q})$ are presented in Fig. 5f, while the derived relation $S_s(z_{rs},\bar{q})$ which results from a combination of $S_s(p_{rs},\bar{q})$ and $z_{rs}(p_{rs},\bar{q})$ is shown in Fig. 5e.

Appendix B

Hysteresis in the $S_r(p_{rs})$ relation

Consider the hysteretic relation between θ and p given in Fig. B1. The solid lines represent the relation for drying, the broken lines for wetting. The most extreme curve for drying corresponds to the soil moisture characteristic given in Fig. 5b. Disregarding the scanning curves, the relations for drying and wetting are used to compute $S_r(p_{rs})$. The result is given in Fig. B2 for a depth of the root zone D_r = 30 cm. The broken line represents the situation for which p_{rs} continuously decreases from pF 4.2 to zero assuming equilibrium conditions in the root zone. This process may be approximated if the root zone is slowly wetted by capillary rise from the subsoil while q_s = 0. Generally wetting is caused by rainfall excess, resulting in a highly non-linear flow process which is complicated by hysteresis. As the pseudo steady-state procedure does not consider flow in the root zone, the total effect must be lumped into the $S_r(p_{rs})$ relation. It should be noted that the nature of the pseudo steady-state procedure hampers the pressure at the lower side of the root zone obtaining low pF values. Even after a long wet period the p_{rs} value may not drop below pF 1.5. Therefore it is assumed that hysteresis effects in the root zone have ceased if the matric pressure p_{rs} has reached a value of e.g. pF 1.5. The resulting numerical representation of the hysteretic $S_r(p_{rs})$ relation for the 13 values of p_{rs} mentioned in Appendix A is given in Fig. B3.

Data on hysteresis in the soil moisture characteristic are usually not available. Therefore a 'hysteresis factor' is introduced, defined as the number of logarithm cycles

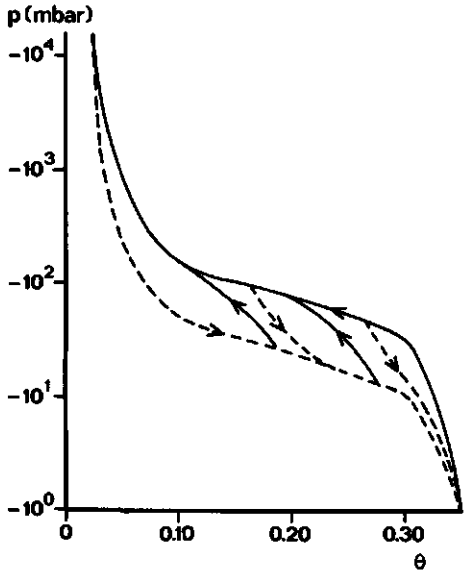

Fig. B1. Soil moisture characteristic showing hysteresis with θ(p) relations for drying (—) and for wetting (---).

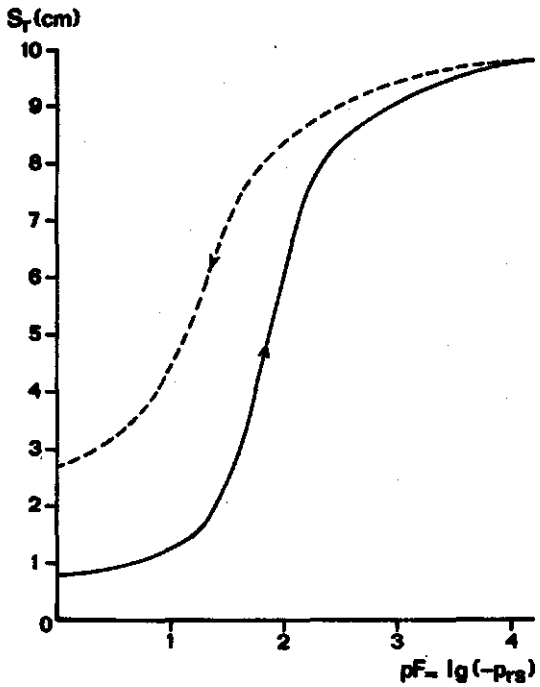

Fig. B2. Saturation deficit curve for the root zone (D_r = 30 cm) showing hysteresis with $S_r(p_{rs})$ relations for drying (-) and for wetting (---).

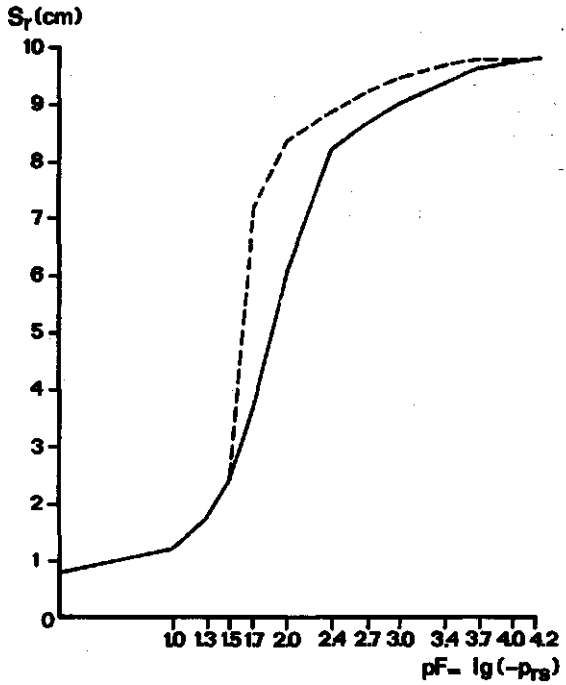

Fig. B3. Numerical representation of the $S_r(p_{rs})$ relation showing hysteresis (hysteresis factor equals 0.5) with $S_r(p_{rs})$ relations for drying (-) and for wetting (---).

over which the $S_r(p_{rs})$ curve for drying is shifted along the p_{rs} axis to obtain the wetting curve. The hysteresis factor applying to Fig. B3 equals 0.5. In the absence of data the hysteresis factor must be calibrated.

A numerical procedure is developed to compute the $S_r(p_{rs})$ relation at the beginning of each time increment. For time step n+1 the scanning curve connecting the curves for drying and wetting is computed such that it joins the drying curve for values of $S_r > S_r^n$ and the wetting curve for values of $S_r < S_r^n$.

Literature

Akker, C. van den, 1972. Een mathematisch model voor de berekening van de gevolgen van een grondwateronttrekking in het geval van twee watervoerende pakketten gescheiden door een semi-permeabele laag. University of Technology Delft, Department of Civil Engineering, 59 p.

Amerman, C.R., 1976. Waterflow in soils: A generalized steady-state, two-dimensional porous media flow model. U.S. Department of Agriculture, ARS-NC-30, 62 p.

Arya, L.M., D.A. Farrell & G.R. Blake, 1975. A field study of soil water depletion patterns in presence of growing soybean roots: I. Determination of hydraulic properties of the soil. Soil Sci. Soc. Am. Proc. 39: 424-430.

Aslyng, H.C., 1963. Report Commission I. Soil physics terminology. Bulletin of the international society of soil science, No. 23, p. 7-10.

Awan, N.M. & T. O'Donnell, 1972. Moving water tables in tile-drained soils. J. Irrig. Drain. Div. Am. Soc. Civ. Eng. 98 (IR3): 459-477.

Awater, R.H.C.M., 1976. Infiltratie Dinxperlo. University of Technology Delft, Department of Civil Engineering.

Awater, R.H.C.M. & P.J.M. de Laat, 1979. Groundwater flow and evapotranspiration; A simulation model. Part 2: Applications. Basisrapport CWG, Provinciale Waterstaat van Gelderland, Arnhem (in preparation).

Bakel, P.J.T. van, 1979. Verdamping en gewasproduktie. Deel 2: Verdamping in relatie tot bodem en gewas. Basisrapport CWG, Provinciale Waterstaat van Gelderland, Arnhem, 49 p.

Bear, J., 1972. Dynamics of fluids in porous media. American Elsevier Publishing Company, Inc., New York, 764 p.

Bolt, G.H., 1975. Report Commission I. Soil physics terminology. Bulletin of the international society of soil science, No. 48, p. 16-22.

Boulton, N.S., 1955. Unsteady radial flow to a pumped well allowing for delayed yield from storage. IAHS Publ. No. 37, Tome II, p. 472-477.

Boulton, N.S., 1963. Analysis of data from non-equilibrium pumping tests allowing for delayed yield from storage. Proc. Inst. Civ. Eng. 26: 469-482.

Bouma, J., 1977. Soil survey and the study of water in unsaturated soil. Soil Survey Papers, No. 13, Soil Survey Institute, Wageningen, 107 p.

Bouma, J. & H.C. van Heesen, 1979. Waterwingebied 't Klooster. Toelichting bij de veldbodemkundige gevoeligheidsanalyse. Stiboka rapport no. 1432, Stichting voor Bodemkartering, Wageningen, 22 p.

Boussinesq, J., 1904. Recherches théoriques sur l'écoulement des nappes d'eau infiltrées dans le sol. J. Math. Pures Appl. 10: 363-394.

Bouwer, H., 1967. Analyzing subsurface flow systems with electric analogs. Water Resour. Res. 3(3): 897-907.

Bouwer, H. & W.C. Little, 1959. A unifying numerical solution for two-dimensional steady flow problems in porous media with an electrical resistance network. Soil Sci. Soc. Am. Proc. 23: 91-96.

Breaster, C., G. Dagan, S.P. Neuman & D. Zaslavsky, 1971. A survey of the equations and solutions of unsaturated flow in porous media. First annual report (part 1). Technion, Haifa, Israel, 176 p.

Brebbia, C.A., 1978. The boundary element method for engineers. Pentech Press, London, 189 p.

Bredehoeft, J.D. & G.F. Pinder, 1970. Digital analysis of areal flow in multi aquifer groundwater systems: A quasi three-dimensional model. Water Resour. Res. 6(3): 883-888.

Brutsaert, W., G.S. Taylor & J.N. Luthin, 1961. Predicted and experimental water table drawdown during tile drainage. Hilgardia 31(11): 389-418.

Buckingham, E., 1907. Studies on the movement of soil moisture. U.S. Dept. Agr. Bur. Soils Bull. 38, p. 29-61.

Carslaw, H.S. & J.C. Jaeger, 1959. Conduction of heat in solids. Oxford University Press, London, 510 p.

Cary, J.W., 1963. Onsager's relations and the non-isothermal diffusion of water vapor. J. Phys. Chem. 67: 126-129.
Cary, J.W., 1966. Soil moisture transport due to thermal gradients: Practical aspects. Soil Sci. Soc. Am. Proc. 32: 3-5.
Cary, J.W. & S.A. Taylor, 1962. The interactions of the simultaneous diffusions of heat and water vapor. Soil Sci. Soc. Am. Proc. 26: 413-416.
Childs, E.C., 1960. The nonsteady state of the water table in drained land. J. Geophys. Res. 65(2): 780-782.
Childs, E.C., 1969. An introduction to the physical basis of soil water phenomena. Wiley, London, 493 p.
Childs, E.C. & N. Collis-George, 1950. The permeability of porous materials. Proc. Roy. Soc. (London) A201: 392-405.
Childs, E.C. & A. Poulovassilis, 1962. The moisture profile above a moving water table. Soil Sci. 13: 272-285.
Colenbrander, H.J., 1970. Analyse van afvoergegevens. In: Hydrologisch onderzoek in het Leerinkbeek gebied (Hydrological research in the Leerinkbeek area, with English summary). Provinciale Waterstaat van Gelderland, Arnhem, p. 121-147.
Cooley, R.L., 1971. A finite difference method for unsteady flow in variably saturated porous media: Application to a single pumped well. Water Resour. Res. 7(6): 1607-1625.
Cooley, R.L. & C.M. Case, 1973. Effect of a water table aquitard on drawdown in an underlying pumped aquifer. Water Resour. Res. 9(2): 434-447.
Crank, J., 1956. The mathematics of diffusion. Oxford University Press, London, 347 p.
Darcy, H.P.G., 1856. Les fontaines publiques de la ville de Dijon, V. Dalmont, Paris, 647 p.
De Wiest, R.J.M., 1966. On the storage coefficient and the equations of groundwater flow. J. Geophys. Res. 71. 1117-1122.
Dooge, J.C.I., 1973. Linear theory of hydrologic systems. U.S. Dept. Agr. Techn. Bull. 1468, 327 p.
Dooge, J.C.I., 1977. Deterministic methods in systems hydrology. Lecture notes, International Institute for Hydraulic and Environmental Engineering, Delft, 283 p.
Douglas Jr., J. & J. Gunn, 1964. A general formulation of alternating direction implicit methods, I. Num. Math. 6: 428-453.
Douglas Jr., J. & B.F. Jones, 1963. On predictor-corrector methods for nonlinear parabolic differential equations. Jour. SIAM 11: 195-204.
Dupuit, J., 1863. Etudes théoriques et pratiques sur le mouvement des eaux dans les canaux découverts et à travers les terrains perméables. 2nd Ed., Dunod, Paris, 304 p.
Edelman, J.H., 1947. Over de berekening van grondwaterstroomingen. Thesis. University of Technology Delft, 77 p.
Elrick, D.E. & D.H. Bowman, 1964. Note on an improved apparatus for soil moisture flow measurements. Soil Sci. Soc. Am. Proc. 28: 450-453.
Ernst, L.F., 1978. Drainage of undulating sandy soils with high groundwater tables. I. A drainage formula based on a constant hydraulic head ratio. J. Hydrol. 39: 1-30.
Ernst, L.F., N.A. de Ridder & J.J. de Vries, 1970. A geohydrologic study of east Gelderland (The Netherlands). Geol. en Mijnb. 49: 457-488.
Feddes, R.A., 1971. Water, heat and crop growth. Thesis. Communications Agricultural University Wageningen, 184 p.
Feddes, R.A. & A.L.M. van Wijk, 1976. An integrated model-approach to the effect of water management on crop yield. Agr. Water Man. 1: 3-30.
Feddes, R.A., P.J. Kowalik & H. Zaradny, 1978. Simulation of field water use and crop yield. Simulation monographs, Pudoc, Wageningen, 189 p.
Feitsma, K.S., 1969. Grondverbetering in het noordwestelijk deel van Oostelijk Flevoland. Cult.tech. Tijdschr. 9: 86-98.
Forchheimer, P., 1886. Über die Ergiebigkeit von Brunnenanlagen und Sickerschlitzen. Zeitschr. Arch. Ing. Ver. 32(7): 539-563.
Freeze, R.A., 1969. The mechanism of natural ground-water recharge and discharge, 1: One-dimenional, vertical, unsteady, unsaturated flow above a recharging or discharging ground-water flow system. Water Resour. Res. 5(1): 153-171.
Freeze, R.A., 1971. Three-dimensional, transient, saturated-unsaturated flow in a groundwater basin. Water Resour. Res. 7(2): 347-366.
Freeze, R.A. & P.A. Witherspoon, 1966. Theoretical analysis of regional groundwater flow. 1: Analytical and numerical solutions to the mathematical model. Water Resour. Res. 2(4): 641-656.
Freeze, R.A. & P.A. Witherspoon, 1968. Theoretical analysis of regional groundwater flow. 3: Quantitative interpretations. Water Resour. Res. 4(3): 581-590.

Gardner, W.R., 1958. Some steady state solutions of the unsaturated moisture flow equation with application to evaporation from a water table. Soil Sci. 85: 228-232.
Gardner, W.R., 1962. Approximate solution of a non-steady-state drainage problem. Soil Sci. Soc. Am. Proc. 26: 129-132.
Guitjens, J.C. & J.N. Luthin, 1971. Effect of soil moisture hysteresis on the water table profile around a gravity well. Water Resour. Res. 7(2): 334-346.
Haines, W.B., 1930. Studies in the physical properties of soil: V. The hysteresis effect in capillary properties and the modes of moisture associated therewith. J. Agr. Sci. 20: 97-116.
Hanks, R.J. & S.A. Bowers, 1962. Numerical solution of the moisture flow equation for infiltration into layered soils. Soil Sci. Soc. Am. Proc. 26: 530-534.
Hele-Shaw, H.S., 1898. Investigation of the nature of surface resistance of water and of stream-line motion under certain experimental conditions. Trans. Inst. Naval Architects 40: 21-46.
Herbert, R., 1968. Time variant ground water flow by resistance network analogues. J. Hydrol. 6: 237-264.
Hillel, D., 1971. Soil and water: Physical principles and processes. Academic Press, New York, 288 p.
Holst, A.F. van, H.C. van Heesen & H. Makken, 1974. Waterwingebied 't Klooster (Hengelo Gld.). Stiboka rapport nr. 1109, Stichting voor Bodemkartering, Wageningen, 17 p.
Hornberger, G.M. & I. Remson, 1970. A moving boundary model of a one-dimensional saturated-unsaturated transient porous flow system. Water Resour. Res. 6(3): 898-905.
Hornberger, G.M., J. Ebert & I. Remson, 1970. Numerical solution of the Boussinesq equation for aquifer-stream interaction. Water Resour. Res. 6(2): 601-608.
Hornberger, G.M., I. Remson & A.A. Fungaroli, 1969. Numeric studies of a composite soil moisture ground-water system. Water Resour. Res. 5(4): 797-802.
Ibrahim, H.A. & W. Brutsaert, 1968. Intermittent infiltration into soils with hysteresis. J. Hydraul. Div. Am. Soc. Civ. Eng. 94 (HY1): 113-137.
Isaacson, E. & H.B. Keller, 1966. Analysis of numerical methods. Wiley, New York, 541 p.
Isherwood, J.D., 1959. Water-table recession in tile-drained land. J. Geophys. Res. 64: 795-804.
Israelson, O.W., 1927. The application of hydrodynamics to irrigation and drainage problems. Hilgardia 2: 479-528.
Jacob, C.E., 1950. Flow of ground water. In: Engineering hydraulics (Ed. H. Rouse). Wiley, New York, p. 321-386.
Jensen, M.E. & R.J. Hanks, 1967. Nonsteady-state drainage from porous media. J. Irrig. Drain. Div. Am. Soc. Civ. Eng. 93 (IR3): 209-231.
Josselin de Jong, G. de, 1961. Moirē patterns of the membrane analogy for ground-water movement applied to multiple fluid flow. J. Geophys. Res. 66(10), 3625-3629.
Josselin de Jong, G. de, 1962. Electrische analogie modellen voor het oplossen van geohydrologische problemen. Water 46: 43-45.
Karplus, W.J., 1958. Analog simulation. Mc Graw-Hill, New York, 427 p.
Kastanek, F., 1971. Numerical simulation technique for vertical drainage from a soil column. J. Hydrol. 14: 213-232.
Kastanek, F., 1973. Calculation of vertical moisture flow in a soil body during evaporation, infiltration and redistribution. In: Ecological studies. Analysis and Synthesis, Vol. 4. Springer Verlag, Berlin, p. 49-58.
Keulen, H. van, 1975. The use of simulation models in the study of soil moisture transport processes. In: Computer simulation of water resources systems (Ed. G.C. Vansteenkiste), North Holland Publishing Company, Amsterdam, p. 291-298.
Kirkham, D. & R.E. Gaskell, 1951. Falling water table in tile and ditch drainage. Soil Sci. Soc. Am. Proc. 15: 37-42.
Klute, A., 1952. A numerical method for solving the flow equation for water in unsaturated materials. Soil Sci. 73: 105-116.
Klute, A., F.D. Whisler & E.J. Scott, 1965. Numerical solution of the nonlinear diffusion equation for water flow in a horizontal soil column of finite length. Soil Sci. Soc. Am. Proc. 29: 353-358.
Kraijenhoff van de Leur, D.A., 1958. A study of non-steady groundwater flow with special reference to a reservoir-coefficient. De Ingenieur 70(19): B87-B94.
Kraijenhoff van de Leur, D.A., 1962. Some effects of the unsaturated zone on nonsteady free-surface groundwater flow as studied in a scaled granular model. J. Geophys. Res. 67: 4347-4362.
Laat, P.J.M. de, 1976. A pseudo steady-state solution of water movement in the unsaturated zone of the soil. J. Hydrol. 30: 19-27.

Laat, P.J.M. de & C. van den Akker, 1976. Simulatiemodel voor grondwaterstroming en verdamping. In: Modelonderzoek 1971-1974. Deel 2: Grondslagen. Interimrapport CWG, Provinciale Waterstaat van Gelderland, Arnhem, p. 145-197.
Laat, P.J.M. de & R.H.C.M. Awater, 1978. Groundwater flow and evapotranspiration; A simulation model. Part 1: Theory. Basisrapport CWG, Provinciale Waterstaat van Gelderland, Arnhem, 64 p.
Laat, P.J.M. de, C. van den Akker & Th.J. van de Nes, 1975. Consequences of groundwater extraction on evapotranspiration and saturated-unsaturated flow. IAHS Publ. No. 115, p. 67-76.
Lamb, H., 1932. Hydrodynamics. 6th Ed., Cambridge University Press, 738 p.
Liakopoulos, A.C., 1965. Theoretical solution of the unsteady unsaturated flow problems in soils. Int. Ass. Sci. Hydr. 10: 5-39.
Lin, C.L., 1972. Digital simulation of the Boussinesq equation for a water table aquifer. Water Resour. Res. 8(3): 691-698.
Luthin, J.N. & G.S. Taylor, 1966. Computer solutions for the drainage of sloping land. Trans. Am. Soc. Agr. Eng. 9: 546-549.
Luthin, J.N. & R.V. Worstell, 1957. The falling water table in tile drainage: I. A laboratory study. Soil Sci. Soc. Am. Proc. 21: 580-584.
Maasland, M., 1959. Water-table fluctuations induced by intermittent recharge. J. Geophys. Res. 64: 549-559.
Miller, E.E. & A. Klute, 1967. Dynamics of soil water. In: Irrigation of agricultural lands. Am. Soc. Agron. Monograph 11: 209-244.
Miller, E.E. & R.D. Miller, 1956. Physical theory for capillary flow phenomena. J. Appl. Phys. 27: 324-332.
Molen, W.H. van der, 1972. Stroming in de onverzadigde zone. Lecture notes. Agricultural University Wageningen, 126 p.
Molz, F.J. & I. Remson, 1970. Extraction-term models of soil moisture use by transpiring plants. Water Resour. Res. 6(5): 1346-1356.
Monteith, J.L., 1965. Evaporation and environment. Proc. Symp. Soc. Exp. Biol. 19: 205-234.
Moore, R.E., 1939. Water conduction from shallow water tables. Hilgardia 12: 383-426.
Muskat, M., 1937. The flow of homogeneous fluids through porous media. Mc Graw-Hill, New York, 763 p.
Nash, J.E. & J.V. Sutcliffe, 1970. River flow forecasting through conceptual models, Part 1: A discussion of principles. J. Hydrol. 10: 282-290.
Neuman, S.P., 1972. Theory of flow in unconfined aquifers considering delayed response of the water table. Water Resour. Res. 8(4): 1031-1045.
Neuman, S.P., 1973. Saturated-unsaturated seepage by finite elements. J. Hydraul. Div. Am. Soc. Civ. Eng. 99 (HY12): 2233-2250.
Neuman, S.P., R.A. Feddes & E. Bresler, 1975. Galerkin method of simulating water uptake by plants. In: Computer simulation of water resources systems (Ed. G.C. Vansteenkiste), North Holland Publishing Company, Amsterdam, p. 325-348.
Nielsen, D.R. & J.W. Biggar, 1961. Measuring capillary conductivity. Soil Sci. 92: 192-193.
Peaceman, D.W. & H.H. Rachford, 1955. The numerical solution of parabolic and elliptic differential equations. Jour. SIAM 3: 28-41.
Penman, H.L., 1948. Natural evaporation from open water, bare soil and grass. Proc. Roy. Soc. London A 193: 120-145.
Philip, J.R., 1955. Numerical solution of equations of the diffusion type with diffusivity concentration-dependent. Trans. Faraday Soc. 51: 885-892.
Philip, J.R., 1957a. The theory of infiltration: 1. The infiltration equation and its solution. Soil Sci. 83: 345-357.
Philip, J.R., 1957b. Evaporation, and moisture and heat fields in the soil. J. Meteorol. 14: 354-366.
Philip, J.R., 1966. The dynamics of capillary rise. In: Water in the unsaturated zone (Eds. P.E. Rijtema & H. Wassink). Symp. Proc. UNESCO/IASH, Vol. 2, p. 559-564.
Philip, J.R., 1969. Theory of infiltration. Adv. Hydrosci. 5: 216-296.
Philip, J.R. & D.A. de Vries, 1957. Moisture movement in porous materials under temperature gradients. Trans. Am. Geophys. Un. 38: 222-232.
Pikul, M.F., R.L. Street & I. Remson, 1974. A numerical model based on coupled one-dimensional Richards and Boussinesq equations. Water Resour. Res. 10(2): 295-302.
Pinder, G.F. & J.D. Bredehoeft, 1968. Application of the digital computer for aquifer evaluation. Water Resour. Res. 4(5): 1069-1093.
Polubarinova-Kochina, P.Ya., 1962. Theory of groundwater movement. Princeton University Press, 613 p.

Poulovassilis, A., 1962. Hysteresis of pore water, an application of the concept of independent domains. Soil Sci. 93: 405-412.
Poulovassilis, A., 1969. The effect of hysteresis of pore water on the hydraulic conductivity. Soil Sci. 20: 52-56.
Prickett, T.A., 1975. Modeling techniques for groundwater evaluation. Adv. Hydrosci. 10: 1-143.
Prickett, T.A. & C.G. Lonnquist, 1969. Comparison between analog and digital simulation techniques for aquifer evaluation. In: The use of analog and digital computers in hydrology. IASH/UNESCO, Paris. Vol. 2, p. 625-634.
Raats, P.A.C. & W.R. Gardner, 1971. Comparison of empirical relationships between pressure head and hydraulic conductivity and some observations on radially symmetric flow. Water Resour. Res. 7(4): 921-928.
Reisenauer, A.E., 1963. Methods for solving problems of multidimensional, partially saturated steady flow in soils. J. Geophys. Res. 68: 5725-5733.
Remson, I., C.A. Appel & R.A. Webster, 1965. Groundwater models solved by digital computer. J. Hydraul. Div. Am. Soc. Civ. Eng. 91 (HY3): 133-147.
Remson, I., A.A. Fungaroli & G.M. Hornberger, 1967. Numerical analysis of soil-moisture systems. J. Irrig. Drain. Div. Am. Soc. Civ. Eng. 93 (IR3): 153-166.
Remson, I., G.M. Hornberger & F.J. Molz, 1971. Numerical methods in subsurface hydrology. Wiley, New York, 389 p.
Richards, L.A., 1928. The usefulness of capillary potential to soil-moisture and plant investigations. J. Agr. Res. 37: 719-742.
Richards, L.A., 1931. Capillary conduction of liquids through porous mediums. Physics 1: 318-333.
Richtmyer, R.D. & K.W. Morton, 1967. Difference methods for initial value problems. Wiley, New York, 405 p.
Rijtema, P.E., 1965. An analysis of actual evapotranspiration. Thesis. Agric. Res. Rep. 659, Pudoc, Wageningen, 107 p.
Rijtema, P.E., 1969. Soil moisture forecasting. Nota 513, Instituut voor Cultuurtechniek en Waterhuishouding, Wageningen, 28 p.
Rijtema, P.E., 1971. Een berekeningsmethode voor de benadering van de landbouwschade ten gevolge van grondwateronttrekking. Nota 587, Instituut voor Cultuurtechniek en Waterhuishouding, Wageningen, 46 p.
Rose, C.W., 1966. Agricultural physics. Pergamon, Oxford, 174 p.
Rose, D.A., 1963a. Water movement in porous materials: Part 1. Isothermal vapour transfer. Brit. J. Appl. Phys. 14: 256-262.
Rose, D.A., 1963b. Water movement in porous materials: Part 2. The separation of the components of water movement. Brit. J. Appl. Phys. 14: 491-496.
Rosema, A., 1974. A mathematical model for simulation of the thermal behaviour of bare soils, based on heat and moisture transfer. Publ. No. 11, Netherlands Interdepartmental Working community for the Application of Remote Sensing techniques, Delft, 92 p.
Rovey, C.E.K., 1975. Numerical model of flow in a stream-aquifer system. Hydrology Paper No. 74, Fort Collins, Colorado, 73 p.
Rubin, J., 1968. Theoretical analysis of two-dimensional, transient flow of water in unsaturated and partly unsaturated soils. Soil Sci. Soc. Am. Proc. 32: 607-615.
Rubin, J., 1969. Numerical analysis of ponded rainfall infiltration. In: Water in the unsaturated zone (Eds. P.E. Rijtema & H. Wassink). Symp. Proc. UNESCO/IASH, Vol. 1, p. 440-451.
Rubin, J. & R. Steinhardt, 1963. Soil water relations during rain infiltration, I. Theory. Soil Sci. Soc. Am. Proc. 27: 246-251.
Rushton, K.R., 1974. Critical analysis of the alternating direction implicit method of aquifer analysis. J. Hydrol. 21: 153-172.
Santing, G., 1958. A horizontal scale model based on the viscous flow analogy for studying groundwater flow in an aquifer having storage. Int. Ass. Sci. Hydr. 44: 105-114.
Santos, A.G. dos & E.G. Youngs, 1969. A study of the specific yield in land-drainage situations. J. Hydrol. 8(1): 59-81.
Schlichter, C.S., 1899. Theoretical investigation of the motion of ground waters. U.S. Geological Survey, Annual Report 19-II, p. 295-384.
Shaw, C.F. & A. Smith, 1927. Maximum height of capillary rise starting with soil at capillary saturation. Hilgardia 2(11): 399-409.
Stallman, R.W., 1961. Relation between storage changes at the water table and observed water-level changes. U.S. Geol. Surv. Prof. Paper 424B: B39-B40.
Stone, H.L., 1968. Iterative solution of implicit approximations of multidimensional partial differential equations. SIAM J. Num. Anal. 5: 530-558.

Streltsova, T.D., 1972. Unsteady radial flow in an unconfined aquifer. Water Resour. Res. 8(4): 1059-1066.
Stroosnijder, L., 1976. Infiltratie en herverdeling van water in grond. Thesis. Agric. Res. Rep. 847, Pudoc, Wageningen, 213 p.
Swartzendruber, D., 1963. Non-Darcy behavior and the flow of water in unsaturated soils. Soil Sci. Soc. Am. Proc. 27: 491-494.
Swartzendruber, D., 1968. The applicability of Darcy's law. Soil Sci. Soc. Am. Proc. 32: 11-18.
Swartzendruber, D., 1969. The flow of water in unsaturated soils. In: Flow through porous media (Ed. R.J.M. De Wiest), Academic Press, New York, p. 215-292.
Taylor, G.S. & J.N. Luthin, 1969. Computer methods for transient analysis of water-table aquifers. Water Resour. Res. 5(1): 144-152.
Taylor, S.A., 1968. Terminology in plant and soil water relations. In: Water deficits and plant growth (Ed. T.T. Kozlowski), Vol. 1, Chapter 3. Academic Press, New York, p. 49-72.
Thames, J.L. & D.D. Evans, 1968. An analysis of the vertical infiltration of water into soil columns. Water Resour. Res. 4: 817-828.
Theis, C.V., 1935. The relation between the lowering of the piezometric surface and the rate and duration of discharge of a well using groundwater storage. Trans. Am. Geophys. Un. 16: 519-524.
Topp, G.C. & E.E. Miller, 1966. Hysteretic moisture characteristics and hydraulic conductivities for glass-bead media. Soil Sci. Soc. Am. Proc. 30: 156-162.
Tyson Jr., H.N. & E.M. Weber, 1964. Ground-water management for the nation's future - Computer simulation of ground-water basins. J. Hydraul. Div. Am. Soc. Civ. Eng. 90 (HY4): 59-77.
Vachaud, G., 1969. Vérification de la loi de Darcy généralisée et détermination de la conductivité capillaire à partir d'une infiltration horizontale. In: Water in the unsaturated zone (Eds. P.E. Rijtema & H. Wassink), Symp. Proc. UNESCO/IASH, Vol. 1, p. 277-287.
Vachaud, G., M. Vauclin & R. Haverkamp, 1975. Towards a comprehensive simulation of transient water table flow problems. In: Computer simulation of water resources systems (Ed. G.C. Vansteenkiste), North Holland Publishing Company, Amsterdam, p. 103-119.
Vachaud, G., M. Vauclin & J. Khanji, 1973. Etude expérimentale des transferts bidimensionnels dans la zone non saturée. Application à l'étude du drainage d'une nappe à surface libre. La Houille Blanche 1: 65-74.
Vauclin, M., G. Vachaud & J. Khanji, 1975. Two dimensional numerical analysis of transient water transfer in saturated-unsaturated soils. In: Computer simulation of water resources systems (Ed. G.C. Vansteenkiste), North Holland Publishing Company, Amsterdam, p. 299-323.
Veer, P. van der, 1978. Calculation methods for two-dimensional groundwater flow. Thesis. Rijkswaterstaat Communications No. 28, Den Haag, 172 p.
Venuri, V. & J.A. Dracup, 1967. Analysis of nonlinearities in ground water hydrology: A hybrid computer approach. Water Resour. Res. 3(4): 1047-1058.
Verhoeven, B., 1953. De inundaties gedurende 1944-1945 en hun gevolgen voor de landbouw. IV. Over de zout- en vochthuishouding van geïnundeerde gronden. Thesis. Versl. Landbouwk. Onderz. 59.5, Staatsdrukkerij, Den Haag, 202 p.
Verma, R.D. & W. Brutsaert, 1970. Unconfined aquifer seepage by capillary flow theory. J. Hydraul. Div. Am. Soc. Civ. Eng. 96 (HY6): 1331-1334.
Verruyt, A., 1970. Theory of groundwater flow. Macmillan, London, 190 p.
Versluys, J., 1916. De capillaire werkingen in den bodem. Thesis. University of Technology Delft, 136 p.
Wachspress, E.L., 1966. Iterative solution of elliptic systems. Prentice Hall Inc., New York, 298 p.
Walton, W.C., 1960. Application and limitation of methods used to analyze pumping test data. Water Well J., March 1960: 45-52.
Walton, W.C. & J.C. Neill, 1960. Analysing ground-water problems with mathematical models and a digital computer. Int. Ass. Sci. Hydr. 52: 336-346.
Watson, K.K., 1967. Experimental and numerical study of column drainage. J. Hydraul. Div. Am. Soc. Civ. Eng. 93 (HY2): 1-15.
Werkgroep Wateronttrekking Gelderse Vallei, 1979. Onderzoek Glindhorst 1974-1979. Waterleiding Maatschappij Gelderland, Velp, 220 p.
Wesseling, J., 1957. Enige aspecten van de waterbeheersing in landbouwgronden. Versl. Landbouwk. Onderz. 63.5, Pudoc, Wageningen, 90 p.

Wind, G.P., 1955. A field experiment concerning capillary rise of moisture in a heavy clay soil. Neth. J. Agric. Sci. 3(1): 60-69.
Wind, G.P., 1972. A hydraulic model for the simulation of non-hysteretic vertical unsaturated flow of moisture in soils. J. Hydrol. 15: 227-246.
Wind, G.P. & A.N. Mazee, 1979. An electronic analog for unsaturated flow and accumulation of moisture in soils. J. Hydrol. 41: 69-83.
Wisler, F.D., A. Klute & R.J. Millington, 1968. Analysis of steady-state evapotranspiration from a soil column. Soil Sci. Soc. Am. Proc. 32: 167-174.
Wit, C.T. de & H. van Keulen, 1972. Simulation of transport processes in soils. Simulation Monographs, Pudoc, Wageningen, 100 p.
Youngs, E.G., 1960. The drainage of liquids from porous materials. J. Geophys. Res. 65: 4025-4030.
Youngs, E.G., 1966. Horizontal seepage through unconfined aquifers taking into account flow in the capillary fringe. In: Water in the unsaturated zone (Eds. P.E. Rijtema & H. Wassink), Symp. Proc. UNESCO/IASH, Vol. 2, p. 897-905.
Youngs, E.G. & S. Aggelides, 1976. Drainage to a water table analyzed by the Green-Ampt approach. J. Hydrol. 31: 67-79.
Zienkiewicz, O.C., 1967. The finite element method in structural and continuum mechanics. Mc Graw-Hill, London, 272 p.